8-2016

A systems biology approach identifies a gene regulatory network in parotid acinar cell differentiation.

Melissa Ann Metzler
University of Louisville

A SYSTEMS BIOLOGY APPROACH IDENTIFIES A GENE REGULATORY NETWORK IN PAROTID ACINAR CELL DIFFERENTIATION

By

Melissa Ann Metzler

B.A., Bellarmine University, 2007

M.S., University of Louisville, 2015

A Dissertation

Submitted to the Faculty of the

School of Medicine of the University of Louisville

In Partial Fulfillment of the Requirements

For the Degree of

Doctor of Philosophy

In Biochemistry and Molecular Biology

Department of Biochemistry and Molecular Genetics

University of Louisville

Louisville, KY

August 2016

A SYSTEMS BIOLOGY APPROACH IDENTIFIES A GENE REGULATORY NETWORK IN PAROTID ACINAR CELL DIFFERENTIATION

By

Melissa Ann Metzler

B.A., Bellarmine University, 2007

M.S., University of Louisville, 2015

A Dissertation Approved on

January 25, 2016

By the following Dissertation Committee:

_____

Douglas S. Darling, PhD, Dissertation Director

_____

Barbara J. Clark, PhD, Committee Member

_____

Ted Kalbfleisch, PhD, Committee Member

_____

Jiaxu Li, PhD, Committee Member

_____

David J. Samuelson, PhD, Committee Member

ACKNOWLEDGEMENTS

This study was undertaken with the help and support of many individuals. I would first like to thank my advisor Dr. Doug Darling who was always available for questions and advise, and whose continued support of myself and this project through difficult periods was essential and much appreciated. His guidance has helped me to develop as a scientist.

I also worked closely with Dr. Srirangapatnam Venkatesh when I first started. His friendly and helpful attitude could always be counted on, and was wonderful to have during my initial training. He is greatly missed by all who knew him.

I am also grateful to Dr. Jim Wittliff and Dr. Sarah Andres who collaborated with the Darling lab. Dr. Andres spent many hours helping to troubleshoot difficult aspects of this challenging project. They helped with my training, were valuable sources of advice, and were always very supportive of the project.

I could also count on advice from Sabine Waigel who I could turn to for technical trouble shooting and questions regarding analysis.

I would also like to thank my committee members, Dr. David Samuelson, Dr. Jiaxu Li, Dr. Barbra Clark, and Dr. Ted Kalbfleisch, for their continued support,

thoughtful questions and advice. Also, Dr. Tom Geoghegan, and Dr. Yong Li who also supported this project. Lastly, I would like to thank my family. Both of my parents, Bob and Connie Metzler, were extremely supportive and helpful during both the ups and downs of this project. Without them none of this would have been possible. And, of course, my husband Jon who has been with me from the beginning, and always encouraged me to keep going. His love and support has always meant so much and helped me immensely during difficult periods

ABSTRACT

A SYSTEMS BIOLOGY APPROACH IDENTIFIES A GENE REGULATORY NETWORK IN PAROTID ACINAR CELL DIFFERENTIATION

By

Melissa Ann Metzler

January 25, 2016

Objective: This project sought to understand the gene regulatory networks that drive parotid salivary gland acinar cells to terminally differentiate, and drive expression of terminal differentiation genes in dedifferentiated ParC5 cells. **Methodology:** Laser capture microdissection was used to isolate acinar cells at multiple time points during differentiation. This important step allowed us to measure gene expression in a single and important cell type. A systems biology approach was taken to measure global mRNA and microRNA expression across acinar cell terminal differentiation in the rat parotid salivary gland. In ParC5 cells, the ER stress activator tunicamycin was used to stimulate Xbp1 activity. **Results:** Profiles of statistically significant changes of mRNA expression, combined with reciprocal correlations of microRNAs and their target mRNAs, suggest a putative network involving *Xbp1* and *Mist1* (BHLHA15). The network suggests that a molecular switch involving Prdm1, *Sox11*, and Pax5 progressively decreases repression of *Xbp1* transcription, in concert with decreased translational

repression by miR-214. Transfection studies validate each of the tested network interactions. Treatment of ParC5 cells with tunicamycin increases expression of Mist1 downstream of Xbp1. However, further downstream effectors of Xbp1 and Mist1 (i.e. PSP, Connexin32) remain unchanged. The Mist1 target gene Rab3D is repressed. However, transfection of Mist1 cDNA, increases Rab3d expression. **Conclusion:** This study identified numerous novel transcription factor expressionpatterns during parotid acinar differentiation, including *Pparg, Klf4,* and *Sox11*. Many differentially expressed microRNAs were also measured which have not previously been described in salivary development. Network analysis identified a gene regulatory network driving expression of terminal differentiation genes. Stimulating Xbp1 activity in ParC5 cells increases Mist1 expression as predicted in the network, but other factors or epigenetic changes may be required for full expression of the network.

TABLE OF CONTENTS

PAGE

LIST OF TABLES

PAGE

LIST OF FIGURES

PAGE

CHAPTER 1: INTRODUCTION

The major salivary glands are exocrine organs that are vital for maintaining oral health. Saliva components provide numerous protective functions in the oral cavity that are unmatched by any other artificial fluid. Millions suffer from gland dysfunction and destruction, and as a result have chronic hyposalivation. These patients generally have poor oral health and reduced quality of life. Regenerating or growing artificial glands for these patients requires increased understanding of how exocrine cells differentiate. This work takes a systems biology approach by measuring both mRNA and microRNA expression changes across acinar cell differentiation and integrating them into a model of gene regulatory interactions that drive differentiation.

1.1 Salivary Gland Anatomy, Cell Types, and Function

1.1.1 Introduction and Basic Anatomy

In mammals, as well as in many terrestrial animals, the salivary glands are a constitutive source of moisture, salt, and proteins which coat the oral cavity and are vital for maintaining oral homeostasis [1-3]. Saliva contributes to many functions in the oral cavity, and as described in a later section, its loss is devastating to oral health and quality of life

There are two main types of glands in mammals: major and minor. Named for their relative size, the major glands are much larger than the minor glands, and are the focus of this study. There are three major paired glands, and they secrete ~ 90% of total saliva. They are the submandibular (SMG), the sublingual (SLG), and the parotid gland (PG). Their locations in humans can be seen in the diagram in Figure 1.1. Both the SMG and the SLG are located under the tongue, while the PG is found in front of and below the ear, flanking the jaw hinge [1].

Gland epithelia can be described as secretory units that exist as clusters of exocrine cells (acini) which are connected by a highly branched duct system and drain into the oral cavity [4]. The three major glands differ slightly in morphology (the SMG is densely packed whereas the branches of the PG are more spaced out) [5, 6]. They also differ with respect to type of secretion, due to different types of acinar cells. The SMG contains mucosal acini which secrete a viscous saliva high in mucin content, while the PG have purely serous acini which do not contain mucins and produce more watery saliva [1, 7] that nonetheless contains a large number of proteins including amylase and the parotid secretory protein (PSP). The parotid is considered responsible for most stimulated flow [8] [9].

The SMG and PG are connected to the oral cavity through their own designated ducts. Each of the paired SMG drains into a single duct know as Wharton's duct under the tongue, and the PG empties into the Stensen duct found opposite the upper second molar in humans [1]. The SLG, on the other hand, may have more than a dozen ducts on the floor of the mouth. The glands are enclosed in

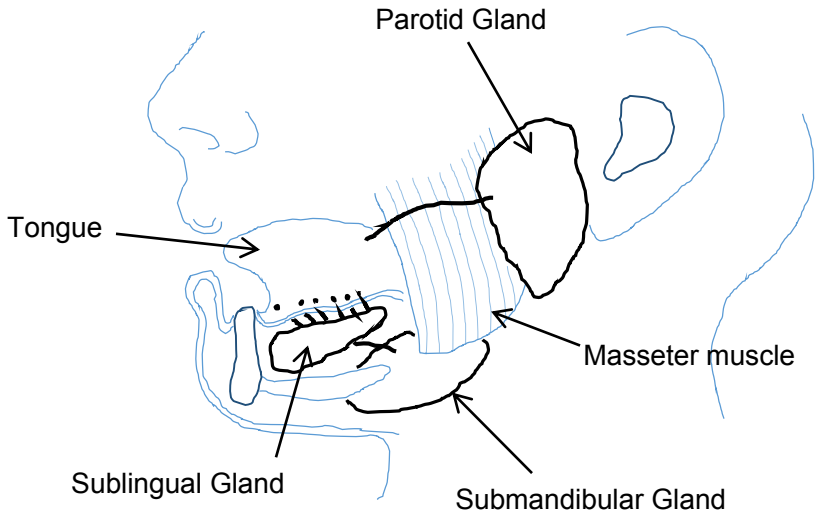

Figure 1.1 Salivary Gland Anatomy. The locations of the three major salivary glands is shown in humans. Both the submandibular and the sublingual glands are found underneath the tongue and are connected to the oral cavity through ducts found on the floor of the mouth. The parotid glands are the largest in humans. They are located on each side of the face in front of the ear, extending down to the lower jaw, and overlapping the masseter muscle. The parotid duct connects to the oral cavity in the back of the mouth, near the upper second molar.

mesenchyme capsules, and are innervated by both parasympathetic and sympathetic fibers which control secretion [1, 2, 10].

Nerves, particularly parasympathetic nerves, are required for secretion. They control both a "resting" or basal flow rate which occurs at all times, and a short term stimulated flow rate where the flow of saliva can be increased 10-fold or more. Also, many types of receptors can indirectly stimulate this increased flow, including mechanoreceptors, olfactory receptors, and gustatory receptors [11]. Evidence suggests that not only can these stimuli alter the flow of saliva but its components as well. For instance saliva collected from the oral cavity after stimulation with sugar has been found to contain more protein than saliva stimulated with citric acid [12]. This level of control makes saliva ideal for maintaining homeostasis of an oral cavity which may undergo many different types of assaults on a daily basis.

1.1.2 Cell Types

The acinar cells produce and secrete most of saliva's components. They are highly specialized terminally differentiated cells, which are vital for fully functioning glands. They are pyramid-shaped cells packed into clusters around a well-defined lumen at the end-points of the ductal branches. The apical cytoplasm is generally filled with electron dense secretory vesicles, and they have a well-developed Golgi complex and rough endoplasmic reticulum [13-15]. There are two types of acinar cells which can be identified by the types of proteins found in the vesicles: mucosal acinar cells contain large amounts of mucin proteins, and serous acinar cells contain densely packed proteins,

including many enzymes, but no mucins, and these vesicles generally appear darker.

In humans, the parotid gland contains purely serous acini, and the submandibular is purely mucosal. The sublingual gland contains a mixture of mucosal and serous cells within a single acinus with mucosal acinar cells forming a cluster which are capped by serous demilune cells [16].

The acini are surrounded by myoepithelial cells which are innervated and are thought to aid secretion through contraction [1, 13].

The ductal cells modify saliva as it passes from the acini, mostly by reabsorbing salt [13]. Saliva is hypotonic to plasma, and this is thought to contribute to taste [10].

1.1.3 Exocrine Secretion

Secretion from parotid acinar cells is fairly complex and has been found to involve several different pathways [17], which can be classified into two main types: regulated secretion, which involves stimulation from the nervous system, and constitutive secretion which does not.

The regulated secretion pathways involve beta-adrenergic stimulation leading to accumulation of intracellular cAMP, and elevation of intracellular Ca^{2+} by muscarinic stimulation, ultimately leading to the release of protein cargo from secretory granules. This type of pathway accounts for 80 – 90% of protein secretion from the parotid [17]. These pathways involve the large secretory granules which are directed towards the apical membrane and densely packed

with protein cargo (i.e. amylase, PSP, RNaseI). The membrane of these mature granules also contain proteins including the SNARE VAMP-2, and two GTP-binding proteins Rab3d and Rab26. VAMP-2 is essential for fusion with the plasma membrane, and the Rab proteins have been found to be vital for granule maturation and recruitment to the plasma membrane [18-20].

1.1.4 Saliva Components and Oral Health

Although saliva has been found to be ~90% water, it contains many protein and salt components which benefit the oral cavity, and make it a difficult fluid to replicate artificially.

Several studies have been done to identify the complete proteome of saliva [21, 22]. The most comprehensive analysis of the whole salivary proteome to date has identified over 1000 different proteins, most coming from the major salivary glands. Individual secretions from the submandibular and parotid gland have also been analyzed. Each gland contributes close to 1000 proteins, with about a 60% overlap between them [23]. These proteins contribute to many functions in the oral cavity ranging from digestion, antimicrobial protection, lubrication, taste, and speech.

One of the main proteins in saliva are mucins which are supplied mostly by the SMG. In humans mucins are expressed from two genes: MUC5B and MUC7, and each gene may have many glycoforms. MUC5B is the more heavily glycosylated (> 80%) and is the main contributor to the viscosity of saliva, which

has a gel-like consistency that coats and forms a barrier on epithelial and enamel surfaces. It also protects against acids.

MUC7 is smaller and does not appear to increase viscosity. It is, unlike MUC5B, specific to salivary glands. MUC5B coats many other surfaces such as in the intestines. MUC7 has been found to bind to several species of bacteria that are found in the oral cavity, and along with agglutinin (an anti-bacterial protein secreted from all three major glands), contributes to the aggregation and clearance of bacteria.

Other types of antimicrobial proteins include enzymes. The most prevalent and probably the most well-known enzyme in human saliva is amylase. This enzyme is produced largely by the parotid gland, and catalyzes the alpha amylase reaction, the first reaction in starch digestion to produce glucose. Aside from aiding in digestion, breaking down starch in the oral cavity allows the taste of sweetness to be perceived [24].

In humans there are five amylase isozymes found in a gene cluster on chromosome 1 [25]. Three of the genes are salivary specific and the remaining two are produced in the pancreas. Interestingly, the salivary amylase genes have variable copy numbers in the human population (from 2-15 copies based on a survey of 50 individuals) [26]. A recent study also found a correlation between amylase copy number and diet, with more copy numbers in populations with a grain heavy diet and less in populations that relay on a low starch diet [26].

A survey of amylase expression throughout the mammalian kingdom further suggests that salivary amylase evolves alongside diet. Pure carnivores, such as cats and dogs, do not produce amylase in their saliva, and ruminants such as sheep have very little amylase [24]. While the exact physiological significant of amylase activity in the oral cavity is still being investigated, the evolution of salivary specific amylase expression suggests it is important in animals with a starch heavy diet.

Saliva has also been reported to contain chitinase activity most likely due to secretions from the parotid [27]. Chitin is a major component of the yeast cell wall and this protein could act as an anti-fungal. Lysozyme is another enzyme found in saliva which acts as an anti-fungal and is thought to contribute to controlling candida growth in the mouth. It has been suggested that the salivary glands, particularly the parotid, can respond to higher candida loads by secreting more lysozyme [28].

There are also many types of antimicrobial proteins in saliva such as the PLUNC (palate, lung, and nasal epithelium clone) family Parotid Secretory Protein (PSP, aka BPIFA2), which is related to the BPI (bactericidal/ permeability-increasing) protein. PSP has been found to have anti-inflammatory as well as antibacterial activity. This protein contains hydrophobic regions, and has been shown to bind to LPS, likely though regions with similarity to Lipopolysaccharide-Binding Protein (LBP) [29]. Several peptides of this protein have been shown to inhibit LSP stimulated secretion of TNFα from macrophages. In a mouse model of sepsis, co-injection of a PSP peptide with *P. aeruginosa* LPS increased survival

compared to the LPS alone. This protein also acts as an agglutinin. Incubation of PSP with *P. aeruginosa* led to the aggregation of the bacteria which has been shown to aid in clearance by inhibiting attachment.

These are just a few examples of known functions for saliva components. Knowledge continues to grow and it is likely that proteins will have more than one function. It is clear that saliva has been adapted for our survival and for our diet; its loss would be devastating for our oral health.

1.2 Gland Dysfunction and Oral Health

1.2.1 Xerostomia and Oral Health

Xerostomia (dry mouth) is a common complaint among the general population, with some surveys finding perceived xerostomia in more than 25% of respondents [30, 31]. Generally, it is reported more often by women and the elderly. Although the presence of xerostomia can be considered subjective, it is often accompanied by hyposalivation which is determined more objectively by a decrease in salivary flow. This is defined by a resting flow rate less than 0.1 ml/min or a stimulated rate less than 0.7 ml/min [32]. The absence or reduction of saliva leads to a dramatic increase in oral health problem such as caries (tooth decay caused by bacteria, commonly called cavities), ulcerations, periodontitis, and opportunistic infections such as candida [31, 33]. Patients also experience discomfort, difficulty chewing, swallowing, and even speaking. This can have a drastic impact on quality of life.

There are many causes of hyposalivation, but they generally fall into three major categories: medication, autoimmune disorder, and radiation therapy.

Many medications list xerostomia as a side effect. Drugs with anticholinergic activity are the most reported, but there are many other classes which are thought to reduce salivary function such as antihistamines, decongestants, tricyclic antidepressants, and others, though in most cases the mechanism is not known [33]. This mostly affects the elderly population which generally report taking more medications. Salivary dysfunction is rarely irreversible in these cases, and salivary flow usually returns to normal when patients stop taking the drug.

Autoimmune disorders are cause by the immune system attacking host tissue, leading to damage. Disorders involving the exocrine glands affects tens of millions of individuals. The most common of these is Sjogren's syndrome (SS) which varies in prevalence from 0.1% to 4.8% of the population. This variation is thought to be due to ethnic and geographical differences. Onset is most common in women in their 40's and 50's, and is the second most common autoimmune disorder behind rheumatoid arthritis. It is usually considered a chronic and progressive disease. A characteristic of SS is immune cell infiltration, particularly of the salivary glands. Overtime the acinar cells atrophy and are replaced with fibrotic and fatty tissue, however, several studies have determined that function is greatly reduced long before cells are lost possibly due to production of nitric oxide (NO) or autoantibodies that target muscarinic receptors [34-36].

Radiation therapy is also responsible for xerostomia in thousands of patients. Every year there are 30,000 – 40,000 new cases of head and neck cancer, and chronic xerostomia is considered the most common complication of treatment. Radiation treatment is part of the standard of care, and is sometimes combined with surgery and chemotherapy. Because of current limitations, the radiation field usually includes some healthy tissue which usually involves the salivary glands. For reasons not completely known, the salivary glands are especially sensitive to radiation [37]. Unlike many radiosensitive cells, they are not highly proliferative. The most recent hypothesis involves acute disruption in the plasma membrane which interferes with muscarinic receptor stimulation without killing the cells (this satisfies the observation that patients experience hyposalivation quickly after therapy begins (~ 1 week), but there is no observed loss of cells). Later damage, and loss of cells, particularly acinar cells is observed (damage can continue to progress for several months after treatment), and this is thought to be due to more "classical" radiation damage, that is, DNA damage of progenitor cells causes lethality when these cells try to re-enter the reproductive cycle and replenish gland tissue. These patients rarely recover gland tissue, and end up suffering from permanent chronic hyposalivation [38-40].

1.2.2 Treatment of Hyposalivation

Most treatments available to patients with xerostomia involve managing symptoms, and preventing oral health problems. Currently, there is no way to regenerate or regrow functioning tissue, and patients generally face a lifetime of managing this disorder.

Commonly patients will consume more water in order the combat the feeling of dry mouth. However, xerostomia is usually not caused by dehydration and thus this is not expected to confer any long-term benefit though it may help with some symptoms such as discomfort, and may aid in chewing and swallowing [31]. There are also an array of saliva substitutes on the market featuring many different formulations. The base for these solutions covers a wide range of options including glycerol, animal mucins, and several types of methylcellulose. Some products contain fluoride, others lemon juice (to stimulate residual gland activity, citric acid is the most effective natural stimulator of salivation), though long-term use of an acid can lead to enamel erosion [31, 41]. Despite the long list of options available, few studies have compared their benefit, and there is currently no accepted gold standard saliva substitute. It is important to note that no artificial substitute contains all of the wide array of components of natural saliva, and so is not likely to confer all the same protective benefits. Also these solutions must be applied every few hours as they are easily washed away [42].

The American Dental Association (ADA) recommends that dentist encourage patients to make changes in their daily life to avoid exacerbating oral complications. These include tobacco cessation, alcohol-free mouth wash, and a reduction in dietary sugar [42]. Patients will also expect to visit a dentist more frequently (every 3-6 months). However, a 2007 review noted that pre-treatment dental consultations for patients with head and neck cancer was low, and compliance with oral care recommendations was poor [43].

There are currently two FDA approved medications used to stimulate saliva flow and alleviate hyposalivation: these are pilocarpine and cevimeline hydrochloride, referred to as "sialogogues." They are cholinergic agonists, and are used to stimulate any remaining gland tissue. These medications must be taken 3 to 4 times a day and side effects include sweating, nausea, and rhinitis. Patients vary in their response to these drugs, usually depending on how much healthy tissue remains. Those with extensive damage and loss of cells may receive no benefit at all [42].

In radiation therapy, several interventions have been developed to protect the salivary glands from damage in the first place. The use of intensity-modulated radiation therapy (IMRT) has been shown to spare the salivary glands by reducing their exposure to radiation, and has been shown to reduce the incidence of xerostomia in these patients [44]. For instance, follow up of phase I/II patients showed that patients receiving IMRT recovered 63% of their flow rate one year after treatment, compared to 3% in the patients that received conventional radiation (these glands received a cumulative dose of 19.9Gy or 57.5Gy respectively, and a baseline of 26Gy is now widely considered a threshold for salivary gland sparing) [45, 46]. Another method to prevent damage is to move one of the submandibular glands out of the field of radiation in a procedure termed salivary gland transfer (SGT). It was developed in 2000 and has been used on hundreds of patients in the last decade [47]. Recent meta-analysis has supported the claim that this treatment is effective in preventing xerostomia [48, 49].

Although these preventative techniques may help many of the hundreds of thousands diagnosed with head and neck cancer every year, these measures will not help all patients, and there are still millions already suffering from gland hypofunction with little effective treatment options available. Therefore, considerable emphasis has been placed on developing therapeutic approaches based on controlling differentiation or regeneration of damaged salivary glands.

1.3 Regenerating Salivary Glands

1.3.1 Stem Cells

Several recent studies have focused on identifying stem cells capable of differentiating into gland cells, particularly acinar cells. In the case of head and neck cancer patients, for instance, the stem cells could be isolated from patients before radiation treatment, and then transplanted back after radiation treatment.

It has long been thought that the salivary glands themselves contain stem cells residing within the ducts, and are mainly responsible for maintaining gland tissue [50, 51]. These ductal progenitors are also thought to be the source of gland regeneration following ductal ligation, when most acinar cells atrophy [52, 53]. However, recent work has suggested that clonal expansion of acinar cells maintains tissue homeostasis, with little contribution from the ducts [54]. However, this does not exclude the possibility that there is a stem cell population in the glands. Many groups have identified different prospective stem cells in the gland, and have exploited their pluripotent potential to grow both ductal and acinar cells *in vitro* and *in vivo*.

Nanduri *et. al.* [55] was able to show immune-histochemical staining of several stem cell markers in the ductal compartment of mouse submandibular glands including c-Kit, CD133, CD24, CD29, and CD49f. Interestingly, culturing gland cells as salispheres, enriches a c-Kit+ population after several days [56]. As reported by Lombaert *et. al.* [57] initial spheres contained both ductal and acinar cells, as well as c-Kit- and c-Kit+ cells. After 2 or 3 days in culture, the acinar cells disappeared and most of the remaining cells were c-Kit+. Over the next several days, acinar cells began to reappear, as indicated by PAS+ staining and IHC for amylase, suggesting these cultures contained stem cells capable of differentiation into acinar cells.

In a rescue experiment, cells from three day cultured spheres were injected into the glands of irradiated mice. The donor was a male expressing a GFP reporter, and the recipients were wild type female mice 30 days after receiving local radiation which destroyed their salivary glands. Glands and salivary flow were examined 90 days after transplantation. Mice that received the transplantation had significantly more salivary flow and increased acinar surface area compared to irradiated, non-transplanted animals. There were many GFP positive cells at the injection site, all ductal cells, and subsequent *in situ* hybridizations confirmed the presence of donor derived acinar cells based on hybridization with the Y chromosome. This indicates that these cells are differentiating and incorporating into the gland rather than relying solely on some paracrine affect to stimulate growth of existing cells.

c-Kit+ cells have also been identified in human submandibular and parotid glands. Salisphere cultures seem to behave in much the same way as the mouse, and c-Kit+ cells could be isolated from 3 day cultures [57].

Bone marrow stem cells have also been investigated for the ability to rescue gland function post-irradiation. As in the salivary gland stem cell experiments, bone marrow stem cells were isolated from a donor mouse (specifically bone marrow mesenchymal stem cells), and transplanted into the glands of an irradiated mouse. Mice that received the stem cells showed a significant increase in saliva production, compared to PBS controls, as well as a preservation of morphological features, including acinar cells. Donor cells were identified in the recipient gland by use of a tracking dye, and in a few cells fluorescence from the dye co-localized with amylase staining indicating transdifferentiation [58].

The use of stem cell based therapies appears promising as it could potentially regrow tissue for patients from their own cells. Several candidate cell populations have been proposed and tested in mice, and one population, c-Kit+ cells, have been isolated in humans. These cells have the ability to differentiate into both ductal and acinar cells both *in vitro* and *in vivo*. However, many patients no longer have progenitor or stem cells remaining, and so alternative therapies continue to be developed. Importantly, there is little understanding of the regulatory pathways which control differentiation into acinar cells.

1.3.2 Bioengineered Glands

While the transplantation of individual stem cells has shown promise, there is also research into constructing three-dimensional structures in culture for grafting into patients. One method, termed the organ germ method seeks to recapitulate the process of development and differentiation in culture starting with isolated epithelial and mesenchymal cells from an embryo, and resulting in a gland germ in culture that can be transplanted [59]. This method has been successful in growing all three of the major salivary glands in mice. Transplantation of the submandibular gland germ in mice was also successful. The gland continued to grow and develop *in vivo*, it expressed terminal differentiation markers such and Aqp5, and amylase, and responded to proper nerve stimulation [60]. While the engineering of a working organ from gland germ cells in culture is impressive, the reliance on embryonic germ cells means this technique could probably not be developed for use on patients in the clinic. Other types of cells and three-dimensional culturing techniques have been investigated for their use in growing differentiated cells *in vitro*, with the ultimate goal of building an implantable artificial salivary gland. This could aid patients with extensive gland damage that no longer possess progenitor cells. By using donor cells and an appropriate scaffold, a working gland could be constructed for them.

The challenges of constructing an artificial gland largely stem from the fact that it is difficult to grow differentiated salivary cells (particularly acinar cells) *in vitro*. Primary cells are generally short lived, and are also known to transdifferentiate in culture [61]. There are several salivary gland cell lines, but none of them harbor all the characteristics of fully differentiated cells. It would be very useful to

develop an understanding of the regulatory pathways to drive and maintain differentiation in culture.

Current work in this area has focused on the role of the culturing scaffold. In creating a three dimensional environment that more closely resembles the *in vivo* structure (rather than culturing cells in a 2D monolayer), several groups have been able to recreate some characteristics of fully differentiated cells. Several cell lines grown on matrigel, for instance, have become more differentiated. HSG cells are a neoplastic cell line derived from human intercalated duct cells from a submandibular gland. When grown on plastic these cells form a flat monolayer, do not express any tight junction (TJ) proteins, which are needed for apical/basal polarity and proper secretion, and do not express Aquaporin5 (AQP5) which is needed for fluid secretion. Culturing on matrigel leads to the formation of three dimensional spheres that express many TJs that are also properly localized to the apicolateral membrane. These cells also express AQP5, they contain electron dense granules, and increased expression of amylase [62]. Similarly, ParC10 cells (a cell line derived from primary rat parotid acinar cells, and immortalized with simian virus 40 (SV40)[63, 64] also organize into lumenized spheres on matrigel, express apically localized TJ proteins, basally localized muscarinic receptor, and increased expression of AQP5 [65].

Unfortunately, matrigel cannot be used for *in vivo* applications as it is derived from a mouse sarcoma cell line [66] and several studies have found it to be tumorigenic [67-69]. Culturing cells on fibrin hydrogels has been investigated, but it has failed to produce the same three dimensional morphology [67]. As an

alternative technique, one group has developed precisely constructed craters lined with poly-lactic-co-glycolic acid (PLGA) nanofibers to mimic a basement membrane. Increasing the curvature of the crater was found to increase cell polarity and expression of AQP5 [70, 71].

These new techniques indicate a limited amount of control over the differentiation process of acinar cells, and we are still a long way from recreating fully differentiated cells in culture. This will take an increased understanding of differentiation *in vivo* in order to identify important factors and networks that drive differentiation, which could then potentially be applied in culture.

1.4 Gland Development and Cell Differentiation

1.4.1 Gland Development and Contribution from Outside Signaling

All three major glands develop by branching morphogenesis, although at different times. The submandibular gland is the first to develop, followed by the sublingual, and finally the parotid. In the rat, parotid development begins around embryonic day 16.5 and continues until postnatal day 25. Development can be characterized by five major events: formation of a prebud thickening in the oral epithelium, an initial bud that protrudes into the surrounding mesenchyme, branching morphogenesis, canalization of the ducts and end buds to form a continuous lumen, and cellular differentiation [1, 13]. Along with the epithelium and mesenchyme, endothelial and neuronal cells also grow alongside the gland. Signaling between these cells types has been found to control many events in development.

It has long been known that the mesenchyme is important for branching morphogenesis. Ex vivo studies involving the salivary glands date back to the 1950's when Grobstein *et. al.* [72] was able to show that branching morphogenesis does not occur when salivary epithelium is mixed with the mesenchyme from a different source. During his experiments, he physically separated the epithelium from the mesenchyme using a filter and concluded that proper branching was due to "diffusible factors" between the two tissues.

Later studies in knockout mice showed that Fgfr2b (fibroblast growth factor receptor 2b) null and Fgf10 (fibroblast growth factor 10) null mice do not have salivary glands. In these animals an initial bud forms, but does not undergo branching morphogenesis [73]. Hoffman *et. al.* [74] profiled the expression of many FGFs and FGFRs in the mouse submandibular gland during branching morphogenesis. They measured expression in the epithelium and mesenchyme separately, and found that Fgfr2b is expressed in the epithelium while Fgf10 and Fgf7 are expressed in the mesenchyme. In functional studies of FGFR signaling, ex vivo glands were incubated with soluble recombinant FGFRs in order to competitively bind ligands. Of all the recombinant proteins used, rFGFR2b had the largest effect on reducing branching morphogenesis. In a rescue experiment, adding exogenous Fgf10 or Fgf7 could restore proper branching [75]. This FGF secretion from the mesenchyme is thought to be stimulating localized cell proliferation at the end buds.

Signaling from the parasympathetic ganglion (PSG) has also been shown to be vital for several functions during organogenesis. The PSG condenses around the

gland soon after the initial bud is formed. It branches and grows alongside the gland, and is also known to be essential for gland regeneration. In ex vivo studies, removal of the PSG around the time of branching morphogenesis stunts growth and reduces the number of branches. Removal does not affect the expression of genes involved in FGF signaling, indicating that the PSG contributes to growth via a completely separate mechanism from the mesenchyme. The PSG was found to contribute to growth via maintaining an adequate progenitor cell population through EGFR (epidermal growth factor receptor) signaling [76]. The PSG has also been found to control ductal cell polarization and lumen formation through secreting vasoactive intestinal protein (VIP) [77].

1.4.2 Acinar Cell Differentiation

Acinar cell terminal differentiation largely occurs during postnatal development. From observational studies in the rat parotid, terminal clusters in the late embryo do not appear to have a lumen, cells contain only a few sporadically located electron dense granules, and the endoplasmic reticulum and Golgi are relatively small. Within the first 24 hours of birth, amylase expression increases along with the number of secretory granules, and a lumen begins to form. Over the next few weeks the exocrine cells become polarized with apically located secretory granules (which progressively increases in size and number), and basally localized nucleus. There is an expansion of the rough ER and Golgi. The expression of cargo proteins such as amylase and RNaseI progressively increases, while the protein DNase I is not detected until the second postnatal

week. The cells are considered fully differentiated around postnatal day 25 (P25) [78, 79].

Unlike the case of branching morphogenesis where many signaling pathways have been identified, not much is known about what drives terminal differentiation. Several studies points to the fact that differentiation is at least partially independent from morphogenesis, and most likely involves a separate set of pathways [6]. For instance, the heterotypic recombination of epithelial cells and mesenchyme that altered gland morphogenesis does not appear to change the cytodifferentiation of the terminal bud cells. Lawson *et. al.* [80] found that when a parotid rudiment is cultured with submandibular mesenchyme the gland structurally resembles the SMG which is denser and tightly packed. However, the acinar cells still develop amylase expression, which is a property of parotid epithelium, not SMG. The reverse observations can be seen when SMG epithelium is cultured with parotid mesenchyme [80]. In another study using the SMG, embryonic epithelia (16 days) was separated from the mesenchyme and grown in culture. Despite the fact that morphogenesis had been disrupted, the cells were able to differentiate and form into distinct ductal and acinar cell lineages. The authors do point out that if the mesenchyme was separated before branching occurred, then cytodifferentiation does not take place, indicating these two process are coupled very early in development but eventually become independent [81]. This also points to the fact that cytodifferentiation may be less dependent on signaling molecules from other tissues, and is instead intrinsic to the epithelial cells themselves, especially in the later stages of development.

Understanding the regulatory networks inside these cells that drives this process will aid in our understanding of differentiation, and is the primary goal of this dissertation.

1.5 Systems Biology and Salivary Gland Development

Organogenesis is a complex process involving many different pathways which are spatially and temporally regulated. These pathways affect many different cellular functions such as proliferation, migration, apoptosis, and lineage specific gene expression to drive the overall patterning of the organ and the differentiation of individual cell types. Many of these pathways are interconnected or occurring in parallel. The goal of systems biology is to build as inclusive a model as possible of all the factors that drive a particular function. These models can then be used as hypothesis driving tools to further test and understand the system.

Cleft formation is an important part of branching morphogenesis, which occurs alongside proliferation and migration to form the overall shape of the organ, and recently systems level modeling has been used to identify controlling factors. Indentations, known as clefts, form spontaneously at the leading edge of the end buds. Once an initial cleft is stabilized it will deepen, and eventually drive the end bud apart into two branches. This occurs many times as the epithelium grows and is important for forming a multibranched structure. This process is thought to involve many functions including cytoskeleton arrangement, cell-cell attachment, and cell-matrix attachment [82]. Recently a mathematical model has been

developed to understand the contribution of these functions to the clefting process [60].

An important part of systems level analysis is expression profiling, where the expression of many molecules are measured under the condition of interest, which can then be used as a starting point to build a model. Several expression profiling experiments in the salivary gland have already increased our knowledge of development. In Ectodysplasin A null Eda $^{-/-}$ mice, for instance, salivary development is delayed, and the profiling of gene expression over the course of branching morphogenesis in the knockout versus wild type indicated a novel signaling pathway, possibly involving C/EPBα, which was counter to ex vivo observations in which Eda was predicted to work by activating the NFκB pathway [83]. This also highlights the importance of measuring changes within the organ *in vivo* rather than under artificial conditions. There has also been an effort to catalogue ex vivo gene expression at several micro anatomic regions of interest in the branching epithelium (i.e. main duct, secondary duct, basement of cleft, end bud), and these expression data have been made available to the field as a searchable gene expression atlas [84]. Using laser capture, these specific regions could be isolated and RNA expression compared between them in order to identify molecules involved in different spatially regulated processes. By comparing expression at the base of the cleft versus the end bud periphery, for instance, the authors identified hundreds of differentially expressed genes, including GSK3β which was expressed much lower in the clefts. This protein is involved in E-cadherin stability. Pharmacological inhibition of GSK3β lead to an

increase in cleft formation which did not progress to secondary ducts [85]. This example highlights how systems level analysis can be used to identify novel interacting molecules and form new hypothesis which can then be interrogated with more traditional approaches.

While many studies have focused on morphogenesis, relatively little attention has been paid to cellular differentiation. Differentiation can be thought of as enduring changes in gene expression which are vital for the unique function of each individual cell type. For instance, salivary acinar cells acquire the expression of a multitude of cargo proteins as well as the cellular machinery necessary for the trafficking, and maturation of exocrine vesicles, and secretion in response to stimulation. The regulatory networks that drive expression of these genes is practically unknown. In order to identify multiple important genes, a systems biology approach could be taken, where expression is profiled across differentiation in order to identify differentially expressed genes in fully developed cells versus the immature cells in the embryo.

Currently, most profiling studies involve measurements of tens of thousands of genes which is far more than current statistical and mathematical modeling approaches can handle as far an integrating all of these components into networks that can describe the whole system. Additional strategies need to be developed that can build hypothesis driving networks or narrow down gene lists to focus modeling on only important subsets.

One way to statistically identify pathways that are involved in biological functions, based on large numbers of measurements, is to use a gene ontology enrichment

analysis [86, 87]. This is a bioinformatics approach which tests for over or underrepresentation of gene ontology (GO) terms in a set of expressed genes. The percentage of genes in each GO terms is compared to a background set (such as the whole genome), which is assumed not to have any bias.

Currently there are several knowledge-based algorithms that predict interactions between genes or gene products based on curated databases developed from literature searches. These programs can be used to filter for many different types of interaction (i.e. enzymatic, protein binding, and transcriptional regulatory). If, for instance, a profiling experiment measures RNA expression changes across several conditions, then filtering for transcription regulatory interactions will probably be the most relevant to that dataset. The direction of the interaction as well as whether it is activating or inhibiting is also predicted.

In these programs, gene lists of interest (i.e. differentially expressed genes) are uploaded and used as "seed nodes." These are the nodes from which networks can be built by adding "edges" between then, signifying an interaction. Several algorithms are available to generate networks from these nodes. For instance, Metacore's "Expand by One Interaction" builds a one-step network around a selected seed node by adding all direct upstream and downstream effectors. Filters can be used to only add genes based on certain criteria (i.e. interaction type, and membership in a gene list of interest). In this way networks can be built one interaction at a time from a list of differentially expressed genes [88].

1.6 MicroRNAs and Cell Differentiation

1.6.1 MicroRNAs

MicroRNAs (aka microRNAs) are small (22-23 nt) endogenous noncoding RNAs which are important regulatory molecules in the cell. They work in the cytoplasm to post-transcriptionally repress gene expression. They act by "targeting" mRNAs through partial base complementarity, usually in the 3'UTR but target sites have also been found in the coding region and 5'UTR. Once targeted, an mRNA is directed to translational inhibition and increased degradation due to message instability. This leads to a decrease in protein expression. Analysis of the human genome has found that most mRNAs contain conserved microRNA target sites. A mRNA may be targeted by many microRNAs and a single microRNA member can have many potential targets, indicating that microRNA based silencing is a common mechanism that participates in numerous functions [89, 90].

MicroRNAs were first identified a little more than 20 years ago in C. elegans, and have since been found throughout the animal kingdom. Several thousand have been identified so far in humans, with most having homologous sequences in mice and rats.

Processing of mature microRNAs is a multistep process that begins with the transcription of an initial long RNA, known as pre-microRNA [91]. This pre-microRNA is transcribed by RNA polymerase II [92] from its own gene. There are also clusters of microRNAs in the genome which are expressed as a single polycistronic transcript. The pre-RNA is then cleaved in the nucleus by the RNaseIII enzyme DROSHA to become ~70bp transcripts called pri-microRNAs, which contain a stem-loop structure. There are also microRNAs which are

processed from the introns of host mRNAs. These RNAs (known as "mirtrons") generally bypass DROSHA processing [93]. Pri-microRNAs are then exported to the cytoplasm via the nucleoprotein exportin-5 [94]. The cytoplasmic pri-microRNA is then process into a mature single stranded microRNA by another RNaseIII enzyme, DICER. The mature microRNA is then loaded into the RNA-induced silencing complex (RISC), a riboprotein complex which can then target mRNAs for silencing.

Interestingly, recent attention is being paid to microRNAs outside the cell. These small RNAs have been found in plasma, milk, and saliva, specifically they are mainly found in exosomes which are nano-sized membrane bound vesicles secreted by many different cell types into the extracellular matrix [95, 96]. These microRNAs have been found to be transferred between cells, and could be serving as some form of cellular communication, and clinically they could be used as biomarkers [97, 98].

The exact mechanism(s) by which microRNAs exert their repressive functions *in vivo* are still being worked out. Uncertainty in this area stems from the fact that the RISC can both repress translation and facilitate mRNA instability. Some of the earliest studies highlighted the role of microRNAs as translational repressors. In fact the first microRNA discovered, lin-4, seems to work exclusively under this model by repressing lin-14 protein expression without any appreciable change in mRNA [99]. However, this has come to be viewed as the exception rather than the rule as many subsequent studies identified a role for microRNAs in mRNA

degradation, and large scale studies have found that degradation explains most of microRNA repression.

In a recent model proposed by Elchhorn *et. al.* [100], translational inhibition and degradation occur sequentially with inhibition occurring first followed by degradation due to deadenylation. At steady state conditions degradation predominates, and inhibition only plays a significant role in cells where transcripts with short poly-A tails are stabilized.

These observations have biological as well as experimental implications. Degradation means that microRNAs induce permanent changes of gene expression that cannot be reversed. This also means that measuring changes in mRNA expression will capture most of the effect of a microRNA, and large scale techniques such as microarrays and RNAseq can be used in identify microRNA targets based on their changing expression.

Soon after microRNAs were identified, much work was done to characterize and predict their target sites, as this is the first step in identifying their biological function. Unlike plant microRNAs, animal microRNAs only share partial complementarity with their target making identification difficult. Extensive mutation studies were carried out on known microRNA:mRNA target pairs in order to identify necessary features. The essential element for microRNA targeting is the "seed" sequence located at the 5' end of the microRNA. It is comprised of either 6, 7, or 8 nt that are complementary to the target, although sometimes 3' pairing (particularly nucleotides 13-16) [101] can be used to compensate for a weak seed sequence [102]. Beyond sequence

complementarity there are several other factors that influence targeting efficiency. Local AU composition was found to be higher immediately downstream of the mRNA target sites [101]. Microarray analysis showed that GC rich regions were less likely to be true targets despite seed region pairing. Also, although target sequences have been found in many transcript regions, true target sites are most likely in the 3'UTR. This is thought to be due to the fact that the ribosome can displace the RISC as it translates the protein, rendering it ineffective.

Using these rules, many algorithms have been developed to identify putative target sites in available genomes and refseq transcripts [103]. Along with sequence pairing, and AU content, many of these programs also take into account conservation of predicted targets across species as an indication of function. Despite the fact that these programs are developed around a similar set of principles, many of their predictions do not overlap, conclusive measurements of their sensitivity and specificity have not been made, and there is currently no gold standard prediction program [104, 105]. Because of this, data driven evidence is essential to supplement predictions in order to identify true target sites.

1.6.2 MicroRNA Functions in Development and Differentiation

Many studies have pointed to the role of microRNAs in cell fate decisions. Knockout mouse models have produced defects in both maintenance of stem cell identity, and in the progression of pluripotent cells into a differentiated phenotype [106]. For instance, global microRNA knockouts in mouse ES cells have defects

in differentiation (when either Dicer or the RNA binding protein DGCR8 is removed in ES cells, mature microRNAs can no longer be expressed). While this technique is not specific, it has proven useful in studying microRNA function. Unfortunately, knocking out single microRNAs often shows no phenotype. This is thought to be due to target overlap in many microRNA families (microRNAs which share the same seed sequence), and the fact that most mRNAs are thought to be targeted by many microRNAs. This redundancy often makes single knockouts uninformative.

In the microRNA knockouts, ES cells no longer express lineage specific markers under differentiation conditions, and they are not able to down-regulate pluripotency factors such as Klf4, and Oct4. Interestingly, in one study, chimeric mice could not be generated by injecting dicer null ES cells into wild type blastocysts indicating a deficiency in differentiation [106].

Tissue specific Dicer knockouts have also been developed, and have identified roles for microRNAs in the differentiation of many cell types including muscle cells, neurons, pancreatic islet cells, osteoblasts, oligodendrocytes, and many others [107]. Subsequent studies, following up on these observations have been able to identify functions of specific microRNAs in differentiation. Studies in muscle, for instance, have revealed an extensive regulatory network composed of both microRNAs and transcription factors that control several functions in differentiating myoblasts, from proliferation to cell fate [108-110].

In the salivary glands, relatively little is known about the contribution of microRNAs to development or differentiation. Several profiling experiments have

been performed on both epithelial and mesenchymal cells during branching morphogenesis [111, 112] but no such studies have been done focusing on acinar cell differentiation. Of the profiling experiments that have been done, many expression changes have been measured, but functions have only been described for a few microRNAs.

In the early branching epithelium of the SMG, a panel of microRNAs were measured in the end buds and primary duct. Expression was compared between the two regions under the hypothesis that microRNAs could be important for spatially controlled gene expression. By using antagomiRs in ex vivo cultures they were able to identify functions for several microRNAs. Knockdown of either mir-200c or miR-34a, which are both highly expressed in the end buds, increased the number of end buds, while knockdown of miR-204 or miR-135, both highly expressed in the main duct, decreased branching.

1.7 Specific Aims

Understanding the process of acinar cell terminal differentiation *in vivo* is vital to better control cell differentiation *in vitro* for the purpose of tissue regeneration and artificial gland construction. In the parotid gland of the rat acinar cells are a single type (serous). This pure cell population could be used as a model of differentiation *in vivo*. In rats, terminal differentiation occurs largely postnatal. The acinar cells morphological changes such as expanded Golgi complex and rough ER, and the accumulation of secretory granules in the apical cytoplasm. The mechanisms that drive these changes remain largely unstudied in the salivary glands, and transcription factors required to activate expression of parotid

specific terminal differentiation markers is unknown. Currently, the ability to generate gland tissue for patients suffering from hyposalivation is not available. Loss of acinar cells is a major factor for these patients and the ability to differentiate acinar cells in culture could be used to grow transplantable tissue for patients.

To address this gap in knowledge, I will use a Systems Biology approach to model gene regulatory networks driving differentiation. I will profile mRNA and microRNA expression across parotid acinar cell terminal differentiation and use network analysis to identify putative transcription regulatory and microRNA:mRNA interactions. Thus I will be able to derive a network driving expression of terminal differentiation markers. The regulatory transcription factors and microRNAs in the network could then be investigated *in vitro* for their ability to control differentiation.

Aim 1 will profile the expression of mRNAs and microRNAs across acinar cell terminal differentiation. Many profiling experiments in the salivary glands have focused on branching morphogenesis, which begins relatively early in development, and does not have much overlap with differentiation, particularly of acinar cells. In the parotid, acinar cell differentiation occurs mostly postnatal, and there is a dearth of knowledge about the gene expression changes that take place during this time period. In this study, both mRNA and microRNA expression was measured at multiple time points spanning terminal differentiation. By using laser capture, measurements were restricted to the

acinar cell lineage. By comparing expression between different stages, molecules that are important for driving differentiation can be identified.

Aim 2 will predict a gene regulatory network driving acinar cell differentiation. Profiling experiments are likely to produce thousands of differentially expressed gene. In this aim, several strategies were employed to identify likely functions, predict interactions, and incorporate genes into regulatory networks. Clustering and regression analysis was used to identify prevailing patterns of gene expression, followed by enrichment analysis to identify contributing biological processes. Interactions between genes of interest and subsequently a gene regulatory network was predicted using the knowledge-based program Metacore, sequence-based predictions, and our own expression measurements.

Aim 3 will validate successive edges of the regulatory network, and investigate the ability of network transcription factors to drive differentiation *in* vitro. One of the main goals of using systems biology to study the salivary glands is to be able to use the knowledge gained to control aspects of development, and to aid in potential clinical solutions such as regeneration or artificial gland construction. In this last section we address the hypothesis that interactions from the proposed regulatory network can be used to drive expression of terminal differentiation genes in de-differentiated cells. We will also use these cells to validate multiple steps in our network.

In this study we were able to identify thousands of differentially expressed mRNAs during differentiation, and dozens of regulated microRNAs many of which have not been studied in acinar cell differentiation. Using these

measurements we developed a gene expression network model incorporating both transcription factors and microRNAs driving expression of terminal differentiation markers, genes that would need to be expressed in regenerated or regrown acinar cells [113, 114]. We validated several of these network interactions in ParC5 cells, a model of dedifferentiated parotid acinar cells.

CHAPTER 2: MATERIALS AND METHODS

2.1 Animals/Tissue Dissection

Parotid tissue was obtained from Sprague Dawley rats (Harlan laboratories) at 9 time points spanning development of the parotid gland, including embryonic day 18 (E18), E20, postnatal day 0 (P0; which is E22), P2, P5, P9, P15, P20, and P25.

Ethics Statement: This study was carried out in strict accordance with the recommendations in the Guide for the Care and Use of Laboratory Animals of the National Institutes of Health. The protocol was approved by the Institutional Animal Care and Use Committee of the University of Louisville (Protocol Number: 11059).

Timed pregnant females were used for the embryonic and early postnatal time points. Birth (P0) in this strain is typically on E22. All animals were euthanized by carbon dioxide inhalation and decapitation of embryos following IACUC-approved procedures. For animals older than P5 the parotid gland was removed, embedded in Tissue-Tek CRYO-OCT Compound (Fisher Scientific) and immediately frozen with a mixture of dry ice and 100% 2-methylbutane. For the embryonic and earlier postnatal time points, heads were divided along the

sagittal plane, and each half was embedded upright. All tissue blocks were stored at -80°C.

2.2 Laser Capture Microdissection

For cryosectioning, blocks were thawed to -30°C. Sections (7 μm) were taken with a Leica cryostat onto clean chilled slides that had been treated with RNaseZap (Ambion), and immediately fixed in 70% ethanol. Xylenes and 100% ethanol were used to remove OCT before staining. For the embryos, tissue was sectioned and stained with hematoxylin and eosin (H&E) until the parotid gland was located. All tissue sections were lightly stained with H&E to identify acinar cells based on the structure of the cells and local vascular landmarks, as validated by immunofluorescence staining of previous samples using anti-parotid secretory protein antibody. Stained sections were dehydrated by washing in 100% ethanol and xylenes before being used for microdissection.

Laser capture microdissection (LCM) was performed on an Arcturus PixCell *IIe LCM* System (Life Technologies/ Thermofisher Scientific) [115, 116]. Caps containing CapSure transfer film carrier were applied to the tissue and cells were adhered to the cap using laser pulses. The cap was then visually inspected under the microscope to ensure that contaminating cells were removed. Only caps that did not contain any detected extraneous tissue, were used in subsequent experiments. Because extracting intact RNA is difficult in RNaseI rich tissues, the aqueous staining steps were kept short (15 – 30 seconds), and no

more than 150 laser pulses were used when capturing tissue in the older animals when RNaseI expression is high.

2.3 RNA Isolation, microarrays, and qPCR arrays

RNA was isolated from the LCM caps using the RNaqueous micro kit (Ambion), per the manufacturer's instructions. Briefly, once cells were isolated onto an LCM cap, lysis buffer was applied immediately. Tubes were then incubated in a heat block at 42°C for 30 min. The lysates were either processed immediately or stored at -80°C. Lysates from multiple caps of the same sample, taken on the same day were combined before proceeding with isolation. At least three independent biological samples (from separate litters) were used for isolation of total RNA at each of the 9 time points. Quantity and quality of the total RNA was assessed using a 2100 Bioanalyzer (Agilent). Samples with a RIN value of at least 7 were used.

For analysis of mRNA expression, the Whole Transcriptome-Ovation Pico RNA amplification system (NuGen Technologies Inc.) was used to prepare amplified cDNA from total RNA for 9 time points of the developing parotid acinar cells. The biotin-cDNA was hybridized to 27 separate rat genome 230 2.0 Affymetrix GeneChips, having 31,099 probe sets.

MicroRNA expression was measured by qRT-PCR at four time points during acinar differentiation: E20, P5, P15, and P25. A total of 372 primer pairs (miRCURY LNA, Exiqon) were used which amplify well annotated rodent microRNA sequences. Triplicate samples were run for each time point. Total

RNA (1 ng) was used to synthesize cDNA (Exiqon's Universal cDNA Synthesis Kit). The cDNA was then applied to microRNA Ready-to-Use PCR, Mouse&Rat panel I, V1.M (Exiqon) per the manufacturer's instructions. Briefly, each 20 µl cDNA reaction was diluted 110x in nuclease free water and then combined 1:1 with 2x SYBR green master mix. The reactions were run on an ABI 7500 RT-PCR system.

2.4 Statistical Analysis of Array Data

2.4.1 Normalization and Filtering

The processing and analysis of the data was carried out in R, and the code used can be found in the supplementary material in Metzler *et. al.* [114].
mRNA: The data were normalized using the *rma* function in the Bioconductor package *affy* [117], with the default settings. Quality was also checked using PCA analysis (Partek). Probes were then filtered according to the following criteria: 1) required mapping to an Entrez Gene ID, 2) removal of duplicate probes which map to the same Entrez Gene ID. To focus on genes involved in the process of differentiation, probes with variability below the 50^{th} percentile across all samples (as measured by the interquartile range) were removed. Data filtering was done using the *nsFilter* function in the Bioconductor package *genefilter* [118].

microRNA: microRNAs were removed that had >50% missing data (i.e. expression was not detected in seven or more samples, which excluded 100 microRNAs), missing values from remaining probes were imputed using R

function *imputeKNN* in Bioconductor package *MmPalateMicroRNA* [119](14.5% of values were imputed) [120]. A median sweep was performed to normalize delta Ct values by subtracting the global median for each array.

2.4.2. Hierarchical Clustering

microRNA: Differentially expressed microRNAs were clustered using the *hclust* function (hierarchical clustering) in the *stats* package in R. Distance *d* was calculated based on the correlation coefficient *r,* with $d = 1-r$. A heatmap was generated from the microRNA clusters using the *heatmap_2* function in the Bioconductor package *Heatplus*

2.4.3 Differential Expression

mRNA: Normalized $\log_2$ values were used for analysis. One-way ANOVA was used to identify differential expression of mRNA, with a false discovery rate (FDR) correction to account for multiple tests [121]. A p-value < 0.05 was considered significant. Comparisons were also made between adjacent time points by empirical Bayes t-tests using the Bioconductor package *limma* [122].

microRNA: Normalized -ΔCT values were used for analysis of microRNA results. Differential expression was analyzed by one-way ANOVA and also by FDR corrected empirical Bayes t-tests comparing pairs of time points.

2.4.4 Expression Patterns and Regression Analysis

Having several time points of measurements allows the identification of dynamic and complex patterns of mRNA and microRNA expression over time. We

extended this by the independent approach of k-means clustering of the per-gene scaled expression data (function *kmeans* in R package *stats*). In addition, regression analysis was used to identify genes that significantly fit into either linear, quadratic, or cubic trends. The trends were then grouped into clusters.

2.5 Network Analysis

All differentially expressed mRNAs were uploaded into Metacore (Thomson Reuters Inc., Carlsbad, CA). Markers of terminal differentiation with increasing expression (i.e. PSP, amylase) were used as initial nodes. The neighborhood around each of these nodes was explored using the *expand* function to identify possible regulating factors. DE genes in the neighborhood were kept for another round of expanding only if their expression pattern over time was consistent with the reported interaction (i.e., activating vs. repressing) and the pattern of the target gene. The *expand* function was used iteratively until no further DE genes were identified. microRNAs predicted to target any nodes were incorporated into the network when their expression patterns had an inverse correlation with the pattern of the target mRNA.

2.6 Cell Culture: Treatments and Transfections

ParC5 and the closely related ParC10 cells are derived from rat parotid acinar cells, and were obtained as a generous gift from Dr. Quissell's laboratory. These cells were maintained at 37°C and 5% CO2 in media as described by [63], and split regularly using 0.25% trypsin EDTA.

2.6.1 Luciferase Assays

Promoter activation: Standard methods were used to clone the target gene promoters upstream of luciferase in pGL4.10 vector. Expression plasmids for selected transcription factors were from OpenBiosystems (Huntsville, AL) or Thermoscientific (Waltham, MA) or were cloned by RT-PCR of rat genomic DNA into pCDNA4. Luciferase reporter plasmids were transiently transfected (list of primers used for cloning can be found in the appendix). Lipofectamine (Invitrogen) was used for luciferase promoter studies. From previous optimization performed in the lab pertaining to ParC5 cells, a Lipofectamine to DNA ratio of 8ul/1ug DNA was used. Cells were plated in 6-well plates at 100,000 cells per well and grown overnight before transfection. Cells were transfected with 2ug/DNA per well. 1ug of luciferase reporter was used, and 50ng of the renilla luciferase (Rluc) expression vector PGL4.73. Several concentrations of expression vector containing the transcription factor of interest were used, and any difference in DNA amount was made up with the vector Bluescript II. The *Mist1* transcription factor expression clone was in pcDNA4 vector, and the spliced *Xbp1* (*Xbp1*-S) expression vector was pFLAG.*Xbp1*p.CMV2 (Addgene; Cambridge, MA). In all experiments, pGL4.73-Renilla luciferase plasmid was co-transfected as an internal control for normalizing transfection efficiency. 48 hours after transfection, cell extracts were prepared using Passive lysis buffer (Promega) and assayed for both firefly and Renilla luciferase activities using the Luciferase Assay and Renilla Luciferase Assay Systems from Promega with a Berthold Lumat LB9501 luminometer. For each experiment, triplicate wells were used to measure normalized luciferase expression (the ratio luciferase/renilla aka

luc/ren) under an experimental condition (expression vector containing the transcription factor of interest), and a control condition (an empty vector). Each experiment was repeated at least three times. A student's t-test was used to test for differential expression between the experimental and control conditions after combing experiments (a p-value of < 0.05 was considered significant).Results are given as means ±SEM.

3'UTR assays: microRNA mimics (Dharmacon, Lafayette, CO) were transfected at 10 pmols/well along with 100 ng of a luciferase reporter (PGL4.25) which contained either a 3'UTR of interest downstream or no 3'UTR.DharmaFeCT Duo (Dharmacon, Lafayette, CO). ParC5 cells were plated in 24-well plates at 25,000 cells/well and were grown overnight before transfection. 3'UTRs were cloned down-stream of firefly luciferase cDNA in PGL4.25 using XbaI and FseI. Primers used to clone 3'UTRs from rat DNA are listed in the appendix. Renilla luciferase plasmid (PGL4.73) (5ng/well) was used as a transfection efficiency control. *et. al.* For each experiment (in triplicate) luc/ren expression was measured under four conditions.

Condition	Treatments	notes
1	microRNA of interest + Pgl4.25-3'UTR	
2	microRNA of interest + PGL4.25-empty	Expression will reflect any effect of the

		microRNA on the empty vector
3	Control microRNA + PGL4.25-3'UTR	Expression will reflect the effect of microRNA transfection
4	Control microRNA + PGL4.25-empty	Expression will reflect any effect of the control microRNA on the empty vector

In order to control for a microRNA specific effect on the empty vector, the following ratios were used to normalize expression.

$$Luc_E = \frac{\left(\frac{luc}{ren}\right) condition1(microRNA\ of\ interest + PGL4.25\_3'UTR)}{\left(\frac{luc}{ren}\right) conditions2(microRNA\ of\ interest + PGL4.25empty)}$$

Where $Luc_E$is the normalized luciferase expression in the experimental condition (transfection of a microRNA mimic that is predicted to target the cloned 3'UTR).

$$Luc_C = \frac{\left(\frac{luc}{ren}\right) condition3(control\ microRNA + PGL4.25\_3'UTR)}{\left(\frac{luc}{ren}\right) conditions4(control\ microRNA + PGL4.25empty)}$$

Where Luc_C is the normalized luciferase expression in the control condition (transfection of a control microRNA that does not target the cloned 3'UTR).

This normalization results in measurements that are the ratio of a ratio. In order to test the null hypothesis that there is no difference between Luc_E and Luc_C, a t-statistic was calculated as in Jacobs et. al. [123].

$$t_{Luc_E,Luc_C} = \frac{\overline{Luc}_E - \overline{Luc}_C}{\sqrt{\frac{s^2_{Luc_E}}{n_{Luc_E}} + \frac{s^2_{Luc_C}}{n_{Luc_C}}}}$$

Where s^2 is the variance and n is the number of experiments. Experiments were repeated at least three times, and p-values were determined from a t-statistic table.

2.6.2 Tunicamycin Treatments and qPCR

Tunicamycin was kept in a stock concentration of 2mg/ml in DMSO. ParC5 cells were treated with either 1µg/ml tunicamycin or an equal concentration of DMSO for eight hours. Media was then removed and replaced, and the cells were allowed to recover overnight. For siRNA pretreatment, cells were transfected with a siRNA pool targeting Xbp1 (Dharmacon, L-085513-02-0005) or a pool of control (non-targeting) siRNAs 24 hours before tunicamycin treatment. siRNAs were transfected at 100nM/well using 8ul of Dharmafect duo per well.

RNA isolation was performed using Trizol. Concentration and quality were assessed by nanodrop. cDNA was synthesized using the High Capacity cDNA Synthesis Kit (ThermoFisher Scientific) per the manufacturer's instructions. qPCR was carried out using Taqman primer/probes (a list can be found in the appendix). RPLP2 was used as an endogenous control and relative expression

was analyzed using the 2^-ΔΔCT method [124]. Experiments were performed at least three times and a t-test was used to compare gene expression between the control condition (i.e. DMSO treatment, control siRNA) and the experimental (i.e. tunicamycin treatment, Xbp1 siRNA).

2.7 Appendix

Table 2.1: Cloning primers

Target Gene	Primers
Sox11 3'UTR	For: 5' cacctctagaATAGAGTTTGCATGCCAGCG 3' Rev: 5' acaaggccggccacaattcgaaCCTCTGTGAAAAACTCCTGC 3' For: 5' caccttcgaaGCATAGGCAAGGTATAGAGG 3' Rev: 5' caccggccggccGAGATCCGTCATGATACGAC 3'
Xbp1 3'UTR	For: 5' cacctctagaTCTTAGAGATCCCCTCTGAG 3' Rev: 5' caccggccggccGCCAGGCTGAACGATAACTG 3'
Klf4 3'UTR	For: 5' cacctctagaATTCCACATCGTGGACATGAC 3' Rev: 5' caccggccggccTGCTTAAAGGCATACTTGGG 3'

s-XBP1 cDNA	For: 5' CACCGCGGCCGCATGCTTGTGGTGGCAGCGG 3' Rev: 5' CACCGGGCCCGGCTCTTTAGACACTAATCAGCTGGG 3'
Mist1 Promoter -515 to +39	For: 5' GGTACCGCAGCCATGTGGTTGG 3' Rev: 5' CTCGAGCACGGGGGACAAGGACACG 3'
500bp PSP promoter -500 to + 21	For: 5' CACCGGTACCCATTATTGCCTCCTCCCAG 3' Rev : 5' GGTGCTCGAGGACAGGAAAGCCTTGTTTC 3'
1kb PSP promoter -1041 to +21	For: 5' CACCCCTTCTCTCGTCACTGAAATGTTTTC 3' Rev : 5' GGTGCTCGAGGACAGGAAAGCCTTGTTTC 3'
1.5kb PSP promoter	For: 5' CACCGGTACCGCTTGGCAGACATGAGATGGAAATCG 3' Rev : 5' GGTGCTCGAGGACAGGAAAGCCTTGTTTC 3'

Intron PSP	For: 5' CAACTTGTCGACCTTGTGGTCTTGTGTGGC 3' Rev: 5' CATTGGTCGACAGCCCAGCTTGAAGATCC 3'

Table 2.2: Taqman primers for qPCR

Gene	Taqman Primers
Xbp1	Rn01443523_m1
Mist1 (aka Bhkha15)	Rn00563466_m1
Rab3d	Rn00756153_m1
Rab26	Rn00592144_m1
PSP	Custom primers For: TTCCCTTCGTCAACCGTATTC Rev: CCCTGAATAGCACTTCCACTC Probe: AAACATCCTATGCCCAGTGCTCCA
Connexin 32	Rn01419045_m1
Tcf3	Rn01452748_m1
Rplp2	Rn01479927_g1

CHAPTER 3: MRNA AND MICRORNA EXPRESSION CHANGES DURING PAROTID ACINAR CELL DIFFERENTIATION

3.1 Introduction

During the postnatal period of salivary gland development, the acinar cell population expands and these cells mature to the fully differentiated phenotype. Drastic changes in cell morphology as well as gene expression occur. It is during this period that acinar cells gain expression of lineage specific genes such as salivary amylase (Amy1a) and the parotid secretory protein (PSP), which are recognized as terminal differentiation markers of parotid acinar cells. The activation of these genes is necessary for the cells to become fully differentiated, however, there is little knowledge about what is driving acinar-specific gene expression. Changing expression has only been studied for a handful of genes during differentiation, and very few studies have measured regulatory molecules such as transcription factors. No large scale profiling experiments have been reported during the last stages of salivary gland development, when terminal differentiation is occurring.

By measuring global mRNA and microRNA expression at multiple time-points during acinar cell differentiation, a whole host of differentially expressed genes can be identified including those involved in the regulation of gene expression.

This study also makes use of laser-capture microdissection (LCM) to specifically isolate acinar cells. Whole salivary glands are a mixture of many different cell types including both epithelial and mesenchymal. The mesenchyme cap that encloses the gland contains both neuronal and endothelial cells. Within the epithelium itself there are both ductal and acinar cells, as well as some myoepithelial cells. By combining histological stains with LCM, acinar cells can be differentiated and isolated away from the ductal cells. Acinar and immature pro-acinar cells can be isolated in this way from many different time points during differentiation. For the measuring of mRNA, cells were isolated from nine time points in triplicate. Two embryonic time points (E18 and E20). Based on morphological studies these represent very immature cells. They have very few electron dense granules (and many cells have none), no lumen, no cellular polarity, and the expression of many cargo protein is undetectable. Six postnatal time points were also measured (P0, P2, P5, P9, P15, P20, and P25).

Analysis of this data revealed thousands of differentially expressed genes, and complex patterns of expression. Enrichment analysis of gene clusters points to the role of ER signaling and the adaptive unfolded protein response in the expression of lineage specific genes. We also identify a novel role for the transcription factor PPARg, which is involved in the differentiation of other cell types but has not been studied in the salivary gland.

Dozens of differentially expressed microRNAs were also identified. By integrating these two data sets, microRNA:mRNA interactions were identified which could be important for driving differentiation.

3.2 Results

3.2.1 mRNA Expression

Using laser-capture microdissection, acinar cells could be isolated from glands at multiple ages without any detectable contamination from ductal cells (Figure 3.3). High quality RNA could be obtained from these cells, as measured by Bioanalyzer. This was especially important to determine as the mature gland expresses high levels of RNaseI which could easily lead to degraded samples not suitable for microarray. By reducing the time spend in the aqueous phase during staining, and using a limited number of laser pulses per slide, a RIN (RNA integrity number calculated by measuring the ratio of the 18S and 28S peaks) of at least 7 out of a possible 10 could be obtained (Figure 3.2). This is generally considered suitable for microarray analysis.

Once RNA was obtained and cDNA generated (see methods), expression was measured by hybridizing to the Affymetrix rat genome array 230, which contains > 30,000 probe clusters.

In order to detect a potential batch effect in the microarray measurements, principal component analysis (PCA) was used to identify the main source of variation, which should be the age group of the sample and not the batch in

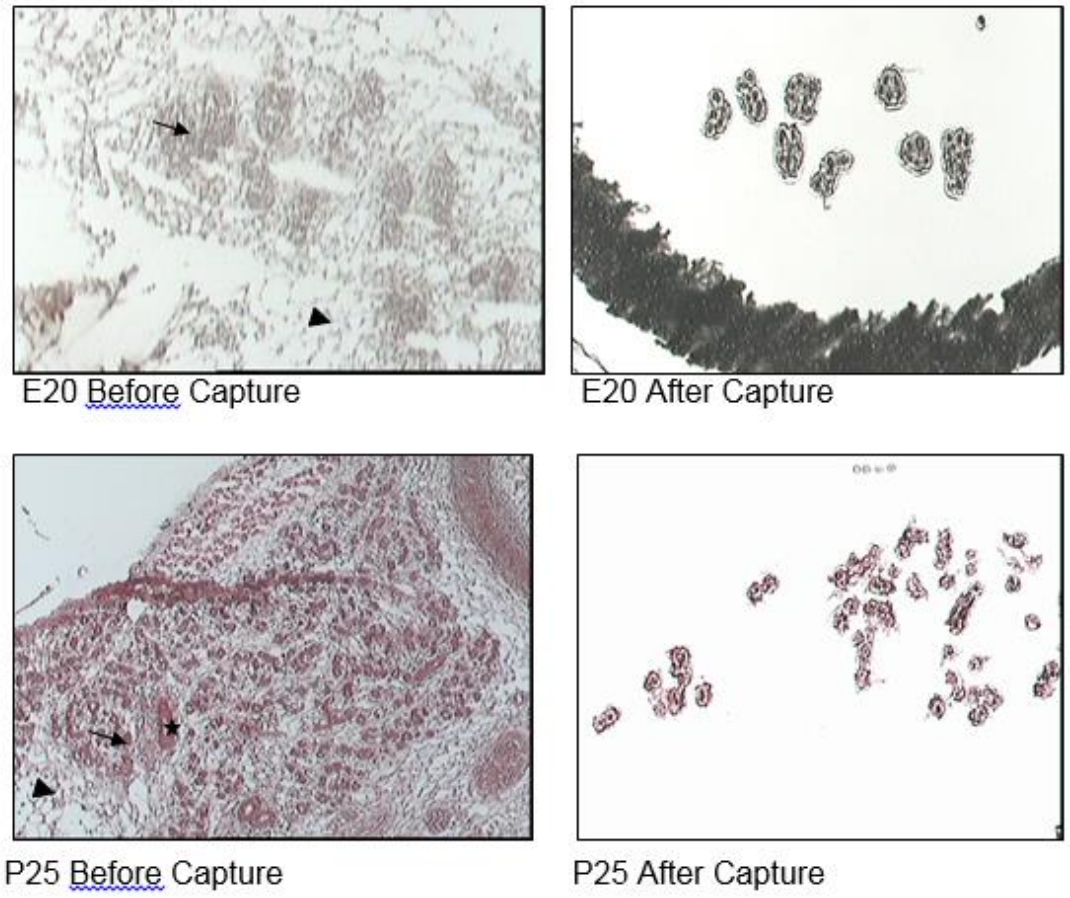

Figure 3.1 Isolation of Acinar Cells by Laser Capture Microdissection. A representative image is shown of a Parotid section from an embryonic day 20 (E20) sample, and a postnatal day 25 (P25) sample. Tissue was stained with H&E. Panels on the left show the section before capture which contains acinar cells (arrow) and surrounding cell types including ductal cells (star), and connective tissue (arrow head). On the right the film-covered caps are shown after the acinar cells have been captured and the sample is now devoid of surrounding tissue.

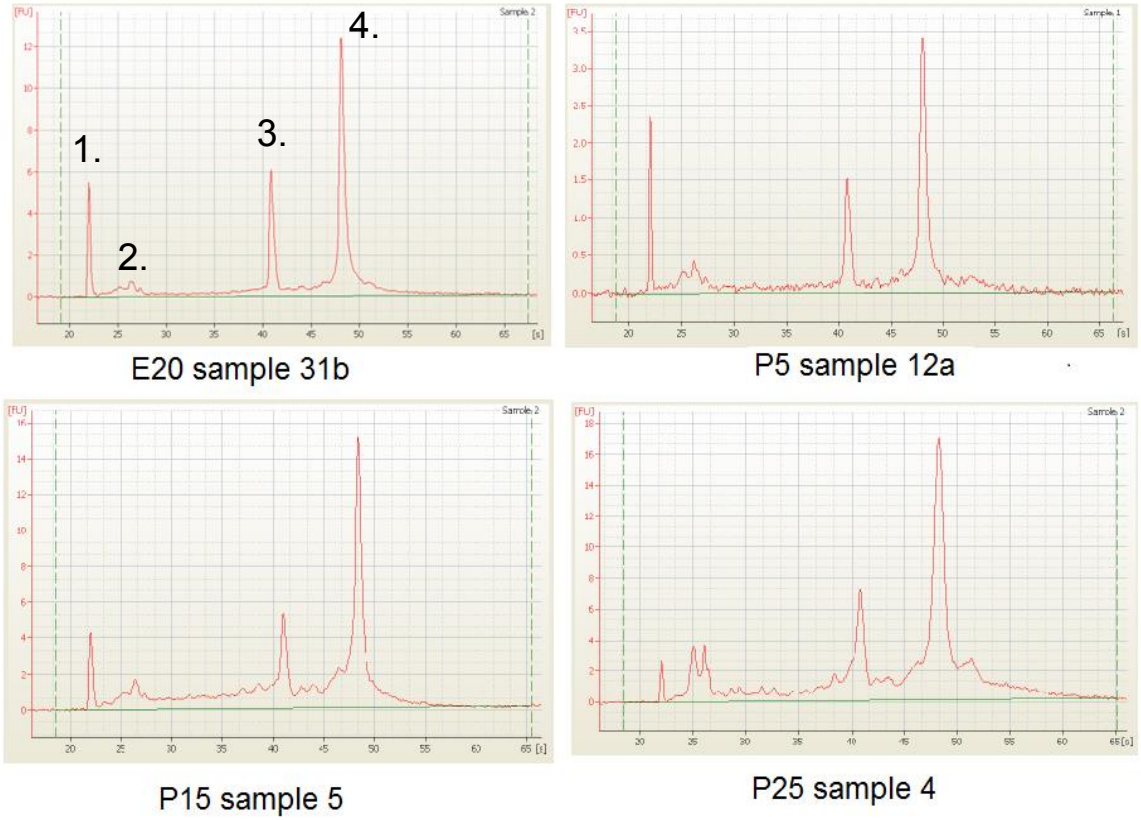

Figure 3.2 Quality RNA Could be obtained from Acinar Cells. Once acinar cells were isolated by LCM, RNA was extracted and quality was assessed by Bioanalyzer (Agilent). This figure shows representative traces for four of the time points isolated: embryonic day 20 (E20), postnatal day 5 (P5), postnatal day 15 (P15), and postnatal day 25 (P25). There are four main peaks on a trace, labeled from left to right on the top left panel. 1.) Control peak introduced in the dye mixture. 2.) 5S RNA and tRNA. 3.) 18S RNA. 4.) 28S RNA. The RNA Integrity Number (RIN) ranging from 1 to 10 is used to assess quality. The higher the number the less degradation is present. A RIN of 7 or more is considered adequate for microarray and qPCR measurements.

which it was run. The first three principal components for each sample were plotted on an x-y-z axis (Figure 3.3). The samples mostly cluster based on their age group, indicating that the batch had little effect on expression variation, and these measurements were carried forward for further analysis.

The measurements were normalized, filtered, and used for significance testing (see methods for the detailed procedure). An overview of the resulting analysis is shown in Table 3.1. 2565 differentially expressed genes were identified by an analysis of variance. In order to validate these expression changes, several of these genes were assayed by qPCR, considered the gold standard of microarray validation. The three gene (Xbp1, PSP, and Nupr1) were measured in all nine time points, and their expression pattern correlated with the microarray measurements (Figure 3.4).

While significance by ANOVA indicates regulated expression changes between some of the time points measured, it does not reveal the direction or the timing of such changes. To identify possible temporal specific patterns across all of the differentially expressed genes, hierarchical clustering was used to group the ages based on patterns of gene expression and the resulting heatmap can be seen in Figure 3.5.

From this analysis (Figure 3.5), four stages are evident during differentiation: An embryonic stage (E18, E20, and P0), early postnatal stage (P2, and P5), mid postnatal stage (P9 and P15), and a late stage (P20 and P25). Fewer gene expression changes occur between time points within a stage, but there are

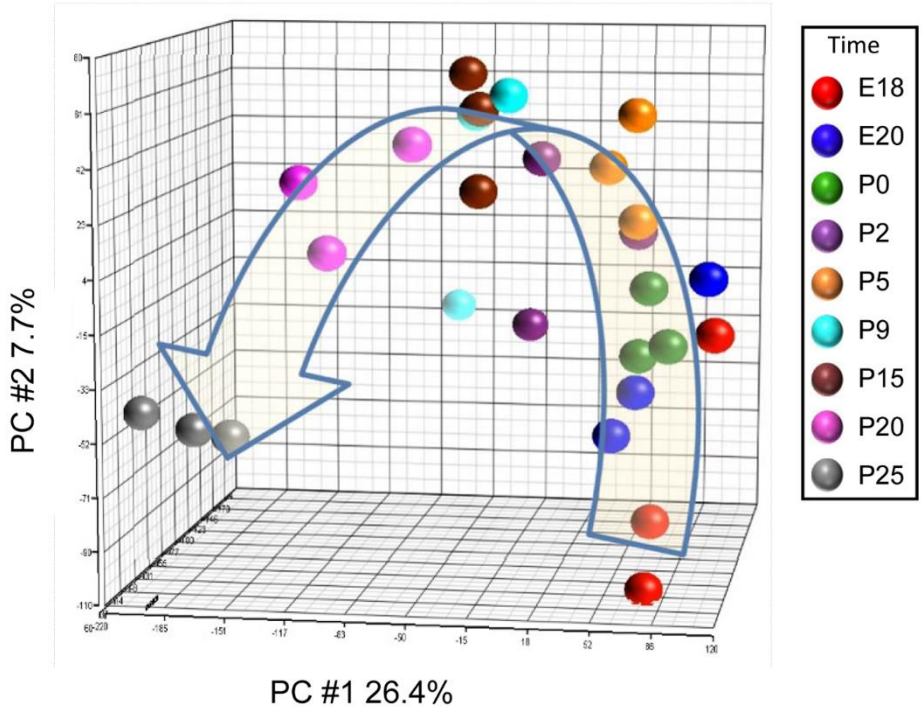

Figure 3.3 Principal Component Analysis (PCA) was used to identify potential batch effects in our microarray data. The first three principal components (PC) were plotted for each sample on an X-Y-Z axis and a view showing the first two PCs is shown in (A.). Points are color coordinated based on their age group. An arrow overlaying the points indicates the progression through time starting with the E18 samples (red) and ending with the P25 samples (gray). The samples largely cluster based on age as expected rather than batch.

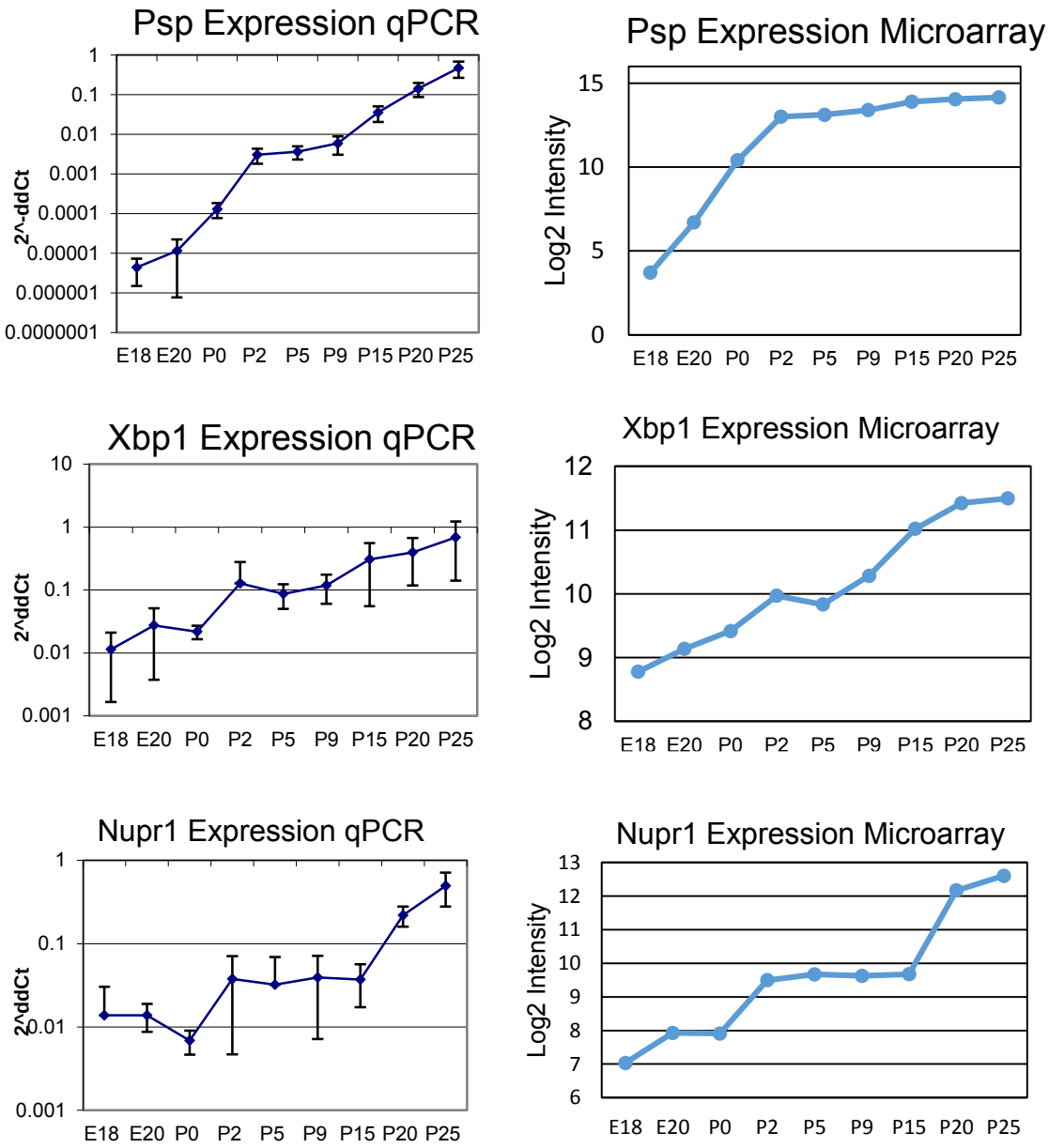

Figure 3.4 Microarray Validation by qPCR. Taqman qRT-PCR was run on triplicate RNA samples spanning nine time points of parotid acinar differentiation, using primers that amplify *Psp*, *Xbp1*, and *Nupr1*. Expression of *Rplp2* was used for normalization. The expression profiles (plotted in Log base 10) replicate the increase in expression seen in the microarrays

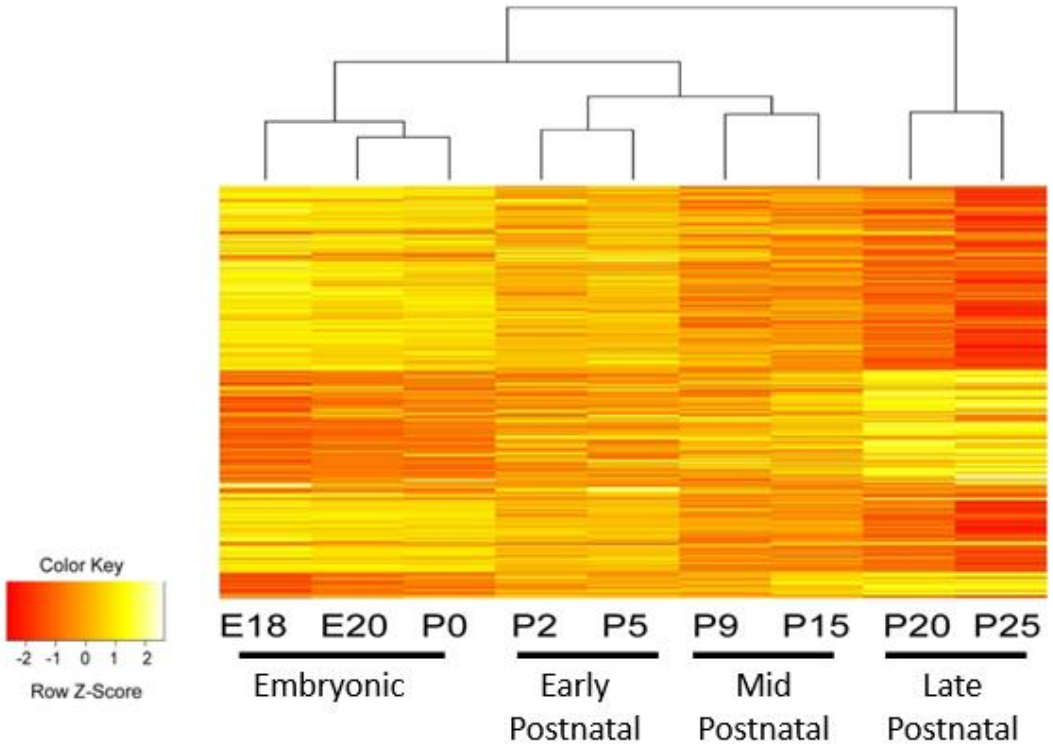

Figure 3.5 Heatmap of Differentially Expressed Genes Identifies Four Stages During Acinar Cell Differentiation. Hierarchical clustering was used to group ages based on the similarity of their gene expression profile for the 2556 differentially expressed genes identified by ANOVA (Table 3.1). Distance was calculated as dissimilarity (1-r) (r=correlation coefficient). A heatmap was then constructed from the resulting dendrogram by scaling gene expression across the time points measured, and coloring them based on their relative expression (red=low expression, and yellow=high expression). This resulted in the identification of four main stages where relative gene expression (represented by color) remains largely constant within a stage but changes dramatically between stages.

Comparison	Number of Differentially Expressed Genes
ANOVA (all nine time-points)	2656
E18 vs E20	2
E20 vs P0	3
P0 vs P2	57
P2 vs P5	0
P5 vs P9	2
P9 vs P15	13
P15 vs P20	48
P20 vs P25	93
Stage 1 vs Stage 2	604
Stage 2 vs Stage 3	124
Stage 3 vs Stage 4	992

Table 3.1: **Differentially Expressed Genes during Acinar Cell Terminal Differentiation.** The number of differentially expressed genes was determined between adjacent time-points and between all combinations of comparisons by ANOVA. We also determined the number of differentially expressed genes between stages as identified in Figure 3.5. Stage 1: E18, E20, and P0; Stage 2: P2, and P5; Stage 3: P9, and P15; and Stage 4: P20, and P25.

many expression changes between stages. This is also evident from the pairwise comparisons between adjacent time points (Table 3.1). A t-test was used to identify both up and down-regulated genes. Only three genes are differentially expressed within the embryonic stage (E18vsE20 and E20vsP0), while in the period immediately after birth (P0vsP2) many genes are up-regulated. There are also many differentially regulated genes between later time points.

We next wanted to be able to identify possible biological processes and pathways that contribute to gene regulation. For large unbiased datasets a common method is to use Gene Ontology enrichment analysis. This will identify over represented processes that are specific to the biological system under study. In order to focus the identification of processes on specific expression patterns the differentially expressed genes (Figure 3.5) were clustered based on their pattern across differentiation. This would also presumably make the analysis more robust, as an unclustered dataset would contain a mixture of expression patterns and their corresponding pathways, and ultimately the underlying assumption of this approach is that there is a common pathway regulating genes with similar expression profiles and term enrichment allows us to make predictions about what those pathways are. The analysis resulted in the identification of eight clusters (Figure 3.6).

The majority of genes are found in the first two clusters which are linear-like patterns either continually decreasing (cluster #1, 1635 genes) or continually increasing (cluster #2, 803 genes). Several clusters only contain a few members

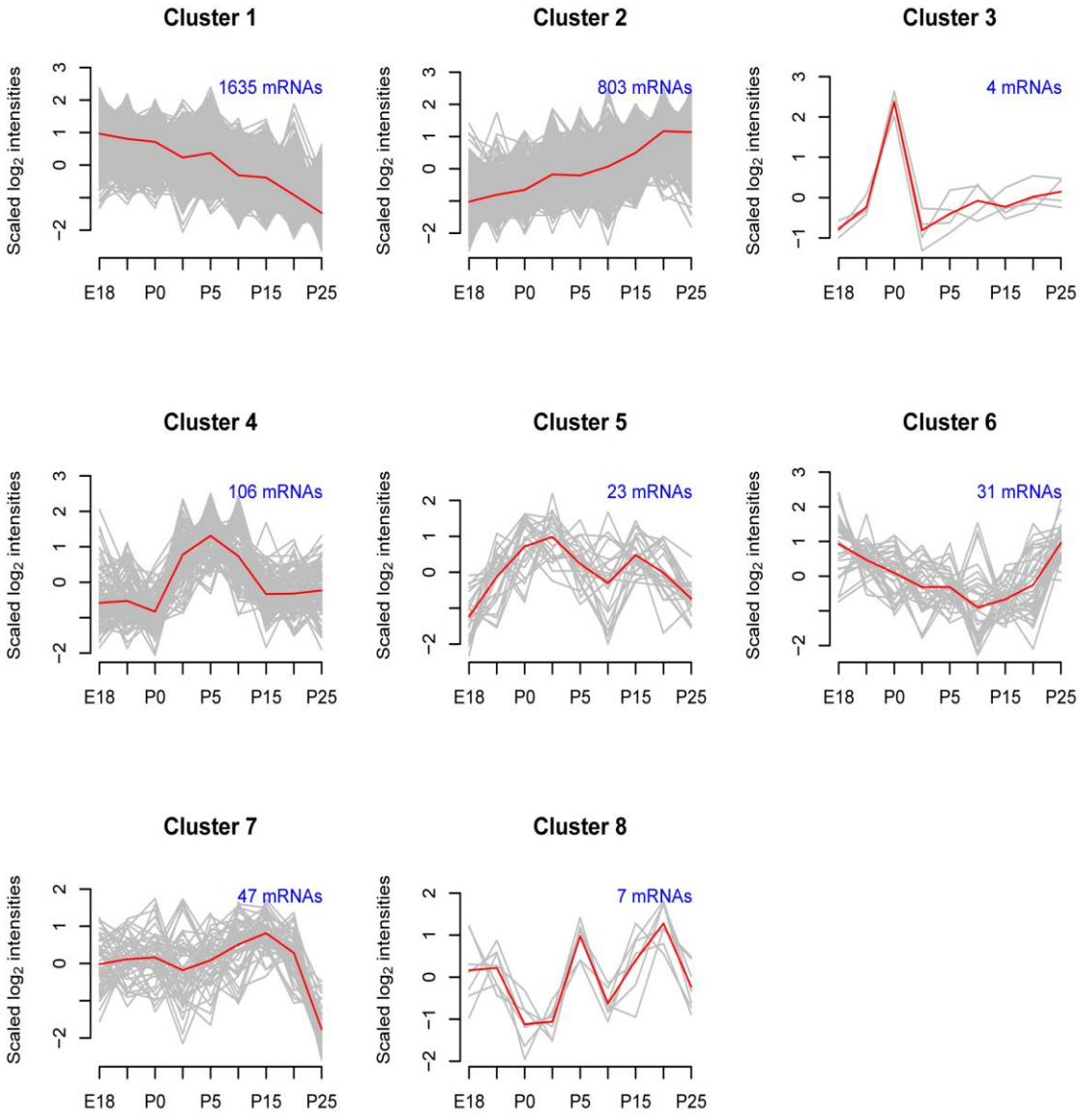

Figure 3.6 K-means Clustering Identifies Eight Patterns of Gene Expression during Acinar Cell Differentiation. K-means clustering was used to group gene expression into eight clusters. This analysis only included those genes determined to be differentially expressed (Table 3.1). For the above graphs, gene expression was standardized to a mean =0 and standard deviation =1. The red line traces the average pattern for the cluster, and the grey lines are each individual observation.

(clusters # 3, 5, and 8) and were not considered for subsequent analysis. Interestingly cluster #4 (106 genes) contains genes which are transiently activated midway through differentiation, they increase in expression shortly after birth, peak around P5 or P9, and then decrease back to basal levels. Genes in cluster #6 (31) increase in expression only in the late stage, while genes in cluster #7 (47) decrease in the late stage.

Enrichment analysis reveals that the genes in cluster #1 are enriched in terms related to mitosis and the cell cycle (Table 3.2). These genes are progressively decreasing across differentiation, and presumably genes promoting mitosis are decreasing as these cells are exiting the cell cycle and becoming fully differentiated.

Cluster #2 contains many of the previously identified acinar cell lineage specific genes such as salivary amylase, PSP, DNase I, and Aquaporin 5 (Aqp5). Processes enriched in this cluster could be involved in driving lineage specific gene expression. Enrichment analysis on this cluster found an overrepresentation of genes involved in ER-nucleus signaling and the adaptive Unfolded Protein Response (UPR) (Table 3.4). In order to identify possible transcription regulators in this cluster, enrichment of transcription factor targets was tested. A knowledge-based program (Metacore) was used which curates known transcription factor targets from the literature, and like GO enrichment can perform an overrepresentation test on a set of genes. Three transcription factors were identified (Table 3.3), two of which are present in the cluster (Xbp1, and

Enrichment by Pathway Maps

Maps	FDR
Cell cycle_The metaphase checkpoint	6.777E-06
Cell cycle_Sister chromatid cohesion	5.312E-04
Cell cycle_Spindle assembly and chromosome separation	8.383E-04
Cell cycle_Role of APC in cell cycle regulation	8.839E-04
Development_NOTCH-induced EMT	5.959E-03
Cell cycle_Start of DNA replication in early S phase	6.013E-03
Development_TGF-beta-dependent induction of EMT via SMADs	6.066E-03
DNA damage_ATM/ATR regulation of G1/S checkpoint	1.772E-02

Enrichment by GO Processes

Processes	FDR
mitotic cell cycle	1.867E-40
cell cycle	2.114E-33
cell cycle process	1.817E-30
cellular component organization	1.555E-23
cellular component organization or biogenesis	3.852E-23
cell division	2.537E-22
mitosis	1.751E-18
nuclear division	1.751E-18
cell cycle phase transition	7.557E-17
organelle organization	1.616E-16

Table 3.2: Processes Relating to Mitosis and the Cell Cycle are Enriched in Cluster of Down-regulated Genes. Clustering differentially expressed genes identified a cluster of 1635 continually decreasing genes (Figure 3.6, cluster #1). GO enrichment analysis of this cluster identified many terms related to the cell cycle. The top ten terms in GO Processes and Pathway maps is tabulated above. The “Processes” column lists the process name and the “FDR” column lists the FDR corrected p-value that DE cluster #2 is enriched in that term compared to a background dataset (rat genome)

Network Object Name	Actual	n	R	N	Expected	Ratio	p-value	z-score	Input IDs
MIST1	5	719	9	12845	0.5038	9.925	5.654E-05	6.522	**1387212_at**
XBP1	20	719	114	12845	6.381	3.134	4.623E-06	5.573	**1371249_at**
GCR-alpha	85	719	1004	12845	56.2	1.512	6.645E-05	4.118	

Table 3.3. DE Cluster #2 is Enriched in Targets for Mist1 and Xbp1. Transcription factor enrichment analysis was run in Metacore on the 803 genes in DE cluster #2. Enrichment is based on the number of downstream target genes identified in the curated Metacore database. Affymetrix rat genome array 230 was used as the background dataset. The columns are as follows: Actual= number of target genes in the dataset, n= number of network objects in the dataset, R= number of target genes in the background set, N= number of network objects in the background set, Expected= number of target genes expected in the dataset, Ratio= Actual/Expected, p-value= FDR adjusted p-value.

Enrichment by GO Processes

Processes	FDR
ER-nucleus signaling pathway	1.825E-04
cellular amino acid catabolic process	3.065E-04
response to endoplasmic reticulum stress	3.416E-04
alpha-amino acid catabolic process	8.107E-04
alpha-amino acid metabolic process	8.609E-04
organonitrogen compound metabolic process	1.173E-03
cellular amino acid biosynthetic process	1.371E-03
endoplasmic reticulum unfolded protein response	1.458E-03
cellular response to unfolded protein	1.568E-03
immune response	1.947E-03

Table 3.4: Processes relating to the Endoplasmic Reticulum are enriched in Cluster of Up-regulated Genes. Clustering differentially expressed genes identified a cluster of 803 continually increasing genes (Figure 3.6, cluster #2). GO enrichment analysis of this cluster identified overrepresentation of terms related to the endoplasmic reticulum. The table above lists the top ten GO Processes. The “Processes” column lists the process name and the “FDR” column lists the FDR corrected p-value that DE cluster #2 is enriched in that term compared to a background dataset (rat genome).

Mist1). Interestingly Mist1 null mice have a defect in acinar cell differentiation of both the pancreas and the salivary glands [125].

Cluster #4 is enriched in lipid metabolism (Table 3.4). This cluster also contains the transcription factor PPARg along with 19 of its known downstream effectors including adiponectin. This expression pattern for PPARg was confirmed by qPCR in a separate set of samples (Figure 3.7). While PPARg has been shown to be involved in the differentiation of other cell types, most notably adipocytes, it has never been identified in acinar cell differentiation before.

In order to identify additional expression patterns of interest, regression analysis was used to identify clusters that significantly follow specific treads. Because this dataset included measurements at nine time-points, complex patterns could be identified that follow quadratic and cubic trends (Figure 3.8). 419 genes were identified that significantly fit a quadratic trend and these genes were clustered into eight patterns. Only eighteen genes followed a cubic pattern and were not subsequently analyzed.

Several of the quadratic clusters were subjected to term enrichment analysis. Cluster #6 contains many known salivary cargo proteins such as DNase I, Chitinase, Prp15, and the immunoglobulin J chain Igj. It had been shown previously that DNase I expression is not detected in the developing salivary gland until the late stage of differentiation, but this adds to the list of late-regulated genes and indicates that the full repertoire of salivary components is not established until the late-stage.

Enrichment by GO Processes

Processes	FDR
regulation of sequestering of triglyceride	1.141E-05
acylglycerol metabolic process	6.743E-05
neutral lipid metabolic process	6.743E-05
lipid metabolic process	1.045E-04
triglyceride metabolic process	4.028E-04
glycerolipid metabolic process	5.269E-04
regulation of lipid storage	7.446E-04
triglyceride biosynthetic process	8.003E-04
glycerolipid biosynthetic process	8.003E-04
neutral lipid biosynthetic process	8.519E-04

Table 3.5: Transiently Activated Gene Cluster is enriched in Processes Relating to Lipid Metabolism. Clustering analysis identified a cluster of transiently up-regulated genes during differentiation (Figure 3.6, cluster #4). GO enrichment analysis identified overrepresented terms relating to lipid metabolism. The table above lists the top ten GO Processes. The “Processes” column lists the process name and the “FDR” column lists the FDR corrected p-value that DE cluster #2 is enriched in that term compared to a background dataset (rat genome).

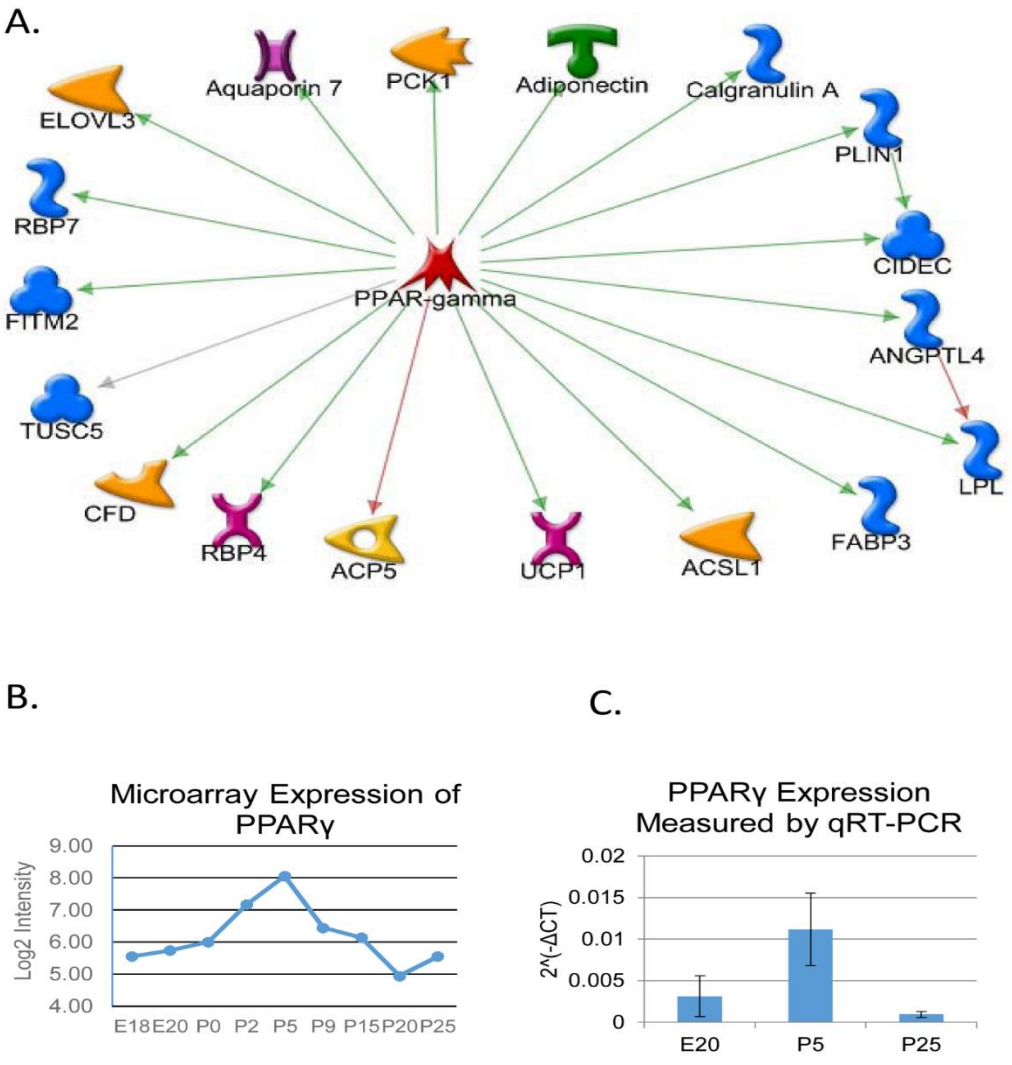

Figure 3.7 PPARg is Transiently Activated during Acinar Cell Differentiation. Cluster #4 (Figure 3.6) was shown to be enriched in genes related to lipid metabolism (Table 3.4) and included the transcription factor PPARg. A.) downstream targets transcriptionally regulated by PPARg that are also in cluster #4. B.) Microarray expression pattern of PPARg confirms that this gene is activated midway through differentiation and then returns to baseline. C.) This expression pattern is validated by qPCR (n=3, p-value= 0.03).

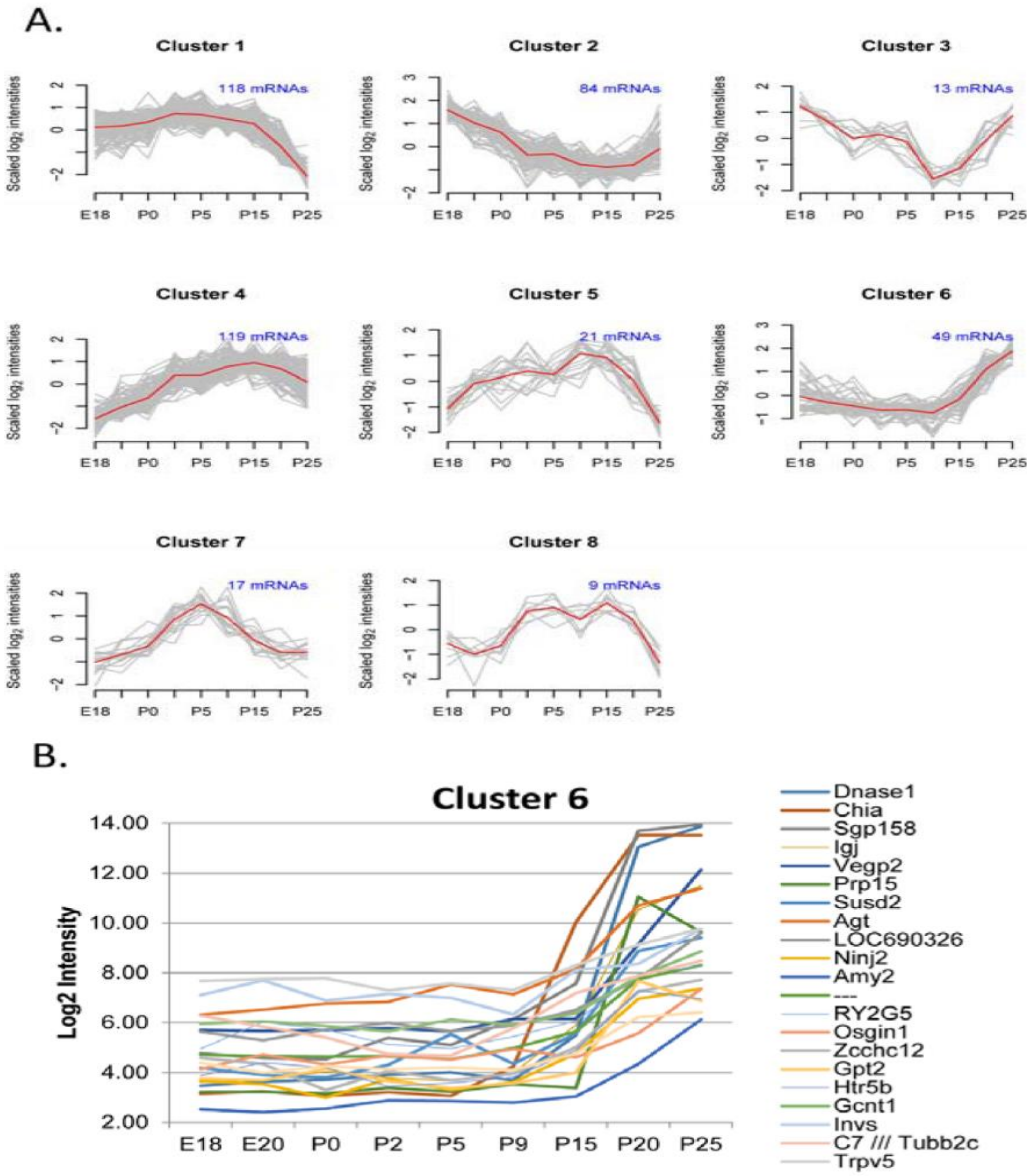

Figure 3.8 Eight Gene Expression Clusters have a Significant Quadratic Trend. A.) Regression analysis was used to identify genes with a significant (adj. p-value= 0.05) quadratic trend. Cluster #6 contains genes which have relatively low expression throughout most of differentiation and then increase dramatically starting between P9 and P15. B.) Non-standardized profiles for genes in cluster #6 with at least a 4-fold change. This cluster contains many extracellular proteins including many saliva components (i.e. DNase I, Chia, and Prp15).

3.2.2 microRNA Expression

Over the last decade microRNAs have come to be recognized as important regulators of gene expression in many processes including development and differentiation. Little is known about their expression and potential targets in acinar cells. To identify a potential role of microRNAs in acinar cell differentiation we profiled their expression across differentiation. By having both mRNA and corresponding microRNA expression patterns, potential target genes can be identified.

As with the microarray study, LCM was used to capture acinar cells at multiple time points across differentiation. Following the observation from the microarray study that there are four stages during differentiation, cells were isolated at four time points in triplicate, each representing one of the four stages (E20, P5, P15, and P25). microRNA expression was measured by a qPCR array designed to amplify 375 well characterized rodent microRNAs. A summary of the analysis is shown in Table 3.6.

qRT-PCR detected 271 microRNAs repeatedly. Analysis by one-way ANOVA identified 79 microRNAs exhibiting significant differential expression (Figure 3.9). Subsequent t-tests between time points (Table 3.6) identified 64 microRNAs with differential expression between the first (E20) and last (P25) time points. These 64 microRNAs encompass all significantly changing microRNAs identified by comparing other pairs of time points. Of these, 52 microRNAs increased in expression and 12 decreased across acinar differentiation.

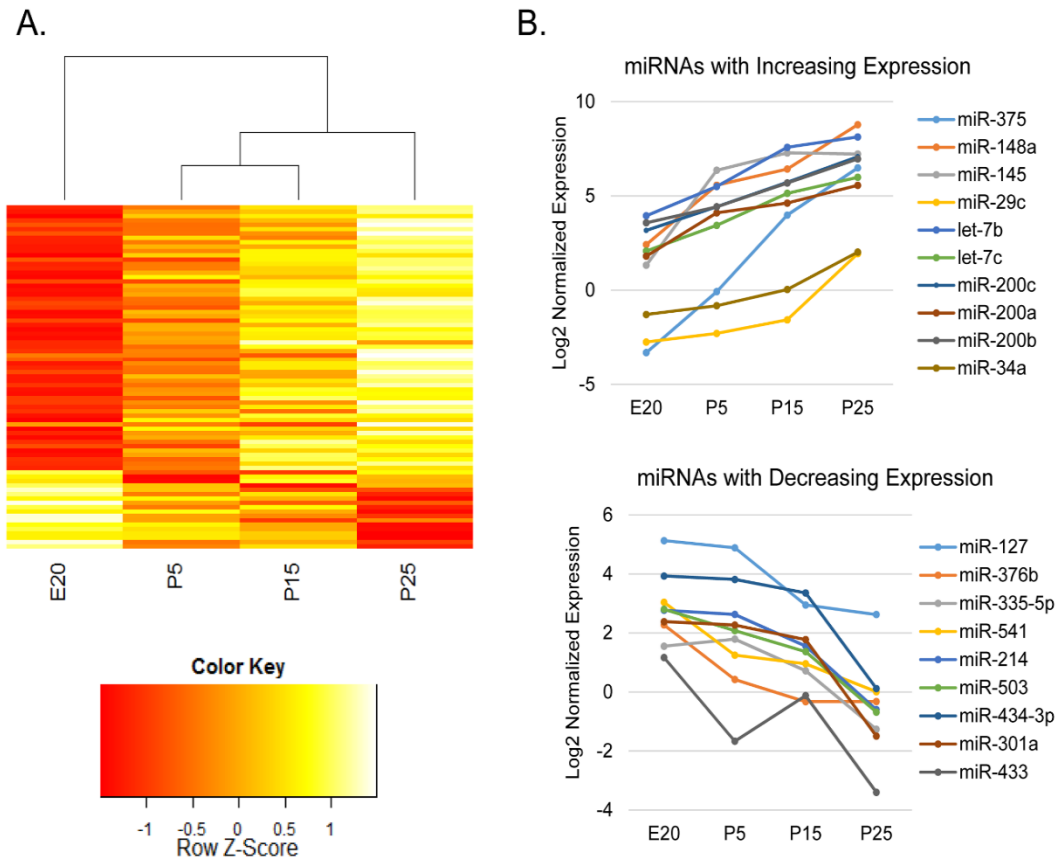

Figure 3.9 Regulated microRNA Expression during Parotid Acinar Cell Differentiation. A.) Heatmap of differentially expressed microRNAs. Ages were clustered based on expression pattern as in Figure 3.5. B.) microRNAs with the largest fold change are shown. Expression is plotted in Log2.

Comparison	Up-regulated microRNA	Down-regulated microRNA
E20 vs. P5	1	0
E20 vs. P15	14	2
E20 vs. P25	52	12
P5 vs. P15	0	0
P5 vs. P25	7	0
P15 vs. P25	0	0

Table 3.6: Summary of microRNA analysis. The number of differentially expressed microRNAs was determined by t-test using the *limma* package in R, for every possible comparison of time points.

Clustering identifies just two major expression profiles (Figure 3.10), either continuously increasing or continuously decreasing. There does not appear to be any microRNAs with transient activation or repression. Table 3.7 lists the ten microRNAs from each group with the largest fold change in expression between the earliest time point (E20) and the latest (P25).

The microRNA with the largest fold change (miR-375) increases in expression more than 800 fold. This microRNA is nearly undetectable by qPCR in the embryonic stage, and progressively increases until P25 when miR-375 has the second highest relative expression of all the microRNAs measured (it is second only to miR-148a, aka miR-148b-2).

miR-375 is one of the few microRNAs that has been previously measured in the adult parotid gland, and may contribute to the formation of adenocarcinoma of the salivary gland. Down-regulation of miR-375 is often measured in tumors, along with up-regulation of its target and proto-oncogene Plag1, a transcription factor thought to increase unregulated cell proliferation by, at least in part, increasing expression of Igf2 [126-128]. In order to identify whether this particular gene is being regulated by miR-375 during cell differentiation the expression profiles of each were used to identify a possible inverse correlation (Figure 3.11). Like its prospective targeting microRNA, Plag1 is also significantly differentially expressed, and is a member of cluster #1 (Figure 3.6) which is made up of progressively decreasing genes. Plag1 expression decreases more than 6-fold across differentiation. Log2 relative expression values were used to calculate a

Up-Regulated microRNAs			Down-regulated microRNAs	
miRname	**Fold change (P25/E20)**		**miRname**	**Fold change (P25/E20)**
mmu-miR-375	895.80		mmu-miR-433	0.04
mmu-miR-148a	82.27		mmu-miR-301a	0.07
mmu-miR-145	59.62		mmu-miR-434-3p	0.07
mmu-miR-29c	25.76		mmu-miR-503	0.09
mmu-let-7b	18.13		mmu-miR-214	0.10
mmu-let-7c	15.07		mmu-miR-541	0.12
mmu-miR-200c	15.03		mmu-miR-335-5p	0.14
mmu-miR-200a	13.55		mmu-miR-376b	0.17
mmu-miR-200b	10.50		mmu-miR-127	0.18
mmu-miR-34a	9.91		mmu-miR-17	0.18

Table 3.7: microRNAs with Largest Fold Change during Differentiation. Fold change between the latest time point (P25) when the parotid gland is fully mature and the earliest time point (E20) when the acinar cells are not terminally differentiated was calculated for each of the differentially expressed microRNAs (Table 3.6). The top ten up-regulated and down-regulated microRNAs are tabulated above.

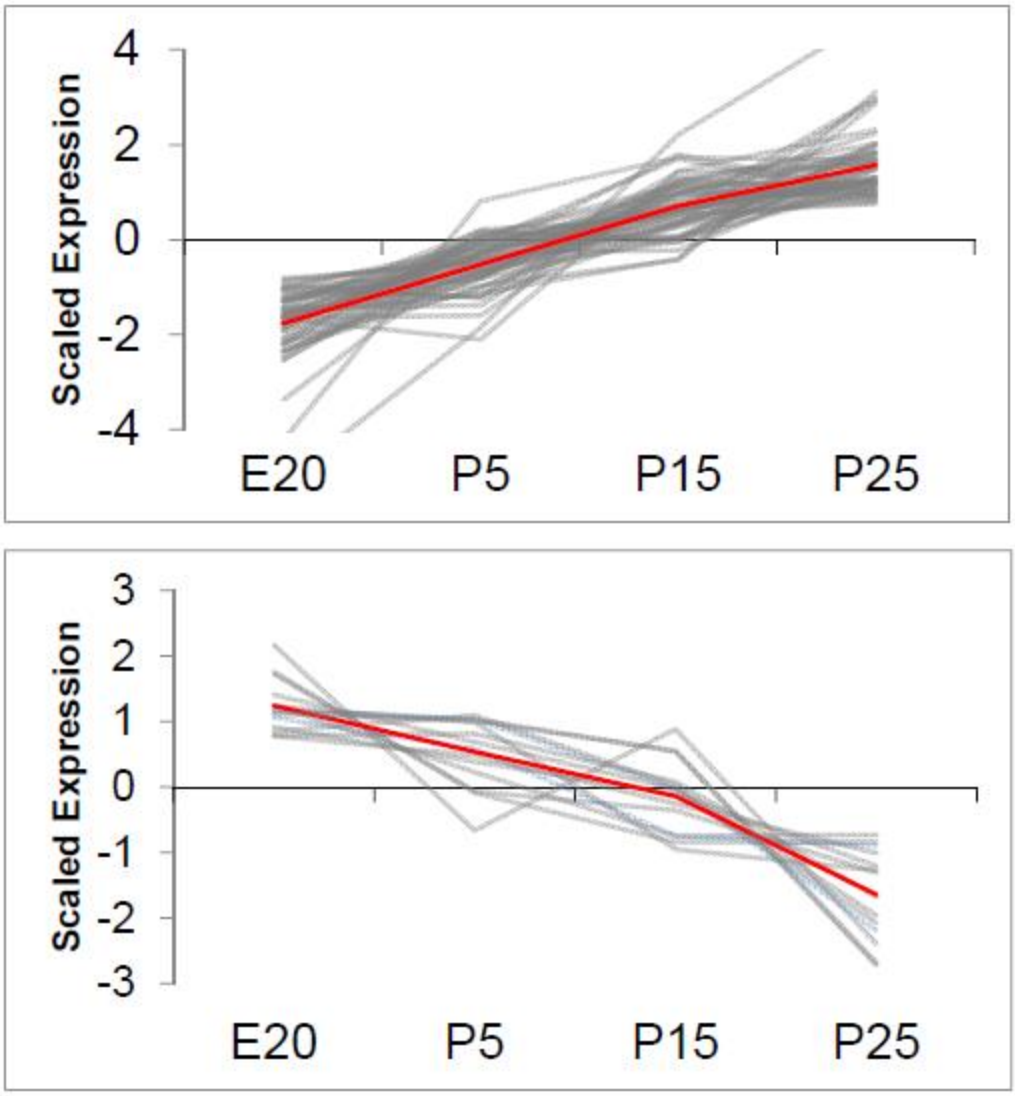

Figure 3.10 Clustering microRNA profiles. K-means clustering was used to group differentially expressed microRNAs into two main clusters: either continually increasing or continually decreasing. For the above graphs, microRNA expression was standardized to a mean =0 and standard deviation =1. The red line traces the average pattern for the cluster, and the grey lines are each individual observation.

A.

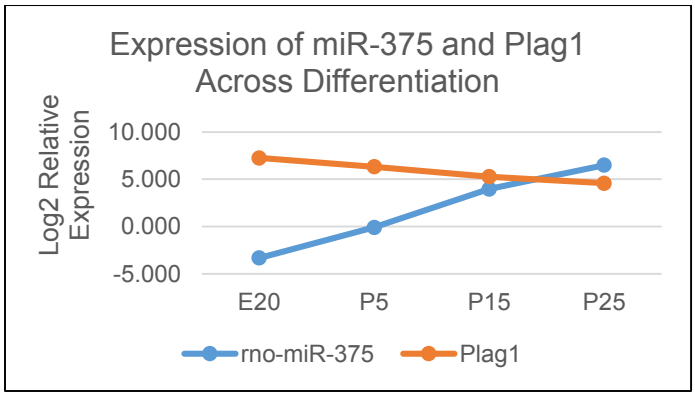

Log2 Expression

	E20	P5	P15	P25	correlation	p-value
Plag1	7.26	6.33	5.27	4.59	1	
miR-375	-3.32	-0.08	4.00	6.49	-.99	0.0002

B.

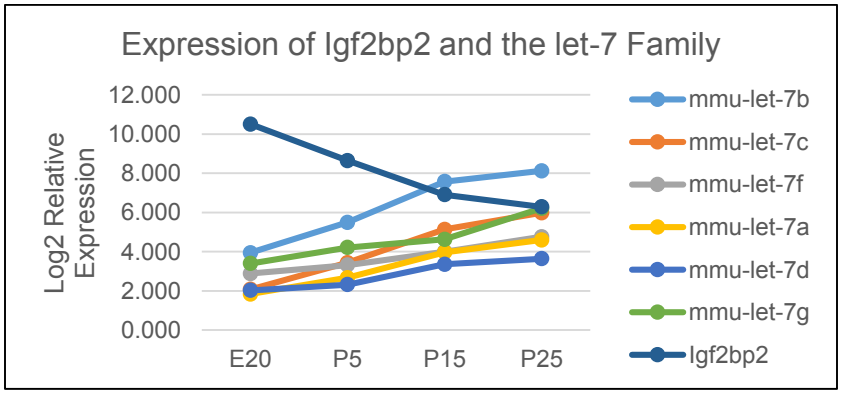

Log2 Expression

	E20	P5	P15	P25	correlation	p-value
Igf2bp2	10.50	8.64	6.90	6.28	1	
let-7a	1.84	2.68	3.97	4.60	-0.99	0.01
let-7b	3.95	5.50	7.58	8.13	-0.99	0.003
let-7c	2.08	3.44	5.13	5.99	-0.99	0.006
let-7d	2.02	2.32	3.35	3.64	-0.97	0.03
let-7f	2.89	3.31	4.00	4.76	-0.95	0.047
let-7g	3.40	4.21	4.63	6.21	-0.90	0.1

Figure 3.11: MicroRNA Expression is Significantly Inversely Correlated with Known Target Genes. A.) Log2 expression of Plag1 and mir-375 from microarray and qPCR measurements respectively is plotted in the top panel. Expression data is tabulated in the bottom panel along with the Pearson correlation coefficient and p-value. B.) Log2 expression is plotted for Igf2bp2 and six members of the let-7 family of microRNAs in the top panel. In the bottom panel expression is tabulated along with the Pearson correlation coefficient between each microRNA and Igf2bp2 and p-value.

Pearson's correlation coefficient, and a t-test used to evaluate significance. This analysis identified a significant inverse correlation ($r = -0.9998$, p-value = 0.0002) indicating that Plag1 is likely a target of miR-375 and that its expression is being progressively down-regulated by this microRNA during differentiation.

Other microRNAs of interest include members of the let-7 family which are known to regulate the cell cycle. There are ten members of this highly conserved family in the genomes of humans and mice [129], and six of them are up-regulated during acinar cell differentiation (Figure 3.11). Their change in expression ranges from 3-fold (let-7d) to more than 18-fold (let-7b). Differentiation and cell cycle progression are often thought of as having opposing roles in the cells. It has often been observed that exiting the cell cycle will stimulate terminal differentiation, while activating the cell cycle is an inhibitor of differentiation [130]. Known direct targets of the let-7 family include Igf2bp2, an mRNA binding protein which is known to enhance the translation of many genes including several oncogenes and activators of proliferation, Igf2, and c-myc [131]. Igf2bp2 decreases significantly across differentiation and its expression profile is inversely correlated significantly with five of the let-7 genes (Figure 3.11).

Several members of the miR-200 family are also significantly up-regulated during differentiation. Previous work identified miR-200c as up-regulated in the end buds (the region of future acinar cell differentiation) during SMG branching morphogenesis. This microRNA was found to have anti-proliferative effects by regulating FGFR signaling through targeting of Vldlr [111]. In our dataset three

members of the miR-200 family (miR-200a, miR-200b, and miR-200c) are significantly upregulated (Figure 3.12). However, its direct target gene, Vldlr, is not differentially expressed, indicating that these microRNAs are acting on a different target during the later stages of gland development.

3.3 Discussion

For the first time, acinar cell specific gene expression was profiled across terminal differentiation *in vivo* by selectively isolating acinar cells at multiple time points starting with immature pro-acinar cells in the late embryo (E18), and ending with fully mature acinar cells at P25. By using a combination of microarray hybridization and qPCR, expression of > 30,000 expression probes and 375 microRNAs were measured at nine time points in triplicate leading to the identification of > 800,000 gene expression measurements during differentiation which represents a large portion of the transcriptome.

Analysis of these measurements led to the identification of individual differentially expressed genes. More than 2500 mRNAs change expression, and were used to cluster the ages into four stages: an embryonic stage (E18, E20, and P0), early postnatal stage (P2, and P5), mid postnatal stage (P9 and P15), and a late stage (P20 and P25). Gene expression changes relatively little between members of the same stage, while large changes are seen between members of different stages.

In order to identify the processes involved in differentiation, the gene expression profiles were clustered and used for gene ontology enrichment analysis. Of

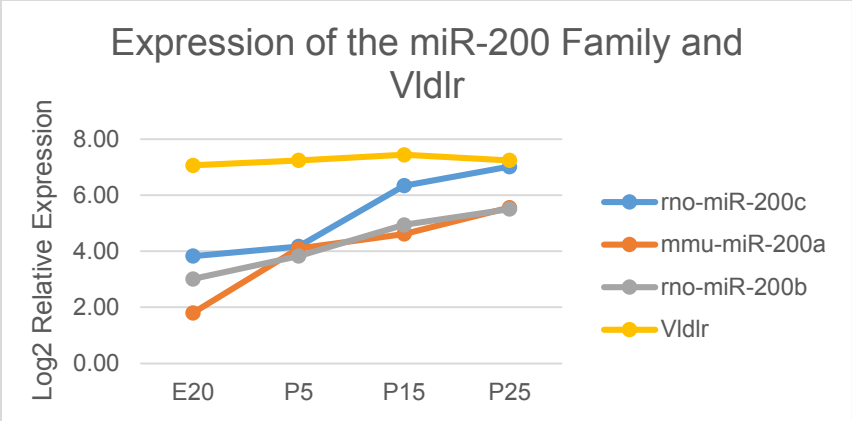

	E20	P5	P15	P25	correlation	p-value
Vldlr	7.07	7.24	7.44	7.24	1	
miR-200b	3.01	3.83	4.94	5.51	0.69	0.51
miR-200c	3.83	4.17	6.34	7.02	0.64	0.56
miR-200a	1.80	4.10	4.62	5.56	0.69	0.51

Figure 3.12: Vldlr Expression is not Inversely Correlated with the miR-200 Family. Log2 expression is plotted for Vldlr and three members of the miR-200 family of microRNAs in the top panel. In the bottom panel expression is tabulated along with the Pearson correlation coefficient between each microRNA and Vldlr and p-value. None of the correlation coefficients are significant indicating that Vldlr is probably not a target of the miR-200 family during differentiation.

particular interest is a large cluster of increasing gene expression that contains many known parotid gland terminal differentiation markers including cargo protein and components of the regulated secretory pathway (i.e. amylase, PSP, Rab3d). GO enrichment identifies ER signaling as an enriched process. Regulation of this cluster is likely to be important for the development of the fully differentiated phenotype, and understanding the components involved in this cluster is vital to understanding how differentiation is controlled. Enrichment analysis using transcription factor targets identified both Mist1 and Xbp1 targets as over-represented, indicating that these two transcription factors could be important regulators of differentiation.

Xbp1 is most known as part of the Unfolded Protein Response (UPR). It is activated in response to ER stress, and binds to Unfolded Protein Response Elements (UPREs) or ER stress elements (ERSE I/II) as a dimer with Atf6 where it up-regulates gene expression. Many of the targets include ER chaperones and members of the ER associated degradation system (ERAD), highlighting its role in ER homeostasis, but there are many other processes it is thought to be a part of. Recently, the role of Xbp1 has expanded to include development and differentiation particularly in cells with a high protein folding burden (i.e. acinar cells, plasma cells, muscle cells). It is involved in the biogenesis and expansion of the ER and Golgi in these cells leading to higher protein production and secretion. Xbp1 is necessary for differentiation of plasma cells from B cells, and Xbp1 -/- mice show disruptions in both salivary gland and exocrine pancreas development [132]. Pancreatic acinar cells show reduced expression of zymogen

granules and associated cargo proteins (i.e. amylase, elastase) at the mRNA level, suggesting disruptions in differentiation. Xbp1 is also required for homeostasis of pancreatic acinar cells [133].

Our results show that Xbp1 activity is enriched in a gene expression cluster containing many lineage specific and terminal differentiation associated genes. These genes increase in expression across differentiation and are likely important for the cells to attain the fully differentiated phenotype. Because we identified Xbp1 as a major regulator in this cluster, its activity is probably necessary for proper mRNA expression, and terminal differentiation.

Mist1 (aka Bhlha15) is the other enriched transcription factor identified in cluster #2 (Figure 3.6). This gene is considered specific to acinar cells, and is reported to be directly downstream of Xbp1. Mist1 -/- mice have disruptions in salivary and pancreatic acinar cell morphology. These cells contain few granules, and lack a polarized cytoplasm (the nucleus is no longer basally located).

In a completely novel observation, Pparg controls the expression of a transient gene cluster. The transcription factor Pparg and 19 of its downstream targets increases in expression shortly after birth, peaks around postnatal day 5, and decreases back to basal levels by the time the gland is fully mature. The Pparg targets include many genes which have not been identified in salivary gland development before, but at least one has been shown to affect the physiology of the adult gland. In our dataset, the hormone adiponectin is produced downstream of Pparg (Figure 3.7). Expression of this protein is mostly associated with

adipose tissue where it is released and acts on other tissue through its receptors (Adipor1 and Adipor2). It has been shown that these receptors are present on acinar cells of the submandibular gland, and adiponectin can increase salivary flow [134]. Our microarray data shows that both adiponectin receptors are expressed throughout differentiation in the parotid (data not shown), and so adiponectin could be acting as an autocrine factor to stimulate secretion for a short period of time postnatally.

This analysis also identified novel microRNA expression changes. This is the first study to measure microRNA expression in the salivary gland during differentiation. 52 microRNAs showed a net increase in expression while 12 had a net decrease. miR-375 had the largest fold-change measured: its expression increased more than 800-fold between embryonic day 18 and postnatal day 25. It showed extremely low expression in the embryo and was undetectable by qPCR in some of these samples suggesting it does not play a role in early gland development, only differentiation. It is likely targeting Plag1 which shows inverse expression in our data. This interaction has been reported in salivary gland cancer where decreased miR-375 leads to increased expression of the oncogenic Plag1 [126], but this is the first report of this interaction in differentiation. Like many oncogenes, Plag1 could also be playing a role in development. For instance, it has been reported to increase proliferation in culture and in tumors through up-regulation of its target gene, the mitogenic Igf2 [128, 135]. Interestingly, in a Plag1 -/- model, small organ size was reported but without the expected decrease in Igf2 expression indicating this transcription

factor is controlling growth through multiple pathways [136]. In the salivary gland, high Plag1 expression in the embryo could be contributing to growth and cellular expansion. miR-375 then would be necessary during later development when cells are exiting the cell cycle and becoming fully differentiated. Many mitogenic factors inhibit differentiation, and so increased miR-375 expression could be promoting differentiation in parotid acinar cells.

A miR-375 knockout mouse line exists [137], but a phenotype relating to the salivary glands has not been investigated. A possible future direction would be to measure acinar cell differentiation by measuring the expression level of salivary acinar cell markers such as amylase and PSP in the knockout versus the wildtype.

The let-7 family of microRNAs could also be influencing proliferation. Six of the let-7 microRNAs increase in expression during differentiation (Figure 3.11) and five are significantly inversely correlated with Igf2bp2, a canonical target of let-7. Igf2bp2 expression decreases 18-fold during differentiation. Interestingly, like the miR-375 target Plag1, Ig2bp2 plays a role in regulating Igf2 expression. Where Plag1 increases transcription of Igf2, Igf2bp2 is an RNA binding protein which has been shown to stabilize Igf2 mRNA and promote translation [138]. Both miR-375 and let-7 could be working together to down-regulate Igf2 signaling during differentiation, which is associated with growth and proliferation.

CHAPTER 4: A GENE REGULATORY NETWORK DRIVING EXPRESSION OF TERMINAL DIFFERENTIATION GENES

4.1 Introduction

Terminal differentiation involves sustained changes in gene expression patterns as progenitor cells mature and take on the fully differentiated phenotype. These changes lead to the directed expression of proteins which are markers of terminal differentiation. In the case of salivary acinar cells, this means that cells acquire expression of secreted cargo proteins as well as all the molecular machinery needed for large scale production and regulated secretion of these proteins into saliva [78]. This specialized differentiation is required for proper saliva production and loss of these cells results in poor oral health and quality of life due to chronic xerostomia which is a common complaint in the general population [30, 32], and is currently difficult to treat. The best treatment option for patients would be one that addressed the underlying cause of xerostomia in many people: acinar cell atrophy [57]. Once destroyed by radiation or autoimmune disease, these cells typically do not grow back by themselves.

Understanding the regulation of gene expression changes during differentiation could aid in efforts to regenerate fully differentiated cells from more naïve progenitors or stem cells. Also, transcription factors needed to drive expression

changes during differentiation could be necessary to maintain homeostasis in the adult gland, and these factors could be used to maintain differentiated cells in culture which could be used for the construction of artificial glands.

In the previous section the global changes in mRNA and microRNA expression were measured across acinar cell differentiation. Transcriptional regulators controlling the terminal differentiation phenotype would presumably be upregulated during this process, and would be captured as differentially expressed genes in our analysis. Also the comparison of microRNA expression profiles with mRNA expression would identify microRNA:mRNA interactions during differentiation. This differential expression data could then be used to identify possible gene regulatory networks driving differentiation.

MicroRNA expression is now being considered in the context of multiple interactions as well as indirect effects, and perturbation of their expression has been predicted to impact whole gene networks. This current understanding has led to several models of how these small RNAs could be impacting gene networks these include feed-back loops with transcription factor targets, or stabilizing gene expression in order to increase robustness in the face of outside perturbation. In this context microRNA expression changes during differentiation could be effecting entire networks down-stream.

For this analysis we used a knowledge-based approach along with our expression measurements to predict transcript regulatory interactions driving the expression of several terminal differentiation genes. We also integrated our

expression data with *in silico* based predictions to identify novel microRNA:mRNA interactions.

This analysis identified an entirely novel tripartite gene regulatory network driving the expression of the terminal differentiation markers PSP, Rab3d, Rab26, and Connexin32. In one arm of the network, pro-stem cell transcription factors decrease across differentiation, a genetic switch activates Xbp1 expression by inhibiting the repressor Pax5, and a pro-differentiation arm activates expression of terminal differentiation genes.

This network also includes several novel microRNA:TF-mRNA interactions. Pro-stem cell TF Klf4 is targeted by miR-200c, and miR-29c. Sox11, another TF involved in stem cell maintenance, is targeted by miR-200a, and miR-30a, and *in vitro* testing of these interactions suggests that these microRNAs are acting cooperatively to decrease expression.

4.2 Results

4.2.1 Knowledge-based Predictions: Regulators of PSP and Amylase

Little is known about the transcriptional regulation of acinar cell lineage-specific genes during terminal differentiation. As we and others have noted, salivary specific cargo proteins such as amylase, PSP, and DNase I are dramatically upregulated during postnatal differentiation [139], but little information has been available regarding the expression of transcription factors which could be necessary for promoter activation. PSP in particular is essentially parotid-

specific, and is one of the most abundant proteins in saliva [140, 141]. In our approach, we measured a large portion of the transcriptome across differentiation, and identified >2500 differentially expressed genes (Figure 3.5), many of which had not been described in parotid development before, including >500 transcription factors (Figure 4.1).

A knowledge-based approach, which uses interactions curated from comprehensive literature searches, was used to predict transcription factors upstream of salivary-specific cargo proteins. Our transcriptome data could then be incorporated to identify differentially expressed transcription factors with expression patterns that correlated with the predicted target gene, indicating a possible interaction with the gene promoter. These genes (e.g. amylase, PSP) were uploaded as seed nodes for network analysis. A network is expanded around a seed node according to selected filters and criteria. Because our data consisted of changes in mRNA expression, edges (interactions between genes) were filtered for transcription regulatory interactions up-stream of the selected seed node. This results in the addition of mostly transcription factors that have at least one literature source supporting direct regulation of the target of interest.

Using this algorithm, up-stream regulators of the amylase enzyme were predicted (Figure 4.2). There are two amylase genes up-regulated during parotid development, Amys (salivary), and Amyp (pancreatic). Up-stream from these genes there are six predicted regulatory transcription factors. Only one is predicted to activate transcription (Gata6), as indicated by a green arrow, and for the others the direction of regulation is unknown (grey arrow). None of these

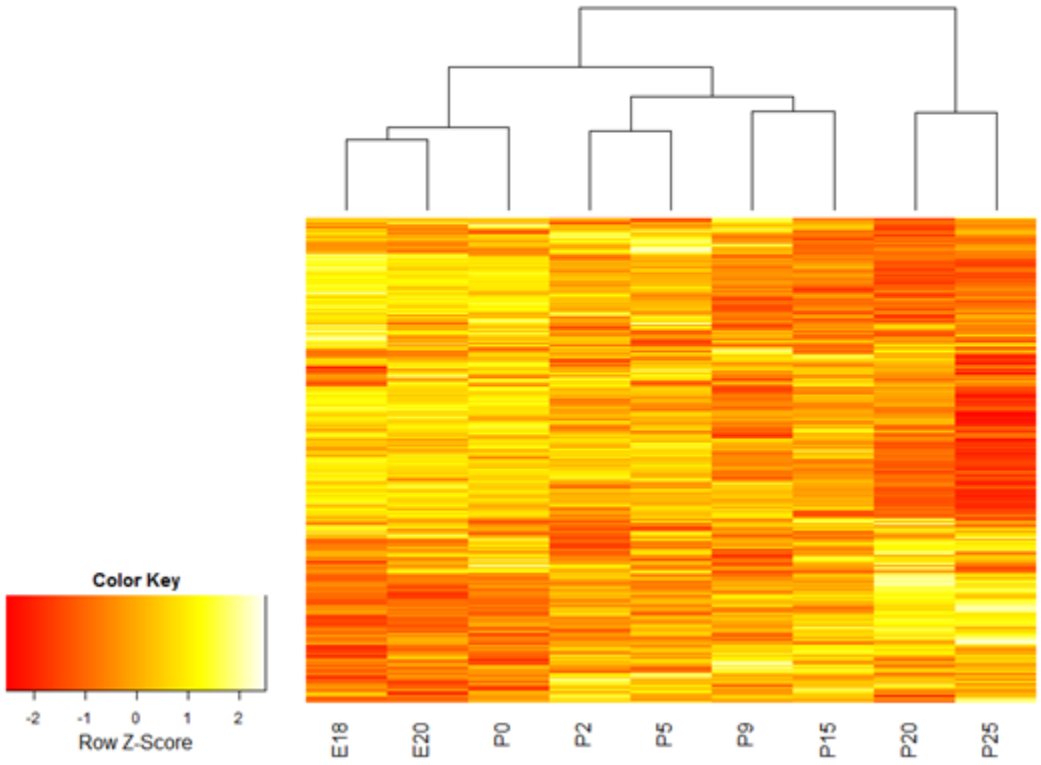

Figure 4.1 Hundreds of Transcription Factors are regulated during Acinar Cell Differentiation. A Heatmap was generated as is Figure 3.5. Using the expression data for 550 transcription factors that were identified in the dataset of 2656 differentially expressed genes (Table 3.1).

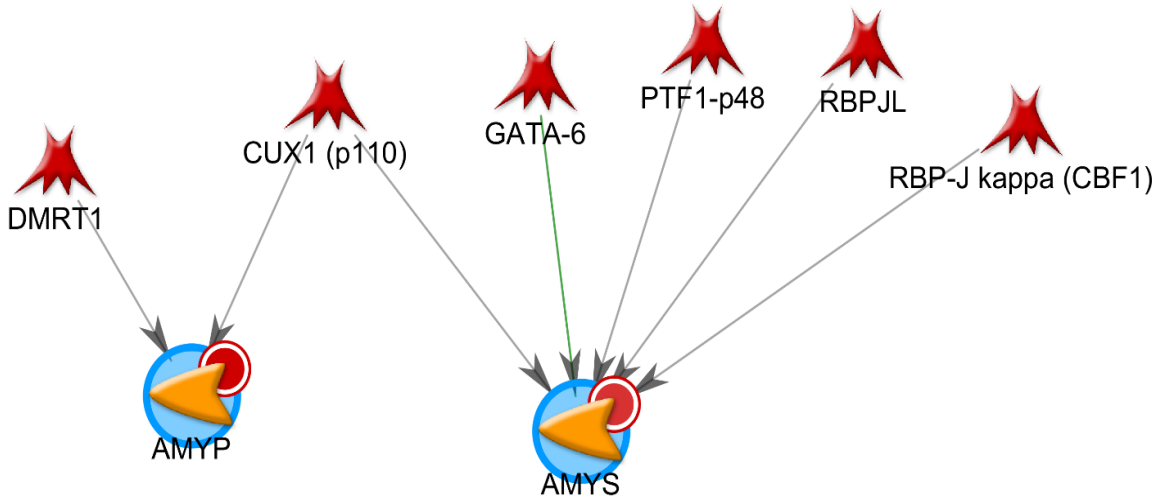

Figure 4.2: mRNA Expression of Knowledge-based Amylase Regulators does not Change during Differentiation: The knowledge-based network analysis software Metacore was used to build a prospective gene regulatory network using the enzyme, and parotid terminal differentiation marker amylase as a seed node. Edges (depicted as arrows) were incorporated by the algorithm based on a comprehensive literature search for up-stream transcription regulators. A green arrow indicates an activating interaction while grey arrows indicate that the direction of interaction is unknown. A circle next to the gene icon indicates that it is significantly differentially expressed as measured by microarray (Figure 3.7). A red circle indicates that net expression increases while a blue circle means expression decreases. Of all the genes in the generated network, only the two amylase genes are differentially expressed.

transcription factors is differentially regulated at the mRNA level. Parotid secretory protein (PSP) is a highly expressed parotid-specific terminal differentiation marker. Three transcription factors are predicted up-stream (Figure 4.3), two of which are up-regulated during differentiation: Elf5 and Ese3. Elf5 expression increases modestly, 1.6-fold, during differentiation, and Ese3 expression increases 3.6-fold. Elf5 is predicted to activate PSP expression (green arrow) while the direction of Ese3 regulation is not known (grey arrow). In order to expand the network to incorporate other potential regulators, Elf5 was used as a seed node with the same filters applied. Stat5a, which is up-regulated, is predicted to up-regulate Elf5 expression. This two-step network predicts PSP regulation through Stat5a and Elf5. Possible microRNA regulation was also investigated, but none of the network genes were predicted targets (based on in silico predictions; Targetscan) of any differentially expressed microRNAs.

4.2.2 Novel Regulator of PSP Expression

Because both Elf5 and Ese3 expression increases modestly compared to PSP expression we hypothesized the existence of novel regulators during differentiation. Also, because this is the first large scale expression study of salivary acinar cell differentiation, there are probably novel cell type specific interactions which would not be identified by a knowledge-based approach. In order to identify new transcription factor interactions, the salivary specific region of the PSP promoter was surveyed for predicted consensus sequences. Two Xbp1 binding sites (CCACG) were identified close to the transcription start site

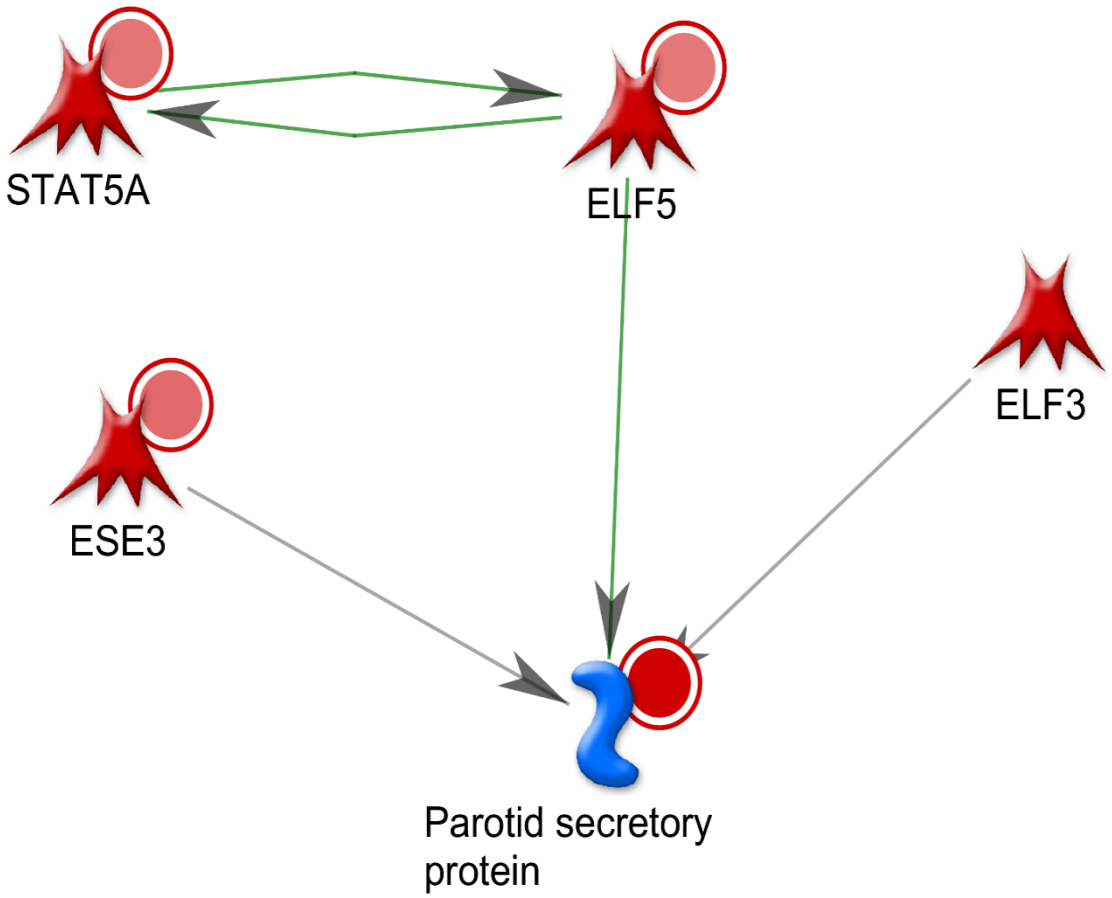

Figure 4.3: Elf5 is a Possible Regulator of PSP during Differentiation. Network shows knowledge-based algorithm predictions of upstream transcription regulators of the parotid secretory protein (PSP, aka Bpifa2). ELF5 is a transcription factor commonly expressed in glandular epithelia, and it is significantly up-regulated across differentiation (Log2 fold change 0.68 between E18 and P25). It is predicted to activate PSP expression (green arrow). No differentially expressed microRNAs targets members of the network.

(-31nt to -35nt, and -44nt to -48nt). Xbp1 expression increases 6.5 fold over the course of terminal differentiation, along with many of its known down-stream effectors. Its targets are significantly enriched in DE cluster #2 (Figure 3.6). Together, this indicates that Xbp1 transcriptional activity is also increasing over this time span.

Luciferase reporters were constructed containing either 500bp or 1000bp of the PSP promoter immediately up-stream of a luciferase gene. Both versions of the promoter showed strong dose dependent induction following co-transfection with an Xbp1 expression vector in ParC5 cells (Figure 4.4). This indicates that Xbp1 could be part of a new transcription regulatory network activating PSP expression during terminal differentiation.

4.2.3 Transcription Regulatory Network Driving PSP Expression through Xbp1

To investigate a possible network, Xbp1 was included with PSP as seed nodes for network analysis, and an interaction between the two genes was added. Using the filtered algorithm, multiple steps of predicted edges were evaluated sequentially up-stream and down-stream of Xbp1 for those with expression changes correlating with the proposed interaction which were then incorporated into the network (Figure 4.5). This led to the identification of multiple steps of transcription regulatory interactions which lead to the expression of acinar cell specific genes. In the network diagram, the terminal differentiation genes are shown at the bottom with each up-stream step acting from above. In the context of this time course experiment, expression changes at the top of the network

A.

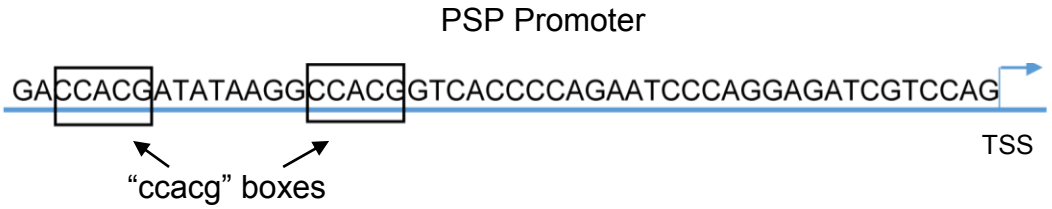

B.

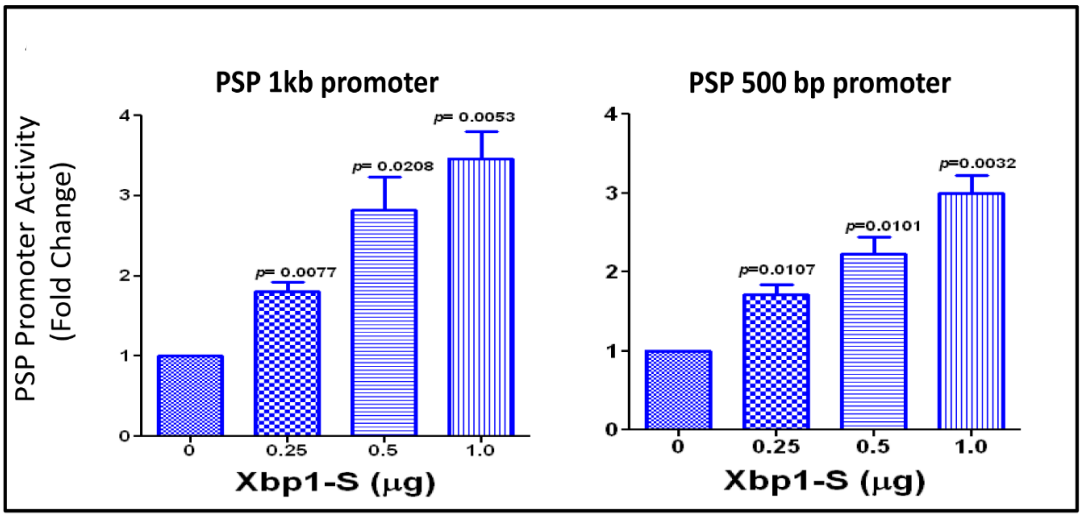

Figure 4.4: Transcription Factor Xbp1 Activates the PSP Promoter: A.) The PSP promoter contains two consensus binding sites for Xbp1 (the CCACG box) just up-stream of the TSS. B.) The PSP promoter was cloned up-stream of a luciferase reporter, and co-transfected into ParC5 cells with an expression vector containing the spliced isoform of Xbp1 (Xbp1-s). Expression was normalized to a renilla control. Xbp1-s activated expression from both the 1kb and 500bp region of the PSP promoter (n=3).

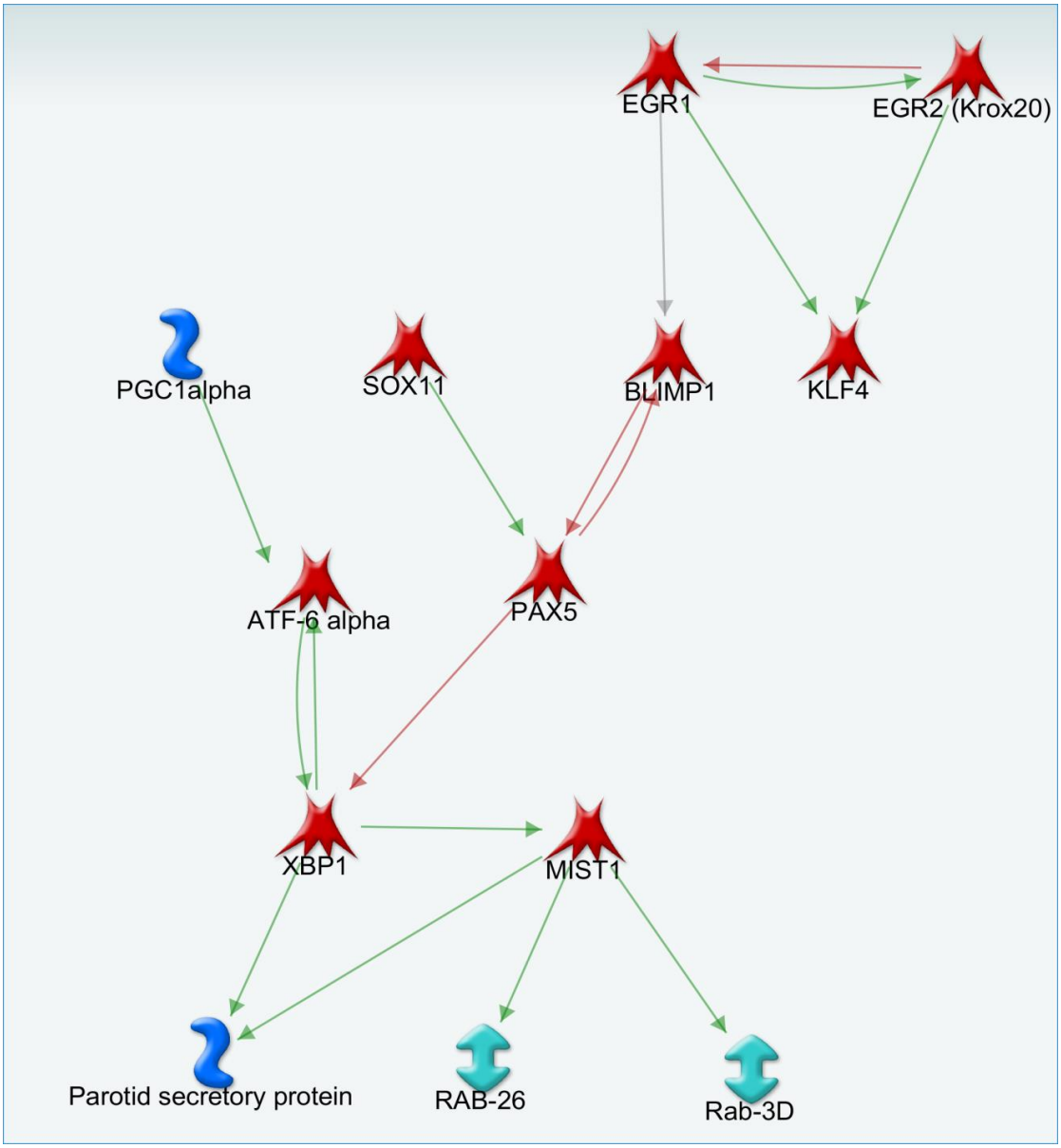

Figure 4.5 Transcription Factor Network. A knowledge-based algorithm was used to add transcription regulatory interactions up-stream and down-stream of Xbp1. Nodes were added if they were differentially expressed (Figure 3.5), and if their expression profile was consistent with the predicted interactions. A green arrow indicates an activating interaction and a red line indicates an inhibiting interaction.

would be required early in differentiation with each subsequent level occurring as time proceeds to drive the network forward to the lineage specific phenotype. In order to develop a comprehensive network from our data, microRNAs were next included based on predicted targeting of network transcription factors. By having expression data for both mRNAs and microRNAs context specific interactions can be predicted. In silico predictions alone (based on sequence complementarity and conservation) often lead to the identification of hundreds of potential targets per microRNA. Many of these genes may not even be expressed in the system under study, or multiple targets expressed each with different (and unknown) affinities for the microRNA leading to competitive binding, the results of which could only be resolved by measuring gene expression under conditions of microRNA perturbation. There are also several pseudogenes that have been identified which contain microRNA binding sites, and have been reported to act as sponges, sequestering microRNAs, and inhibiting them from binding protein coding genes. By having expression data, true interactions during differentiation can be identified from sequence based predictions.

The prediction algorithm Targetscan [142] was used to identify microRNA targets for the 64 differentially expressed microRNAs (Figure 3.9), leading to the identification of 5184 potential target sites in 851 unique mRNAs. Importantly, these genes are significantly enriched in DE cluster #1, and deficient in DE cluster #2 (Figure 3.6) (Fisher's exact test p-value < 0.05) Table 4.1 indicating that microRNAs may have an important impact on overall gene expression trends

Targets of DE microRNAs are over represented in cluster #1 and under represented in cluster #2			
DE cluster (Figure 3.6)	odds.ratio	p.value.greater	p.value.less
clust1	1.21	**0.01**	0.99
clust2	0.83	0.99	**0.02**
clust3	0.00	1.00	0.33
clust4	0.73	0.94	0.09
clust5	0.68	0.85	0.29
clust6	1.21	0.34	0.77
clust7	1.47	0.09	0.95
clust8	0.45	0.89	0.39

Table 4.1: microRNA Target Genes in Enriched in Cluster of Up-regulated Genes during Differentiation. Using Targetscan, target genes were predicted for each differentially expressed (DE) microRNA. A Fisher's exact test was used to test for over or under representation of a gene cluster (Figure 3.6) in the list of predicted targets. There are three data columns. Odds.ratio: odds of drawing a gene from that cluster in the list of interest (predicted targets) compared to a background list (rat genome), p.value.greater: probability that the genes in that cluster are over represented in the list of interest, p.value.less: probability that the genes in that cluster are underrepresented in the list of interest.

during differentiation. Of the genes in DE cluster #1 (which have progressively decreasing expression), 32% are predicted to be direct targets of microRNAs that are part of DE cluster #2 (progressively increasing).

microRNA target predictions were then filtered for only those interactions that involved genes in the regulatory network, and microRNAs were incorporated into the network if their expression profile was inversely correlated with the predicted target mRNA (Figure 4.6). This lead to the identification of eight microRNA:mRNA interactions involving seven microRNAs and four genes.

The hypothetical network (Figure 4.6) suggests that expression of *Egr1* early in development maintains expression of *Klf4 [143].* Similarly to the parotid, *Egr1* is highly expressed in hematopoietic stem cells and decreases on differentiation [144]. *Klf4* is involved in stem cell maintenance and inhibits terminal differentiation [145]. As development proceeds, the observed increases of miR-29c, miR-375, miR-148, and miR-200c may drive the observed decreased expression of *Klf4* mRNA. *Sox11* is initially strongly expressed, and is an activator of the *Pax5* gene, which is an inhibitor of *Xbp1* transcription factor gene expression [146]. Increasing expression of miR-200a and miR-30a may combine to repress expression of *Sox11*, thereby decreasing stimulation of *Pax5*. *Prdm1* (*Blimp1*) mRNA increases transiently during mid-differentiation, which may inhibit *Pax5*. The *Prdm1-Pax5-Xbp1* genes are reported to form a genetic switch which regulates the timing of differentiation of antibody secreting plasma

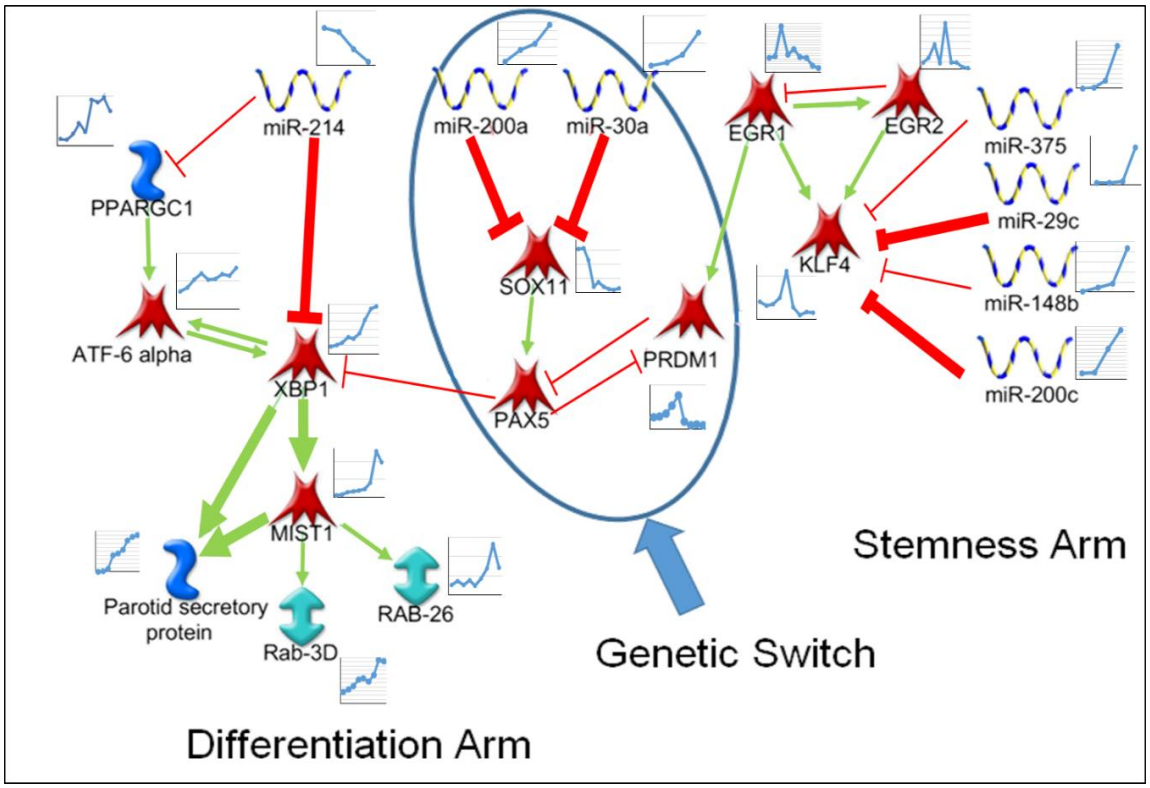

Figure 4.6: Gene Regulatory Network Driving Expression of Terminal Differentiation Genes. Network containing predicted edges from both knowledge-based resources and in silico based predictions of microRNA:mRNA interactions. Edges connecting nodes are either a green arrow indicating activation or a red line indicating repression. A small graph next to each node plots the relative expression for that gene across differentiation. The network is divided into three main arms, a stemness arm on the right, a genetic switch in the middle, and a differentiation arm of the left where transcription factors such as Xbp1 and Mist1 drive expression of differentiation markers such as PSP.

B cells [147, 148]. This genetic switch has not previously been seen in parotid differentiation, and may contribute to the observed increase of *Xbp1* mRNA.

The observed decrease of miR-214 which may target *Xbp1* mRNA, combined with the positive feedback loop between *Xbp1* and *Atf6* alpha [149, 150], would help maintain the observed elevated expression of *Xbp1*. Down-stream of Xbp1, along with PSP, is Mist1 (Bhlha15). Xbp1 is known to regulate the expression of transcription factor Mist1. This basic helix-loop-helix family member is highly expressed in serous acinar cells as well as other protein secreting cells, such as plasma cells. Mist1 is considered necessary for plasma cell differentiation, and in knockouts acinar cell maturation is impaired during development leading to disorganized cells that lack cytoplasmic and plasma membrane polarity, and contain far fewer secretory granules [125, 151, 152]. Among Mist1 target genes are Rab3d and Rab26 which are necessary for secretory vesicle maturation. All three of these genes (Mist1, Rab3d, and Rab26) significantly increase (at the mRNA level) during differentiation.

4.2.4 Testing Transcription Factor and MicroRNA Interactions

Several of the proposed regulatory interactions (edges) of this network were directly tested by transfection experiments. According to the network, *Xbp1* is directly up-stream of *Mist1* (Bhlha15) [153] [132]. *Mist1* and *Xbp1 in vivo* expression increases 21-fold and 6.5-fold respectively between the earliest and latest time points (Figure 4.7). Their expression pattern was significantly correlated across the time points measured

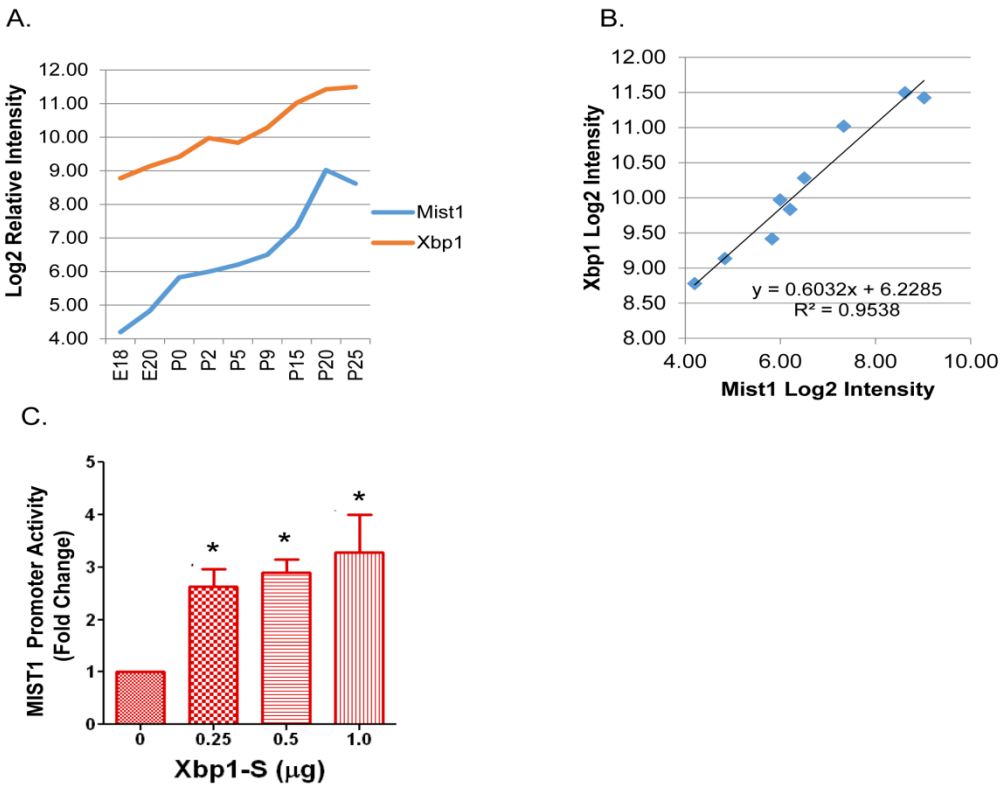

Figure 4.7: Xbp1 regulates Mist1 Expression. A.) Both Xbp1 and Mist1 increase expression significantly during acinar cell differentiation. B.) Mist1 and Xbp1 expression is significantly correlated. C.) The Mist1 promoter was cloned in front of a luciferase vector and co-transfected in ParC5 cells with an expression vector containing the spliced version of Xbp1 (Xbp1-s). Activity significantly increased with increasing concentration of Xbp1-s (n=3).

(correlation coefficient= 0.97, p-value= $1.4*10^{-5}$) (Figure 4.7). Transfections of a *Mist1* promoter (-500 - +15) luciferase construct into immortalized rat parotid acinar cells (ParC5 cell line) confirmed direct activation of the *Mist1* promoter by the spliced (activated) form of *Xbp1* (Figure 4.7). This experimentally supports the predicted interaction in this network. Possible regulation of the *Psp* gene by the *Mist1* transcription factor was also investigated. This interaction was not predicted by a knowledge-based algorithm, but to further identify novel interactions with terminal differentiation markers, a region of the PSP gene containing two E-box sites was cloned into a luciferase reported in order to test activation. These two consensus sequence sites are not in the promoter region. Though the promoter is the most common binding site, transcription factors have also been shown to regulate gene expression through binding sites within introns. Co-transfection of *Mist1* cDNA did not lead to activation of the *Psp* 500 bp promoter alone(not shown), nor did it activate a 1.5 kb *Psp* promoter construct even in the presence of the *Mist1* dimerization partner *Tcf3*/E2A [154] (Figure 4.8). The E-box regions flank exon three in the PSP gene, and this promoter+intron/exon construct was significantly activated 2.3-fold by co-transfection with *Mist1* and *Tcf3* cDNAs (p=0.0227), whereas the 1.5 kb *Psp* promoter was not activated (Figure 4.8). Neither *Tcf3* nor *Mist1* alone significantly activated the *Psp* reporter construct (not shown). *Tcf3* was included in these experiments as a heterodimerization partner with *Mist1*. Since *Tcf3* mRNA was not differentially expressed (p=0.25), it is not included in the proposed regulatory network, however, it is constitutively expressed throughout

A.

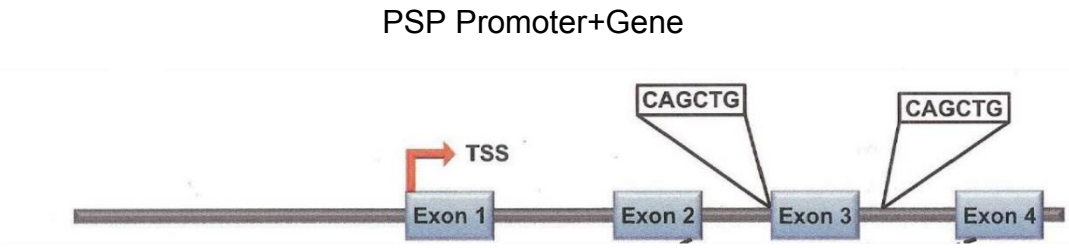

B.

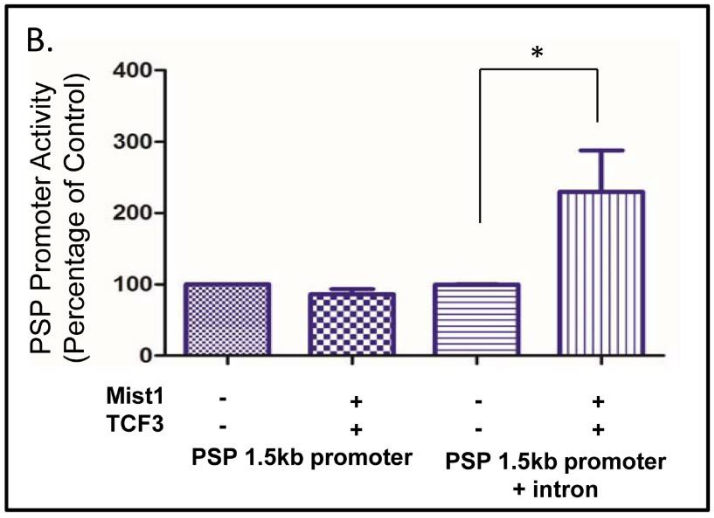

Figure 4.8: Mist1 and Tcf3 Activate PSP Expression from the Introns. A.) The promoter region of PSP does not contain a Mist1 consensus sequence, however, there are two E-box sites in the introns flanking exon 3.B.) Two regions of the PSP gene were cloned up-stream of a luciferase reporter. In the first clone, only 1.5kb of the promoter was used (PSP 1.5kb promoter), and in the second, regions of the PSP gene containing the introns of interest were included (PSP 1.5kb promoter + introns). These clones were co-transfected with expression vectors containing Mist1 and Tcf3. These transcription factors activated expression only in the clone containing the introns (n=4, p-value = 0.26).

acinar cell differentiation. While *Tcf3* is typically present in most cell types, it apparently has inadequate levels in the ParC5 cells used for transfections. Overall, these experiments indicate that the increase of *Mist1* expression during acinar differentiation contributes to the increase of *Psp* gene expression through binding sites flanking exon 3. Several microRNA:mRNA interactions were also tested using a luciferase reporter. Four microRNAs, which increased expression late in differentiation, are predicted to target *Klf4* mRNA. Figure 4.9 shows the Log2 relative expression of miR-29c during acinar differentiation compared to that of *Klf4* mRNA. *Klf4* does not decrease in expression until stage 3 in postnatal development when miR-29c increases. Expression of these two genes are negatively correlated across acinar differentiation (Pearson's r= -0.79; p = 0.011). In order to test potential microRNA target genes, cells were co-transfected with a microRNA mimic and a luciferase expressing plasmid containing a 3'UTR of interest. Transfection experiments confirmed repression of rat *Klf4* by miR-29c (Figure 4.9). Several other microRNAs are predicted to target *Klf4*, among them miR-200c, which has relatively low expression in the embryo and early postnatal gland but significantly increased in expression by P15. It has been shown that *Klf4* is targeted by miR-200c [155, 156], and luciferase assays confirmed this interaction in a parotid cell line (Figure 4.9).

Xbp1 mRNA increased expression 6.5-fold across differentiation, while its targeting miR-214 decreased more than 10-fold (Figure 4.9). *Xbp1* 3'UTR contains a known miR-214 binding site in humans [157]. Although this sequence is not conserved in rats, the rat 3'UTR contains an alternate miR-214 predicted

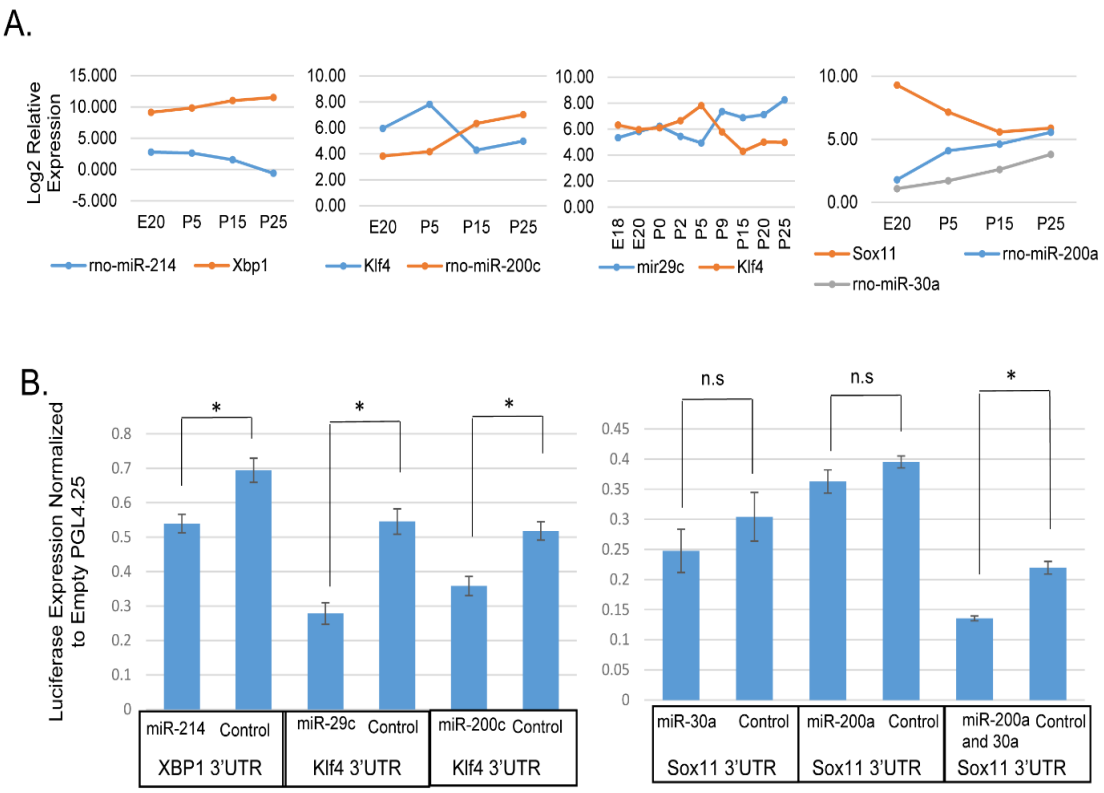

Figure 4.9: Several microRNAs Target Transcription Factors in the Network. A.) log2 expression is plotted for five of the network microRNAs (Mir-214, miR-200c, miR-29c, miR-200a, and miR-30a) and their corresponding predicted target (Xbp1, Klf4, and Sox11) respectively. Each of the microRNA:mRNA pairs is inversely correlated. B.) Each of the 3'UTRs containing the microRNA target was cloned downstream of a luciferase reporter, and was co-transfected in ParC5 cells with a microRNA mimic. Expression was normalized to renilla and to an empty (no 3'UTR) luciferase vector as in Jacobs *et. al.* [123]. Neither miR-200a nor miR-30a alone down-regulated expression from the Sox11 3'UTR but expression was inhibited when both were transfected together (n=3 for miR-29c, miR-200a, miR-200c, and miR-200a/30a) (n=4 for miR-30a and miR-214) (p = 0.014, 0.012, 0.025, 0.28, 0.23, and 0.017 respectively).

binding site, which was cloned into a reporter, and co-transfection experiments demonstrate repression of rat *Xbp1* by miR-214 (Figure 4.9).

Sox11 expression decreased significantly after birth, and it is predicted to be targeted by several differentially expressed microRNAs. Assays with miR-200a, and miR-30a did not show any repression of the reporter, however, a construct containing binding sites for both miR-200a and miR-30a was repressed when co-transfected with both microRNAs (Figure 4.9), indicating that these microRNAs are acting cooperatively to repress expression. Taken together, these microRNA transfection experiments provide experimental support for five of the edges in the proposed network.

4.3 Discussion

In this section expression measurements spanning nine time-points during acinar cell differentiation were integrated into gene regulatory networks containing both transcription factors and microRNAs. These networks were used to identify factors important for the regulation of terminal differentiation markers.

Our knowledge-based approach identified several transcription factors regulating the cargo protein gene PSP. Both Elf5 and Ese3 have been reported to activate the PSP promoter [158], but our data shows their expression changes are modest in the mature acinar cells compared to the embryo.

In order to identify major regulators of PSP, we predicted and validated several novel interactions activating the PSP promoter. Both Xbp1 and Mist1 activate

PSP expression, and, as shown in the last chapter, these two transcription factors increase significantly during differentiation.

Using these novel and knowledge-based transcription interactions along with in silico based microRNA target predictions, gene regulatory interactions driving expression of terminal differentiation genes were predicted. When expression co-variance supported the interaction, it was included in a network, leading to the identification of a gene regulatory network which drives the expression of several differentiation markers such as PSP, connexin32, Rab3d, and Rab26 (Figure 4.6).

This putative network provides a context for changes in transcription factors which regulate differentiation. The network identifies two main branches; initial expression of stemness factors (*Sox11*, *Klf4, and EGR1, none of which have been describe before in parotid differentiation*) which inhibit differentiation, and subsequent switch to an *Xbp1* pathway which drives and maintains markers of terminal differentiation. Our network suggests that Klf4 is initially stimulated by Egr1 and, remarkably, subsequently repressed by 4 different microRNAs which increase strongly in the late stages. We demonstrate that either miR-200c or miR-29c can down-regulate the expression of *Klf4*. By affecting its expression, these microRNAs could be important drivers of terminal differentiation. This is one example of the broad observation that microRNAs have extensive roles driving parotid differentiation.

Sox11 expression was elevated in embryonic stage acinar cells, decreasing dramatically immediately after birth apparently due to concerted action by both miR-200a and miR-30a. *Sox11* is important in neurogenesis and involved in stem cell survival [58], and its down-stream factor, Tead2, is involved in maintaining ES cell identity and inhibiting differentiation [159]. In our mRNA profiles, *Tead2* directly parallels *Sox11* expression across parotid differentiation. Hence, repressing *Sox11* promotes differentiation and also diminishes a stemness program. *Sox11* directly activates transcription of the *Pax5* gene [146]. *Sox11* is not expressed in normal lymphoid progenitor cells, however, in mantle cell lymphoma tumors it activates *Pax5* thereby blocking differentiation [146]. While *Pax5* probes were not present in the microarray used in the current experiments, we infer that its expression decreases downstream of *Sox11* expression changes. Pax5 is a transcriptional inhibitor of *Xbp1*, and decreasing its expression would contribute to *Xbp1* activation. The *Prdm1-Pax5-Xbp1* genetic switch is well characterized in differentiating immune plasma cells [147, 148], and we suggest is active in parotid acinar cells, with the additional regulation by *Sox11*.

Parotid acinar expression of *Xbp1* is apparently maintained low in the embryo by dual repression entailing both direct repression by miR-214, and indirectly by *Sox11* activating the Pax5 repressor.

Downstream of *Xbp1*, the serous exocrine specific transcription factor *Mist1* is up-regulated. We confirm direct regulation of the *Mist1* promoter by *Xbp1* in a parotid cell line (Figure 4.7). Xbp1 and Mist1 likely work as 'scaling' factors, a

concept developed by Mills *et. al.* [160] which contributes to quantitative differentiation.

CHAPTER 5: GENE REGULATORY NETWORK AND DIFFERENTIATION *IN VITRO*

5.1 Introduction

In the previous section single edges of a gene regulatory network were validated *in vitro*. In this section multiple successive interactions (edges) will be tested in a cell culture model of parotid acinar cells.

The ParC5 cell line was derived from rat parotid acinar cells [63], and have since lost expression of many terminal differentiation genes (Figure 5.1). This ability to spontaneously de-differentiate in culture has made acinar cells difficult to maintain. The ability to drive differentiation in culture would be beneficial towards the goal of maintaining the acinar cell phenotype in culture and using these cells to construct artificial glands.

Work with the similar cell line ParC10 has shown increased differentiation when cultured on matrigel. The 3D spheres that form express polarized tight junction (TJ) proteins, and increased expression of aquaporin5 (Aqpr5). However this does not translate into other three dimensional culture matrices such as fibrin hydrogels, which have been used in the formation of artificial organs (because matrigel is tumorigenic it cannot be used for this purpose). The ability of

transcription factors to drive differentiation in these cells has not been investigated.

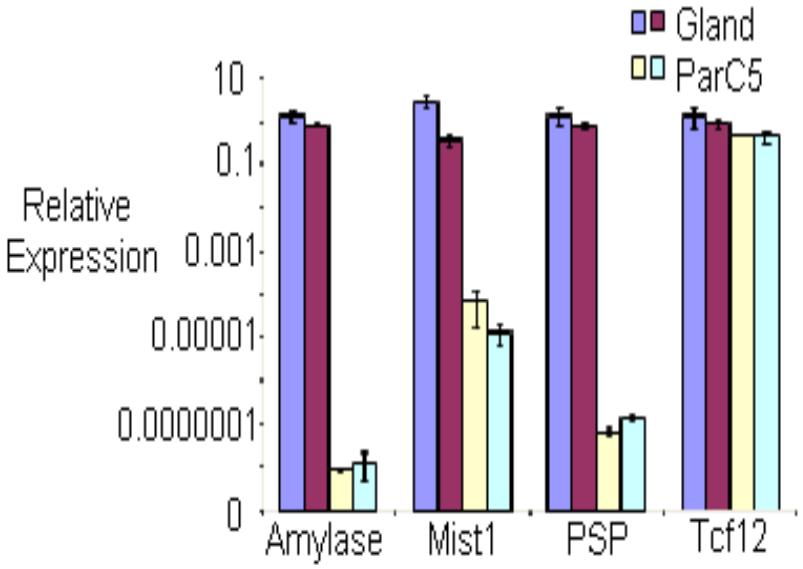

Figure 5.1: ParC5 Cells are No Longer Terminally Differentiated. Gene expression was compared between ParC5 cells and an adult parotid gland (rat) by qPCR. Expression was normalized to Gapdh. Relative expression is plotted in a log10 scale. Both Amylase and PSP are reduced more than 100,000-fold and Mist1 more that 10,000-fold while the ubiquitous transcription factor Tcf12 remains unchanged.

The gene regulatory network from the previous section includes transcription regulatory interactions that drive the expression of terminal differentiation genes. The TF Xbp1 and Mist1 seem to be especially involved in acinar cell specific expression *in vivo*, and this section addresses the hypothesis that they can also drive expression *in vitro*.

A method for activating Atf6 and Xbp1 was investigated in ParC5 cells. Both are activated as part of the unfolded protein response (UPR). Atf6 protein is cleaved into an active form which can then up-regulate transcription. Xbp1 has a unique mechanism of activation. It is actually ubiquitously transcribed in cells and is translated into a weakly activating transcription factor. However, when the endoribonuclease Ire1 is activated in response to ER stress, 26nt of Xbp1 mRNA is spliced out in the cytoplasm leading to the translation of a highly active transcription factor. In our study we used the ER stress agonist tunicamycin to induce splicing of endogenous Xbp1and activation of Atf6 in all cells which should lead to a robust response (Figure 5.2).

Measurements of down-stream effectors showed that Xbp1 can robustly induce expression of Mist1. Other genes further down-stream in the network such as PSP, Connexin32, and Rab3d are not induced upon Xbp1 activation suggesting there are additional unknown factors, possibly epigenetic, that are regulating transcription of differentiation genes.

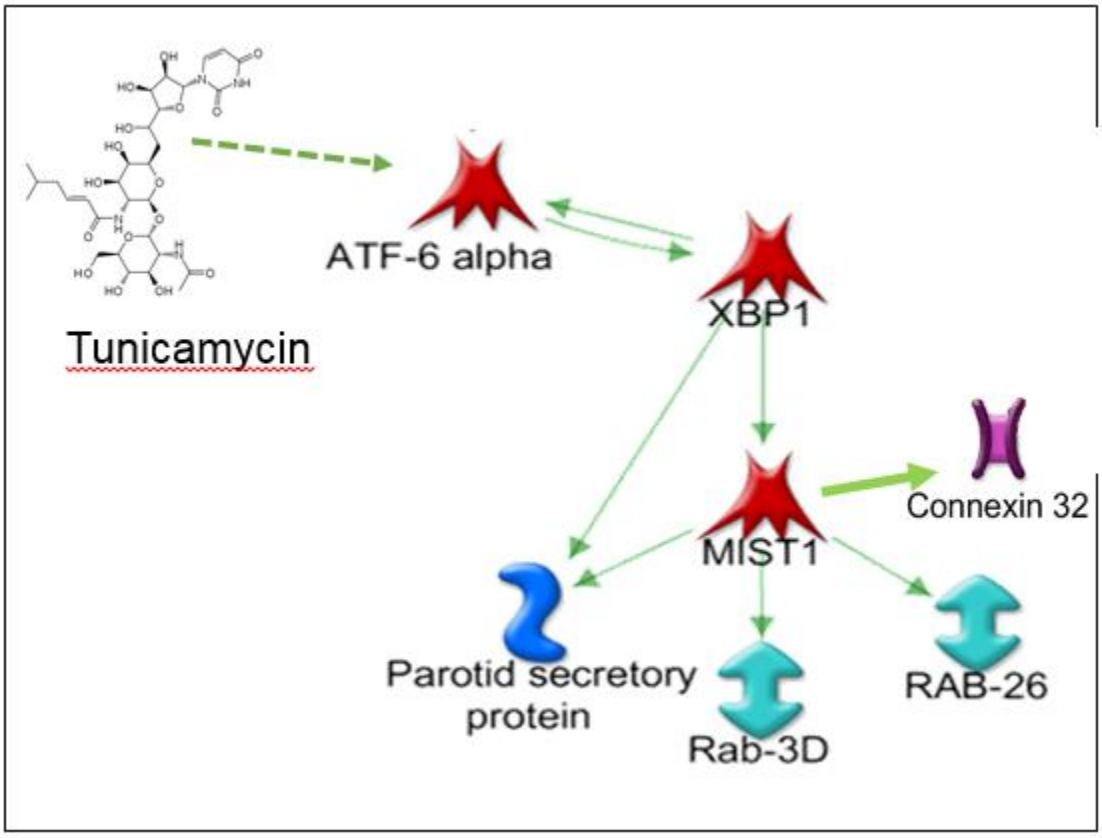

Figure 5.2: Tunicamycin Treatment will Activate Endogenous Transcription Factors in the Differentiation Arm of the Network: Tunicamycin is an activator of the unfolded protein response. It will activate the transcriptional activity of Atf6 to increase Xbp1 expression and the RNase activity of Ire1 which will cleave Xbp1 mRNA into the active form. Based on our network model (Figure 4.6) this will increase the expression of differentiation markers down-stream.

5.2 Results

5.2.1 Tunicamycin Treatments

ParC5 cells were maintained in supplemented DMEM/F12 media as described by Quissell *et. al.* [63]. After 8 hours of 1 ug/ml tunicamycin treatment (or DMSO for controls), cells were allowed to recover overnight (~ 16 hours) before RNA was extracted and gene expression was measured by qPCR. The $2^{-\Delta\Delta CT}$ method was used to calculate normalized relative gene expression [124]. Rplp2 was used for normalization as its expression was found to be the most stable of a selected panel of housekeeping genes. Differential expression was evaluated using a t-test with a p-value < 0.05 considered significant.

Both Xbp1 and Mist1 expression increases significantly after tunicamycin treatment (Figure 5.3). Total Xbp1 mRNA amount increases ~4-fold, and its activity as a transcription factor is most likely increasing much higher due to the fact that tunicamycin not only increases Xbp1 transcription (through activation of Atf6), but also its splicing to an active form (through activation of the endoribonuclease Ire1). Downstream of Xbp1, Mist1 expression increases more than 100-fold. Knock down of Xbp1 by siRNA, confirms that it regulates Mist1 expression in ParC5 cells (Figure 5.4). The dramatic > 100-fold increase of Mist1 during tunicamycin treatment is completely dependent on Xbp1 increase.

Cells were pretreated with siRNA targeting either Xbp1 or a non-targeting control before treatment with tunicamycin or DMSO. Xbp1 expression was reduced 80% by the siRNA regardless of treatment with either tunicamycin or DMSO. Mist1

A.

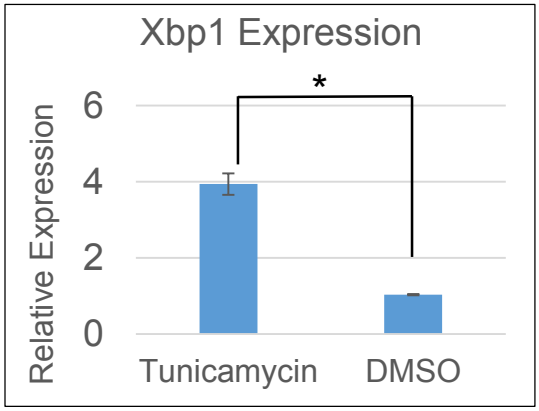

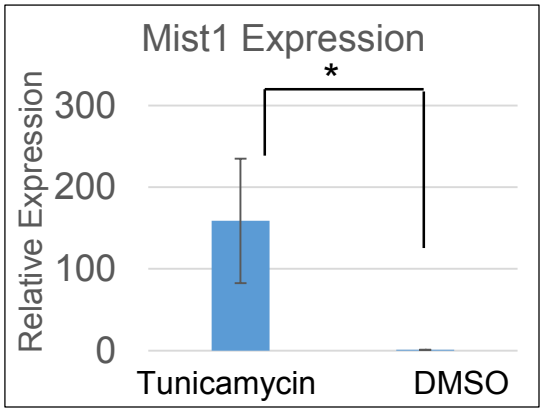

B.

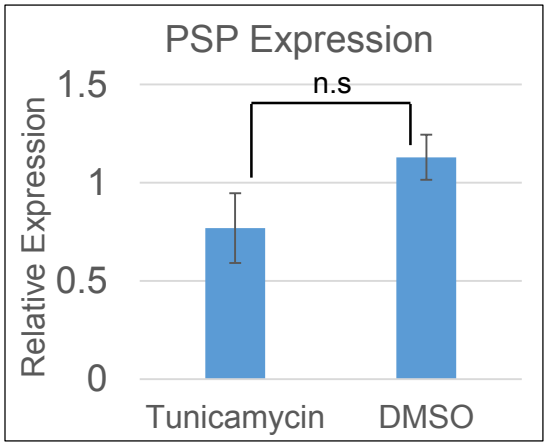

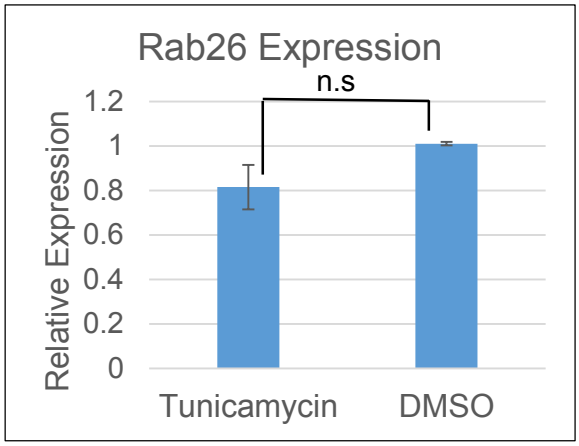

C.

Treatment	Connexin 32 (CT)
Tunicamycin	Undetermined
DMSO	Undetermined
0.25uM 5Aza + DMSO	Undetermined
0.25uM 5Aza + Tun	Undetermined

Figure 5.3: Tunicamycin Dramatically Increases Xbp1 and Mist1 but not PSP, Rab26, or Connexin32. ParC5 cells were treatment with 1µg/ml tunicamycin for 8 hours, and gene expression was measured 16 hours later. Expression was normalized to Rplp2. A.) Both Xbp1 and Mist1 expression increased after treatment compared to a DMSO control (n=3, p-values= 0.03, and 0.025). Mist1 expression increased more than 100-fold. B.) Neither PSP nor Rab26 showed any change in expression after tunicamycin treatment. (n=3, p-values= 0.18, and 0.3) C.) Connexin32 was not detected by qPCR under any treatment. Along with tunicamycin cells were also treated with 5-Aza-2′-deoxycytidine, a DNA methyltransferase inhibitor which has been shown to restore expression of some genes silenced by promoter methylation.

expression was reduced 80% by the siRNA, but only in cells that also received tunicamycin treatment. In the DMSO treatment group, Mist1 expression did not change when pretreated with siRNA targeting Xbp1 (Figure 5.4). This indicates that the increase in Mist1 expression after tunicamycin treatment is due to promoter activation by Xbp1, and there is also a low basal level of Mist1 expression that is independent of Xbp1.

Several genes down-stream of Xbp1 and Mist1 were also measured after tunicamycin treatment. The cargo protein and terminal differentiation marker PSP did not change expression, and the gap junction protein connexin32 was undetectable by qPCR in either condition (Figure 5.3). This indicates there are other factors needed for promoter activation. In the case of Connexin32. We also investigated the possible role of epigenetics.

Epigenetic markers have long been known to control lineage specific gene expression. Histone modifications, largely at the promoter, can control DNA availability leading to either silencing or activation, and DNA methylation can silence nearby genes. The promoter of connexin32 has been shown to contain a CpG island, and in the liver its expression can be silenced through methylation [161]. Treatment of ParC5 cells with DNA methyltransferase inhibitors (DNMTi) was investigated as a means to reverse silencing of terminal differentiation genes.

5-Aza-2′-deoxycytidine (5-Aza) is a cytosine analog that is incorporated into DNA, and will inhibit the methyl transferase enzyme by covalently trapping it to

A.

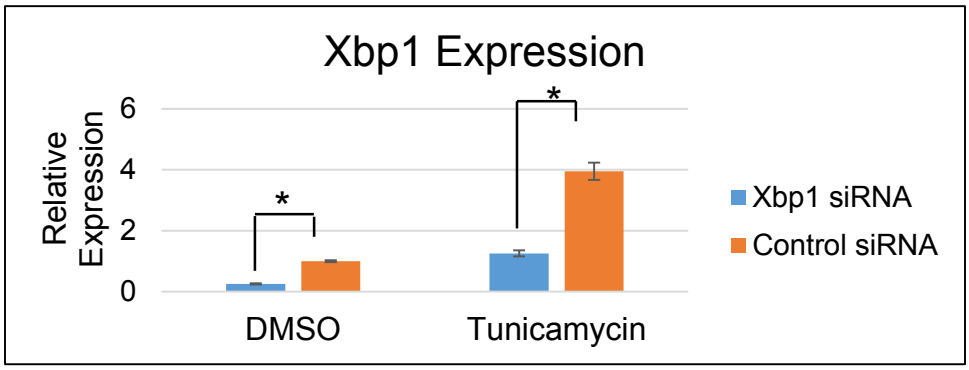

B.

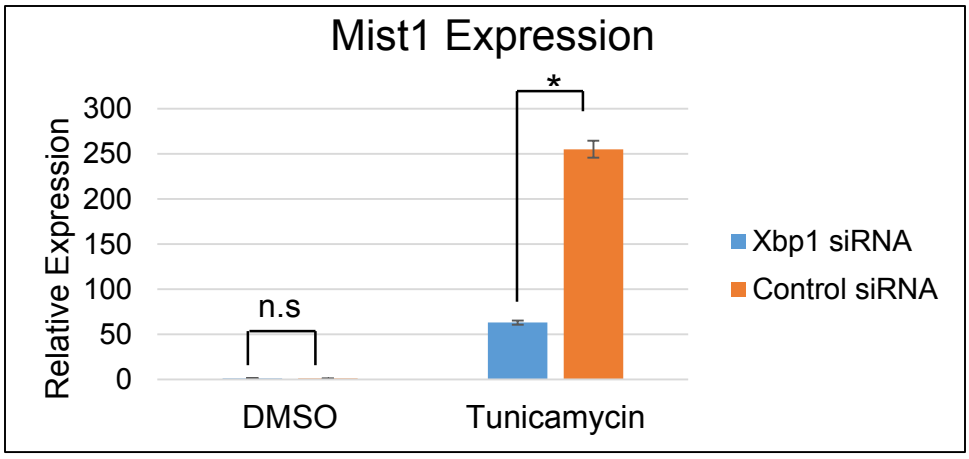

Figure 5.4 Mist1 is Regulated Downstream of Xbp1 in Cells Treated with Tunicamycin not DMSO. Cells were pre-treated with a siRNA targeting Xbp1 or a non-targeting control before tunicamycin or DMSO. A.) Xbp1 expression was measured by qPCR. Expression is significantly reduced after pre-treatment with the Xbp1 siRNA compared to a control siRNA regardless of whether the cells were subsequently treated with DMSO or tunicamycin (p-values= 0.00004, and 0.003). B.) Mist1 expression was measured by qPCR. Expression is significantly reduced after pre-treatment with Xbp1 siRNA compared to control siRNA only when cells were subsequently treated with tunicamycin (right panel). Expression remained unchanged in cells treated with DMSO following siRNA (left panel). (p-values= 0.086, and 0.0025)

the DNA. While this has been shown in many cell types to produce a hypomethylated genome, it has the potential to be toxic due to the formation of DNA lesions during replication.

ParC5 cells were treated with 0.25 μM of 5-Aza over 24 hours, and then were treated with tunicamycin. Expression of Connexin32 was measured by qPCR. As seen in Figure 5.3, Connexin32 remained undetected in all conditions.

Because of the sensitivity of these cells to 5-Aza, relatively low concentrations and a short duration of treatment was used. DNA methylation is generally not occurring continuously, but only during DNA replication and so several replication cycles of treatment is needed to induce a hypomethylated genome. The non-responsiveness of the genes measured could be due to the inability of this short treatment to induce hypomethylation.

Surprisingly, treatment with tunicamycin resulted in decreased Rab3d expression (Figure 5.5), and no change in Rab26 (Figure 5.3). Rabs are proteins on the cytosolic side of the secretory vesicle which direct the secretory pathway. Our network predicts that Mist1 activates expression of Rab3d and Rab26 in acinar cells, and that these gene products are necessary for the differentiated phenotype. The ability of tunicamycin to drastically increase Mist1 expression suggests that it should also increase expression of downstream effectors, but this does not seem to be the case in ParC5 cells.

The possibility of Mist1 acting as a repressor in these cells was next investigated. Though Mist1 commonly activates gene expression, it has also been shown to

A.

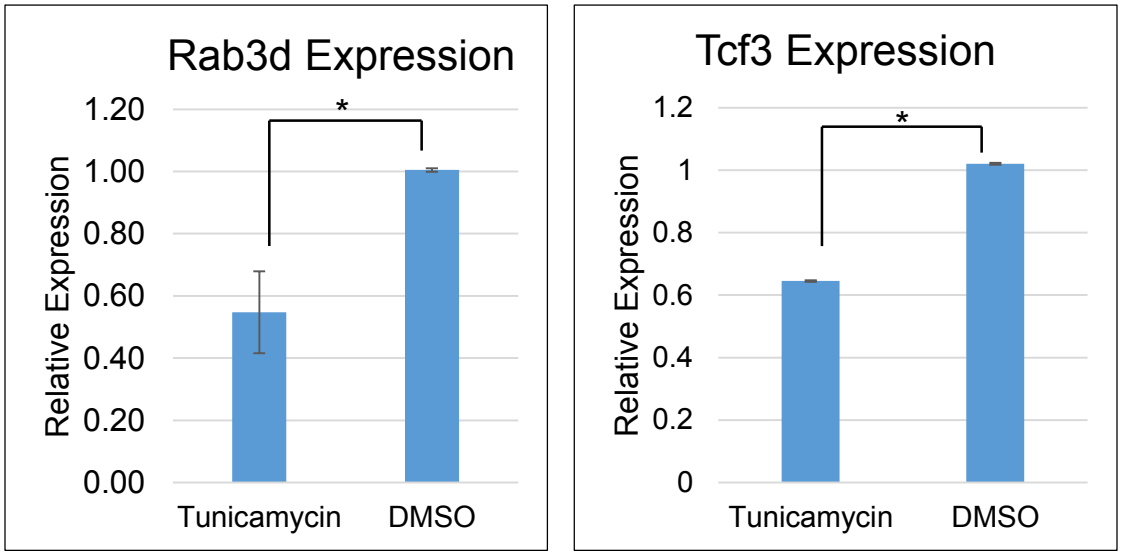

B.

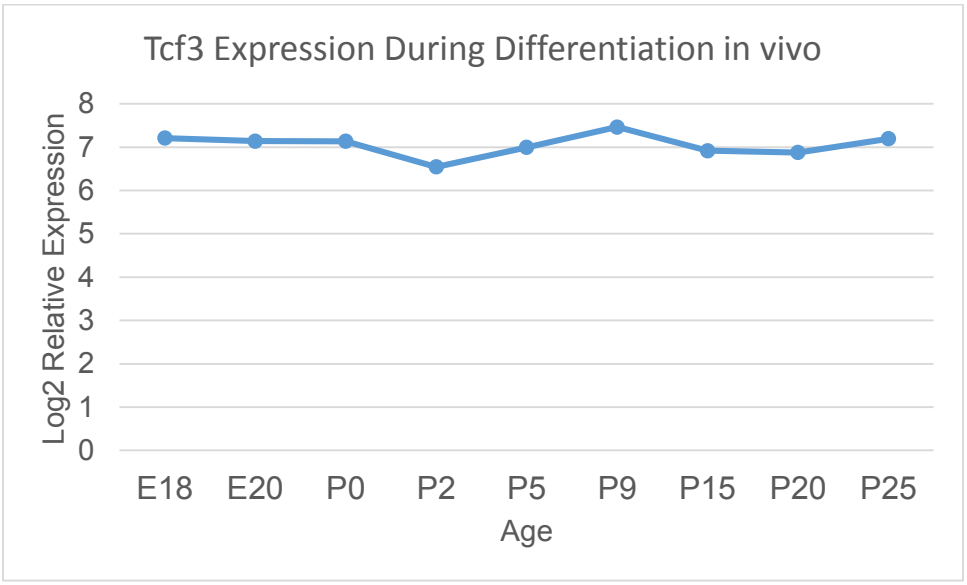

Figure 5.5: Rab3d and Tcf3 Expression is Down-regulated by Tunicamycin. A.) ParC5 cells were treatment with 1µg/ml tunicamycin for 8 hours, and gene expression was measured 16 hours later. Expression was normalized to Rplp2. Rab3d and Tcf3 expression is significantly down-regulated after treatment with tunicamycin (n=3. P-value = 0.006, and 0.03). B.) Tcf3 expression during differentiation by microarray.

repress expression in some contexts, but the exact mechanism is unknown[152]. ParC5 cells were transfected with an expression vector containing the Mist1 coding region, and qPCR was used to measure the expression of Rab3d and Rab26. Both Rab3d and Rab26 expression was increased after transfection of Mist1 (Figure 5.6) indicating that it is acting as a transcriptional activator and not a repressor.

We next examined the possibility that Mist1 must form a heterodimer in order to activate transcription. Mist1 is a member of the basic helix-loop-helix family of transcription factors which commonly bind DNA as heterodimers. Mist1 has been shown to form a dimer with Tcf3 which can bind E-box regions of DNA, and our work suggests that a Mist1/Tcf3 dimer activates PSP expression (Figure 4.5). However, the functions of this dimer remain largely untested in the literature.

Tcf3 expression was measured by qPCR, and was shown to decrease after treatment with tunicamycin (Figure 5.5). If a Mist1/Tcf3 heterodimer is required to activate Rab3d expression then decrease in Tcf3 expression could result in decreased dimer formation regardless of the expression increase in Mist1, and this could be causing the reduction in Rab3d expression.

Our *in vivo* microarray measurements show that Tcf3 is moderately expressed at every time point measured during differentiation (Figure 5.5) indicating that a Mist1/Tcf3 dimer could be biologically relevant for *in vivo* development.

Tcf3 either alone or with Mist1 was transfected into ParC5 cells and Rab3d expression was measured by qPCR (Figure 5.7). Transfection of Tcf3 alone did

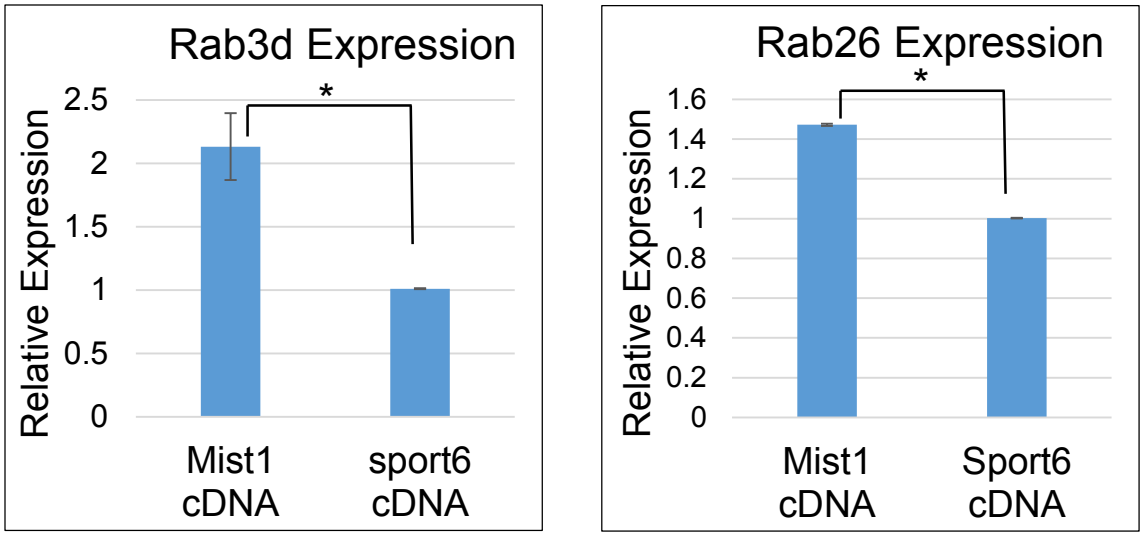

Figure 5.6: Mist1 is not acting as a Repressor in ParC5 Cells.

An expression vector containing Mist1 was transfected into ParC5 cells. Gene expression was measured by qPCR 24 hours later. Expression was normalized to Rplp2. Both Rab3d and Rab26 expression increased in cells transfected with Mist1 compared to an empty vector. (Fold-change= 2, and 1.4 respectively, n=3, p-values= 0.016, and 0.008).

A.

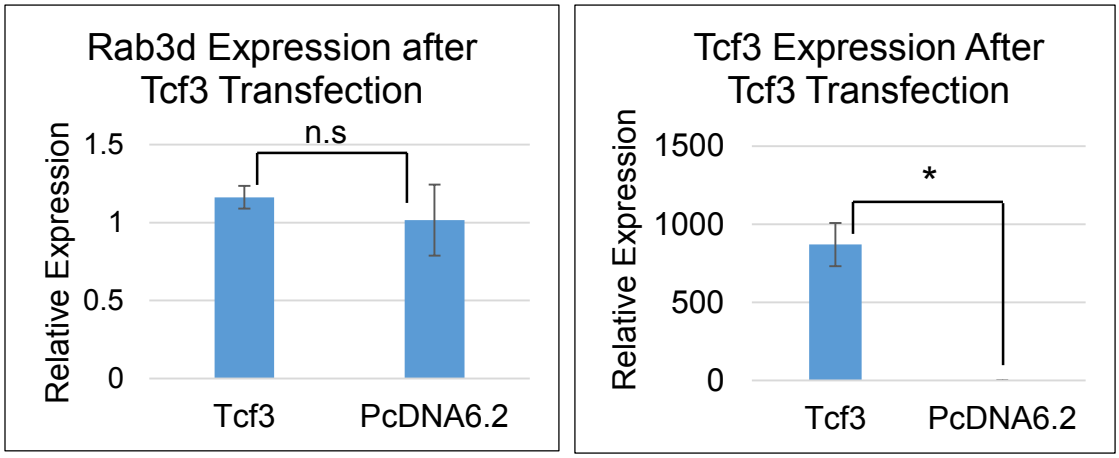

B.

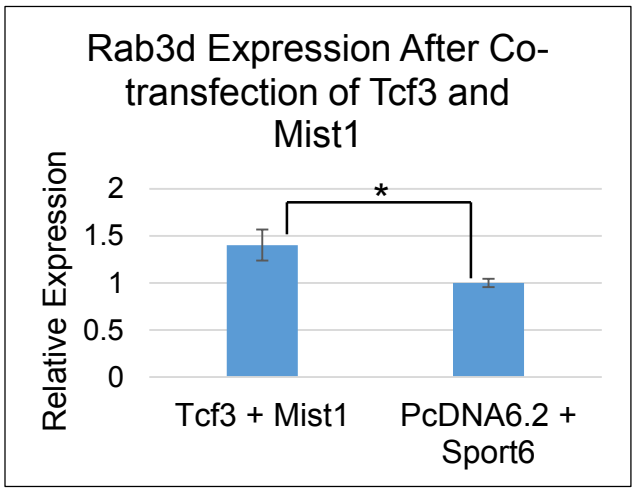

Figure 5.7: Tcf3 does not contribute to Mist1 Activation of the Rab3d Promoter. A.) ParC5 cells were transfected with an expression vector containing the transcription factor Tcf3 and expression was measured by qPCR 24 hours later. Rab3d expression was not changed significantly by Tcf3 transfection alone (n=3, p-value= 0.4). B.) Mist1 and Tcf3 were co-transfected into ParC5 cells, and expression of Rab3d was measured by qPCR 24 hours later. Rab3d expression increased significantly. (Fold-change =1.4, n=3, p-value = 0.05), but its expression did not increase anymore that with Mist1 alone (Figure 5.6).

not alter Rab3d expression which could be due to the low basal levels of Mist1 in untreated cells. When co-transfected, Rab3d expression did not increase more than Mist1 alone, indicating that heterodimer formation is likely not necessary for promoter activation of Rab3d. Mist1 could be acting as a homodimer as it has been reported to do in the pancreas [162].

Rab3d expression decrease could be due to other factors that are impacted by tunicamycin treatment. Tunicamycin disrupts protein folding by inhibiting n-linked glycosylation, and this triggers the ER stress response which activates Xbp1. However, inhibition of glycosylation by tunicamycin is also known to alter the activity of glycosylated transcription factors (e.g. SP1) [163, 164]. This is not likely having an impact of Mist1 activity, which has no known or predicted glycosylation sites, but there could be other transcription factors acting on the Rab3d promoter which are impacted by altered glycosylation states.

5.3 Discussion

In this section, several successive edges of the network were validated in a cell culture system. Treatment of ParC5 cells with the UPR activator tunicamycin activated the transcription of both Xbp1 and Mist1, transcription factors that we identified in the previous sections as important for acinar cell differentiation.

Overall, this sections validates both Xbp1 and Mist1 activation downstream of Atf6 in our predicted network, and shows that Mist1 activation after stimulation is due nearly entirely to Xbp1. This supports our hypothesis that Xbp1 is the main driver of Mist1 expression during differentiation. We showed that Xbp1 is capable

of strong Mist1 induction, which is what we observe from our *in vivo* measurements.

There also seems to be a low baseline Mist1 expression that is Xbp1 independent suggesting the presence of other minor regulators. These regulators may or may not be involved in Mist1 expression *in vivo* but they could be used to explain the different acinar phenotypes that are seen in Mist1 $^{-/-}$ mice,, where the parotid acinar cells lack polarity and are completely disorganized [151], and Xbp1 $^{-/-}$ mice where acinar cells in the salivary glands are smaller than wild type but are not structurally any different [165]. Measuring Mist1 expression in Xbp1 $^{-/-}$ cells could help to establish alternative regulation.

Genes further downstream in the network (i.e. PSP, Connexin32) were not activated by tunicamycin treatment. This is probably due to unknown factors that are involved in full expression of the network. While our microarray and qPCR data allowed us to measure gene expression changes on a large scale, it does not capture all the information about gene expression activation. Our dataset does not contain information about epigenetic changes during differentiation, any signaling pathways coming from outside the cell, or any post-transcriptional modifications that could change transcription factor activation. A combination of these factors is most likely involved in the gene regulatory network (Figure 3.6) during differentiation.

CHAPTER 6: SUMMARY

This is the first study to measure comprehensive changes in gene expression during parotid acinar cell differentiation. The control of this cell type's differentiation is poorly understood, and this study increases our knowledge greatly. The networks identified could potentially be used as drivers of differentiation in progenitor cells, which would be a step forward in being able to regenerate salivary gland for patients suffering chronic xerostomia.

In the first results chapter (chapter 3), both mRNA and microRNA expression were measured at several time-points spanning differentiation. This allowed the identification of complex expression patterns, including the novel involvement of Pparg, as well as the identification of mRNA:microRNA interactions which had not been studied in the salivary gland differentiation before.

One of the main goals of Systems Biology is to use big datasets to generate novel hypothesis. By integrating mRNA and microRNA data, we were able to identify two separate microRNAs families targeting the pro-mitogenic, IGF2 at different levels of expression, leading to the hypothesis that microRNA expression controls cell cycle exit which could be necessary for driving differentiation. miR-375 represses the transcription factor Plag1, which is an activator of the IGF2 promoter, and several members of the let-7 family repress

IGF2BP2 an mRNA binding protein that promotes IGF2 translation. This hypothesis could be tested *in* vivo using microRNA knockout mice, or a constitutively active IGF2 transgene, and potentially these microRNAs could be used to study differentiation *in* vitro.

This study is the first to identify stages specifically in the acinar cell lineage, indicating that large gene expression changes occur rapidly in these cells at specific time points as they differentiate. Importantly, strong changes of gene expression were observed even several weeks after birth, the late stage of differentiation, emphasizing the prolonged nature of parotid differentiation.

Clustering differentially expressed genes, combined with GO and transcription factor enrichment identified for the first time the prevailing pathways and regulatory genes during differentiation. Surprisingly, a novel role was predicted for the transcription factor PPARg. Its expression, along with 19 of is downstream effectors were transiently up-regulated mid-way through differentiation. The transcription factor targets of both Xbp1 and Mist1 are enriched in a cluster of genes that increase during differentiation.

64 microRNAs are differentially expressed during differentiation (52 are up-regulated and 12 are down-regulated). These include miR-375 which increases more than 800-fold, and likely inhibits Plag1 expression, making it an important regulator of proliferation in the postnatal period and possibly of differentiation by inhibiting mitogenic factors.

In chapter 4, mRNA and microRNA expression measurements were integrated into a model gene regulatory network driving the expression of terminal differentiation markers PSP, Rab3d, Rab26, and Connexin32. This network incorporates three main arms.

In the pro-stemness arm, pro-stem cell transcription factors such as Klf4 and Sox11 are expressed relatively highly in the embryo, and decrease during differentiation due to targeting by several microRNAs. As shown in chapter 3 with the let-7 family, several microRNAs are acting together to regulate a target gene. In the genetic switch, expression of Pax5 decreases across differentiation due to decreased expression of Sox11 and transient up-regulation of Prdm1 which represses expression. Finally, in the pro-differentiation arm, Xbp1 expression increases due to decreased repression by Pax5 and miR-214. At the same time, Xbp1 expression is activated by increasing Atf6. Terminal differentiation markers are activated downstream of Xbp1 and Mist1.

These transcription regulatory networks are likely necessary for promoting differentiation in a progenitor cell or a stem cell, and would need to be activated in cells used for salivary regeneration. This network provides several prospective targets which could be activated (Xbp1, Mist1) or repressed (Klf4, Sox11) in order to drive differentiation in culture and regrow acinar cells for transplantation.

Individual interactions from the network were validated *in vitro* by luciferase assay, and in chapter 5, multiple steps of the network were tested at once in a cell culture model. Using tunicamycin, transcription of Xbp1 and Mist1 was

activated, but genes further downstream (PSP, Rab3d, Connexin32) were not. This could be due to epigenetic changes in the cell line used, or the absence of extracellular signaling that could be involved in differentiation *in vivo* such as signaling between the epithelium and that mesenchyme or the parasympathetic ganglion.

Future work is needed to expand this network to incorporate factors not included in the current design such as extracellular signaling pathways and epigenetic changes which are important for differentiation. Nonetheless, the genes identified in this network and in the analysis of expression changes during differentiation, provide additional targets and markers for research into bioengineering or regeneration of salivary glands.

REFERENCES

1. Tucker A, editor Salivary gland development. Seminars in cell & developmental biology; 2007: Elsevier.
2. Amano O, Mizobe K, Bando Y, Sakiyama K. Anatomy and Histology of Rodent and Human Major Salivary Glands:—Overview of the Japan Salivary Gland Society-Sponsored Workshop—. Acta histochemica et cytochemica. 2012;45(5):241.
3. Amerongen AV, Veerman EC. Saliva--the defender of the oral cavity. Oral Dis. 2002;8(1):12-22. Epub 2002/04/09. PubMed PMID: 11936451.
4. Nicolescu MI, Bucur A, Dinca O, Rusu MC, Popescu LM. Telocytes in parotid glands. Anat Rec. 2012;295(3):378-85.
5. Ball WD. Development of the rat salivary glands. III. Mesenchymal specificity in the morphogenesis of the embryonic submaxillary and sublingual glands of the rat. Journal of Experimental Zoology. 1974;188(3):277-88.
6. Denny P, Ball W, Redman R. Salivary glands: a paradigm for diversity of gland development. Critical Reviews in Oral Biology & Medicine. 1997;8(1):51-75.
7. Jaskoll T, Zhou YM, Chai Y, Makarenkova HP, Collinson JM, West JD, et al. Embryonic submandibular gland morphogenesis: stage-specific protein localization of FGFs, BMPs, Pax6 and Pax9 in normal mice and abnormal SMG phenotypes in FgfR2-IIIc(+/Delta), BMP7(-/-) and Pax6(-/-) mice. Cells Tissues Organs. 2002;170(2-3):83-98. PubMed PMID: 11731698.
8. Pattipati S, Patil R, Kannan N, Kumar BP, Shirisharani G, Mohammed RB. Effect of transcutaneous electrical nerve stimulation induced parotid stimulation on salivary flow. Contemporary clinical dentistry. 2013;4(4):427.
9. Milne R, Dawes C. The relative contributions of different salivary glands to the blood group activity of whole saliva in humans. Vox sanguinis. 1973;25(4):298-307.
10. Proctor GB, Carpenter GH. Regulation of salivary gland function by autonomic nerves. Autonomic Neuroscience. 2007;133(1):3-18.
11. Hector MP. Reflexes of salivary secretion. 1999.
12. Mackie D, Pangborn R. Mastication and its influence on human salivary flow and alpha-amylase secretion. Physiology & behavior. 1990;47(3):593-5.
13. Patel VN, Hoffman MP, editors. Salivary gland development: a template for regeneration. Seminars in cell & developmental biology; 2014: Elsevier.
14. Tamaki H, Yamashina S. Structural integrity of the Golgi stack is essential for normal secretory functions of rat parotid acinar cells: effects of brefeldin A and okadaic acid. Journal of Histochemistry & Cytochemistry. 2002;50(12):1611-23.
15. Doine AI, Oliver C, Hand AR. The Golgi apparatus and GERL during postnatal differentiation of rat parotid acinar cells: an electron microscopic cytochemical study. The journal of histochemistry and cytochemistry : official journal of the Histochemistry Society. 1984;32(5):477-85. PubMed PMID: 6143779.
16. Yamagishi R, Wakayama T, Nakata H, Adthapanyawanich K, Kumchantuek T, Yamamoto M, et al. Expression and Localization of α-amylase in the Submandibular and Sublingual Glands of Mice. Acta histochemica et cytochemica. 2014;47(3):95.

17. Gorr S-U, Venkatesh S, Darling D. Parotid secretory granules: crossroads of secretory pathways and protein storage. Journal of dental research. 2005;84(6):500-9.
18. Nashida T, Imai A, Shimomura H. Relation of Rab26 to the amylase release from rat parotid acinar cells. Archives of oral biology. 2006;51(2):89-95. doi: 10.1016/j.archoralbio.2005.06.005. PubMed PMID: 16076461.
19. Nguyen D, Jones A, Ojakian GK, Raffaniello RD. Rab3D redistribution and function in rat parotid acini. Journal of cellular physiology. 2003;197(3):400-8. doi: 10.1002/jcp.10373. PubMed PMID: 14566969.
20. Takuma T, Arakawa T, Tajima Y. Interaction of SNARE proteins in rat parotid acinar cells. Archives of oral biology. 2000;45(5):369-75.
21. Walz A, Stühler K, Wattenberg A, Hawranke E, Meyer HE, Schmalz G, et al. Proteome analysis of glandular parotid and submandibular-sublingual saliva in comparison to whole human saliva by two-dimensional gel electrophoresis. Proteomics. 2006;6(5):1631-9.
22. Hu S, Xie Y, Ramachandran P, Ogorzalek Loo RR, Li Y, Loo JA, et al. Large-scale identification of proteins in human salivary proteome by liquid chromatography/mass spectrometry and two-dimensional gel electrophoresis-mass spectrometry. Proteomics. 2005;5(6):1714-28.
23. Denny P, Hagen FK, Hardt M, Liao L, Yan W, Arellanno M, et al. The proteomes of human parotid and submandibular/sublingual gland salivas collected as the ductal secretions. Journal of proteome research. 2008;7(5):1994-2006.
24. Boehlke C, Zierau O, Hannig C. Salivary amylase-the enzyme of unspecialized euryphagous animals. Archives of oral biology. 2015.
25. Butterworth PJ, Warren FJ, Ellis PR. Human α-amylase and starch digestion: An interesting marriage. Starch-Stärke. 2011;63(7):395-405.
26. Perry GH, Dominy NJ, Claw KG, Lee AS, Fiegler H, Redon R, et al. Diet and the evolution of human amylase gene copy number variation. Nature genetics. 2007;39(10):1256-60.
27. Suzuki M, Fujimoto W, Goto M, Morimatsu M, Syuto B, Iwanaga T. Cellular expression of gut chitinase mRNA in the gastrointestinal tract of mice and chickens. Journal of Histochemistry & Cytochemistry. 2002;50(8):1081-9.
28. Yeh C-K, Dodds MW, Zuo P, Johnson DA. A population-based study of salivary lysozyme concentrations and candidal counts. Archives of oral biology. 1997;42(1):25-31.
29. Abdolhosseini M, Sotsky JB, Shelar AP, Joyce PB, Gorr S-U. Human parotid secretory protein is a lipopolysaccharide-binding protein: identification of an anti-inflammatory peptide domain. Molecular and cellular biochemistry. 2012;359(1-2):1-8.
30. Villa A, Connell CL, Abati S. Diagnosis and management of xerostomia and hyposalivation. Therapeutics and clinical risk management. 2015;11:45.
31. Cassolato SF, Turnbull RS. Xerostomia: clinical aspects and treatment. Gerodontology. 2003;20(2):64-77.
32. Sasportas LS, Hosford AT, Sodini MA, Waters DJ, Zambricki EA, Barral JK, et al. Cost-effectiveness landscape analysis of treatments addressing xerostomia in patients receiving head and neck radiation therapy. Oral surgery, oral medicine, oral pathology and oral radiology. 2013;116(1):e37-e51.
33. Saleh J, Figueiredo MAZ, Cherubini K, Salum FG. Salivary hypofunction: An update on aetiology, diagnosis and therapeutics. Archives of oral biology. 2015;60(2):242-55.
34. Bayetto K, Logan R. Sjögren's syndrome: a review of aetiology, pathogenesis, diagnosis and management. Australian dental journal. 2010;55(s1):39-47.
35. Peri Y, Agmon-Levin N, Theodor E, Shoenfeld Y. Sjögren's syndrome, the old and the new. Best Practice & Research Clinical Rheumatology. 2012;26(1):105-17.

36. Dawson L, Fox PC, Smith PM. Sjögrens syndrome—the non-apoptotic model of glandular hypofunction. Rheumatology (Oxford). 2006;45(7):792-8.
37. Grundmann O, Mitchell G, Limesand K. Sensitivity of salivary glands to radiation: from animal models to therapies. Journal of dental research. 2009;88(10):894-903.
38. Dirix P, Nuyts S, Van den Bogaert W. Radiation-induced xerostomia in patients with head and neck cancer: a literature review. Cancer. 2006;107(11):2525-34. Epub 2006/11/02. doi: 10.1002/cncr.22302. PubMed PMID: 17078052.
39. Guchelaar HJ, Vermes A, Meerwaldt JH. Radiation-induced xerostomia: pathophysiology, clinical course and supportive treatment. Support Care Cancer. 1997;5(4):281-8. Epub 1997/07/01. PubMed PMID: 9257424.
40. Konings AW, Coppes RP, Vissink A. On the mechanism of salivary gland radiosensitivity. International Journal of Radiation Oncology* Biology* Physics. 2005;62(4):1187-94.
41. Wolff A, C Fox P, Porter S, T Konttinen Y. Established and novel approaches for the management of hyposalivation and xerostomia. Current pharmaceutical design. 2012;18(34):5515-21.
42. Plemons JM, Al-Hashimi I, Marek CL. Managing xerostomia and salivary gland hypofunction: executive summary of a report from the American Dental Association Council on Scientific Affairs. The Journal of the American Dental Association. 2014;145(8):867-73.
43. Brosky ME. The role of saliva in oral health: strategies for prevention and management of xerostomia. J Support Oncol. 2007;5(5):215-25.
44. Hsiung C-Y, Ting H-M, Huang H-Y, Lee C-H, Huang E-Y, Hsu H-C. Parotid-sparing intensity-modulated radiotherapy (IMRT) for nasopharyngeal carcinoma: preserved parotid function after IMRT on quantitative salivary scintigraphy, and comparison with historical data after conventional radiotherapy. International Journal of Radiation Oncology* Biology* Physics. 2006;66(2):454-61.
45. Bhide S, Newbold K, Harrington K, Nutting C. Clinical evaluation of intensity-modulated radiotherapy for head and neck cancers. The British journal of radiology. 2014.
46. Ship J, Eisbruch A, d'Hondt E, Jones R. Parotid sparing study in head and neck cancer patients receiving bilateral radiation therapy: one-year results. Journal of dental research. 1997;76(3):807-13.
47. Jha N, Seikaly H, Harris J, Williams D, Liu R, McGaw T, et al. Prevention of radiation induced xerostomia by surgical transfer of submandibular salivary gland into the submental space. Radiotherapy and oncology. 2003;66(3):283-9.
48. Sood AJ, Fox NF, O'Connell BP, Lovelace TL, Nguyen SA, Sharma AK, et al. Salivary gland transfer to prevent radiation-induced xerostomia: A systematic review and meta-analysis. Oral oncology. 2014;50(2):77-83.
49. Klijn C, Durinck S, Stawiski EW, Haverty PM, Jiang Z, Liu H, et al. A comprehensive transcriptional portrait of human cancer cell lines. Nat Biotechnol. 2015;33(3):306-12. doi: 10.1038/nbt.3080. PubMed PMID: 25485619.
50. Man YG, Ball WD, Marchetti L, Hand AR. Contributions of intercalated duct cells to the normal parenchyma of submandibular glands of adult rats. Anat Rec. 2001;263(2):202-14.
51. Denny PC, Liu P, Denny PA. Evidence of a phenotypically determined ductal cell lineage in mouse salivary glands. Anat Rec. 1999;256(1):84-90. PubMed PMID: 10456989.
52. Burford-Mason AP, Cummins MM, Brown DH, MacKay AJ, Dardick I. Immunohistochemical analysis of the proliferative capacity of duct and acinar cells during ligation-induced atrophy and subsequent regeneration of rat parotid gland. J Oral Pathol Med. 1993;22(10):440-6. PubMed PMID: 7907370.

53. Takahashi Y, Shiba A, Shiba K. [Differences in whole salivary total protein concentration and protein fractions among the groups of dentulous subjects, edentulous subjects and periodontitis patients]. Nihon Hotetsu Shika Gakkai Zasshi. 2004;48(5):723-32. PubMed PMID: 15818005.
54. Aure MH, Konieczny SF, Ovitt CE. Salivary Gland Homeostasis Is Maintained through Acinar Cell Self-Duplication. Dev Cell. 2015;33(2):231-7.
55. Nanduri LS, Lombaert IM, van der Zwaag M, Faber H, Brunsting JF, van Os RP, et al. Salisphere derived c-Kit+ cell transplantation restores tissue homeostasis in irradiated salivary gland. Radiother Oncol. 2013;108(3):458-63. doi: 10.1016/j.radonc.2013.05.020. PubMed PMID: 23769181.
56. Nanduri LS, Maimets M, Pringle SA, van der Zwaag M, van Os RP, Coppes RP. Regeneration of irradiated salivary glands with stem cell marker expressing cells. Radiother Oncol. 2011;99(3):367-72. Epub 2011/07/02. doi: 10.1016/j.radonc.2011.05.085. PubMed PMID: 21719134.
57. Lombaert I, Brunsting JF, Wierenga PK, Faber H, Stokman MA, Kok T, et al. Rescue of salivary gland function after stem cell transplantation in irradiated glands. PloS one. 2008;3(4):e2063.
58. Gadi J, Jung S-H, Lee M-J, Jami A, Ruthala K, Kim K-M, et al. The transcription factor protein Sox11 enhances early osteoblast differentiation by facilitating proliferation and the survival of mesenchymal and osteoblast progenitors. Journal of Biological Chemistry. 2013;288(35):25400-13.
59. Nakao K, Morita R, Saji Y, Ishida K, Tomita Y, Ogawa M, et al. The development of a bioengineered organ germ method. Nature methods. 2007;4(3):227-30.
60. Ogawa M, Oshima M, Imamura A, Sekine Y, Ishida K, Yamashita K, et al. Functional salivary gland regeneration by transplantation of a bioengineered organ germ. Nature communications. 2013;4.
61. Nelson J, Manzella K, Baker OJ. Current cell models for bioengineering a salivary gland: a mini-review of emerging technologies. Oral Dis. 2013;19(3):236-44.
62. Maria OM, Maria O, Liu Y, Komarova SV, Tran SD. Matrigel improves functional properties of human submandibular salivary gland cell line. The international journal of biochemistry & cell biology. 2011;43(4):622-31.
63. Quissell DO, Barzen KA, Redman RS, Camden JM, Turner JT. Development and characterization of SV40 immortalized rat parotid acinar cell lines. In vitro cellular & developmental biology Animal. 1998;34(1):58-67. doi: 10.1007/s11626-998-0054-5. PubMed PMID: 9542637.
64. Turner JT, Redman RS, Camden JM, Landon LA, Quissell DO. A rat parotid gland cell line, Par-C10, exhibits neurotransmitter-regulated transepithelial anion secretion. The American journal of physiology. 1998;275(2 Pt 1):C367-74. PubMed PMID: 9688590.
65. Baker OJ, Schulz DJ, Camden JM, Liao Z, Peterson TS, Seye CI, et al. Rat parotid gland cell differentiation in three-dimensional culture. Tissue engineering Part C, Methods. 2010;16(5):1135-44. doi: 10.1089/ten.TEC.2009.0438. PubMed PMID: 20121592; PubMed Central PMCID: PMC2943407.
66. Kibbey MC. Maintenance of the EHS sarcoma and Matrigel preparation. Journal of tissue culture methods. 1994;16(3-4):227-30.
67. McCall AD, Nelson JW, Leigh NJ, Duffey ME, Lei P, Andreadis ST, et al. Growth factors polymerized within fibrin hydrogel promote amylase production in parotid cells. Tissue Engineering Part A. 2013;19(19-20):2215-25.

68. Ishii E, Greaves A, Grunberger T, Freedman M, Letarte M. Tumor formation by a human pre-B leukemia cell line in scid mice is enhanced by matrigel and is associated with induction of CD10 expression. Leukemia. 1995;9(1):175-84.
69. Fridman R, Kibbey MC, Royce LS, Zain M, Sweeney TM, Jicha DL, et al. Enhanced tumor growth of both primary and established human and murine tumor cells in athymic mice after coinjection with Matrigel. Journal of the National Cancer Institute. 1991;83(11):769-74.
70. Soscia DA, Sequeira SJ, Schramm RA, Jayarathanam K, Cantara SI, Larsen M, et al. Salivary gland cell differentiation and organization on micropatterned PLGA nanofiber craters. Biomaterials. 2013;34(28):6773-84.
71. Sequeira SJ, Soscia DA, Oztan B, Mosier AP, Jean-Gilles R, Gadre A, et al. The regulation of focal adhesion complex formation and salivary gland epithelial cell organization by nanofibrous PLGA scaffolds. Biomaterials. 2012;33(11):3175-86.
72. Grobstein C. Inductive epithelio-mesenchymal interaction in cultured organ rudiments of the mouse. Science. 1953;118(3054):52-5.
73. Knosp WM, Knox SM, Hoffman MP. Salivary gland organogenesis. Wiley Interdisciplinary Reviews: Developmental Biology. 2012;1(1):69-82.
74. Hoffman MP, Kidder BL, Steinberg ZL, Lakhani S, Ho S, Kleinman HK, et al. Gene expression profiles of mouse submandibular gland development: FGFR1 regulates branching morphogenesis in vitro through BMP-and FGF-dependent mechanisms. Development. 2002;129(24):5767-78.
75. Steinberg Z, Myers C, Heim VM, Lathrop CA, Rebustini IT, Stewart JS, et al. FGFR2b signaling regulates ex vivo submandibular gland epithelial cell proliferation and branching morphogenesis. Development. 2005;132(6):1223-34.
76. Knox SM, Lombaert IM, Reed X, Vitale-Cross L, Gutkind JS, Hoffman MP. Parasympathetic innervation maintains epithelial progenitor cells during salivary organogenesis. Science. 2010;329(5999):1645-7. doi: 10.1126/science.1192046. PubMed PMID: 20929848; PubMed Central PMCID: PMC3376907.
77. Nedvetsky PI, Emmerson E, Finley JK, Ettinger A, Cruz-Pacheco N, Prochazka J, et al. Parasympathetic innervation regulates tubulogenesis in the developing salivary gland. Dev Cell. 2014;30(4):449-62.
78. Redman RS, Sreebny LM. Morphologic and biochemical observations on the development of the rat parotid gland. Dev Biol. 1971;25(2):248-79. Epub 1971/06/01. PubMed PMID: 5562853.
79. Lawson KA. Morphogenesis and functional differentiation of the rat parotid gland in vivo and in vitro. Journal of embryology and experimental morphology. 1970;24(2):411-24.
80. Lawson KA. The role of mesenchyme in the morphogenesis and functional differentiation of rat salivary epithelium. Journal of embryology and experimental morphology. 1972;27(3):497-513.
81. Cutler LS. The dependent and independent relationships between cytodifferentiation and morphogenesis in developing salivary gland secretory cells. Anat Rec. 1980;196(3):341-7.
82. Yamamoto S, Fukumoto E, Yoshizaki K, Iwamoto T, Yamada A, Tanaka K, et al. Platelet-derived growth factor receptor regulates salivary gland morphogenesis via fibroblast growth factor expression. Journal of Biological Chemistry. 2008;283(34):23139-49.
83. Melnick M, Phair RD, Lapidot SA, Jaskoll T. Salivary gland branching morphogenesis: a quantitative systems analysis of the Eda/Edar/NFκB paradigm. BMC developmental biology. 2009;9(1):32.
84. Hoffman M, Yamada K. Salivary Gland Molecular Anatomy Project [cited 2015]. Available from: http://sgmap.nidcr.nih.gov/sgmap/sgexp.html.

85. Musselmann K, Green J, Sone K, Hsu J, Bothwell I, Johnson S, et al. Salivary gland gene expression atlas identifies a new regulator of branching morphogenesis. Journal of dental research. 2011;90(9):1078-84.
86. Rivals I, Personnaz L, Taing L, Potier M-C. Enrichment or depletion of a GO category within a class of genes: which test? Bioinformatics. 2007;23(4):401-7.
87. Laukens K, Naulaerts S, Berghe WV. Bioinformatics approaches for the functional interpretation of protein lists: From ontology term enrichment to network analysis. Proteomics. 2015;15(5-6):981-96.
88. Bessarabova M, Ishkin A, JeBailey L, Nikolskaya T, Nikolsky Y. Knowledge-based analysis of proteomics data. BMC bioinformatics. 2012;13(Suppl 16):S13.
89. Friedman RC, Farh KK-H, Burge CB, Bartel DP. Most mammalian mRNAs are conserved targets of microRNAs. Genome research. 2009;19(1):92-105.
90. Lewis BP, Burge CB, Bartel DP. Conserved seed pairing, often flanked by adenosines, indicates that thousands of human genes are microRNA targets. Cell. 2005;120(1):15-20.
91. Lee Y, Ahn C, Han J, Choi H, Kim J, Yim J, et al. The nuclear RNase III Drosha initiates microRNA processing. Nature. 2003;425(6956):415-9.
92. Maniataki E, Mourelatos Z. A human, ATP-independent, RISC assembly machine fueled by pre-miRNA. Genes & development. 2005;19(24):2979-90.
93. Ruby JG, Jan CH, Bartel DP. Intronic microRNA precursors that bypass Drosha processing. Nature. 2007;448(7149):83-6.
94. Kim VN. MicroRNA precursors in motion: exportin-5 mediates their nuclear export. Trends in cell biology. 2004;14(4):156-9.
95. Simons M, Raposo G. Exosomes–vesicular carriers for intercellular communication. Current opinion in cell biology. 2009;21(4):575-81.
96. Gallo A, Tandon M, Alevizos I, Illei GG. The majority of microRNAs detectable in serum and saliva is concentrated in exosomes. PloS one. 2012;7(3):e30679.
97. Lotvall J, Valadi H. Cell to cell signalling via exosomes through esRNA. Cell adhesion & migration. 2007;1(3):156-8.
98. Zhang J, Li S, Li L, Li M, Guo C, Yao J, et al. Exosome and Exosomal MicroRNA: Trafficking, Sorting, and Function. Genomics, proteomics & bioinformatics. 2015;13(1):17-24.
99. Bartel DP. MicroRNAs: genomics, biogenesis, mechanism, and function. Cell. 2004;116(2):281-97.
100. Eichhorn SW, Guo H, McGeary SE, Rodriguez-Mias RA, Shin C, Baek D, et al. mRNA destabilization is the dominant effect of mammalian microRNAs by the time substantial repression ensues. Molecular cell. 2014;56(1):104-15.
101. Grimson A, Farh KK-H, Johnston WK, Garrett-Engele P, Lim LP, Bartel DP. MicroRNA targeting specificity in mammals: determinants beyond seed pairing. Molecular cell. 2007;27(1):91-105.
102. Brennecke J, Stark A, Russell RB, Cohen SM. Principles of microRNA-target recognition. PLoS Biol. 2005;3(3):e85.
103. Peterson SM, Thompson JA, Ufkin ML, Sathyanarayana P, Liaw L, Congdon CB. Common features of microRNA target prediction tools. Frontiers in genetics. 2014;5.
104. Sethupathy P, Megraw M, Hatzigeorgiou AG. A guide through present computational approaches for the identification of mammalian microRNA targets. Nature methods. 2006;3(11):881-6.
105. Witkos T, Koscianska E, Krzyzosiak W. Practical aspects of microRNA target prediction. Current molecular medicine. 2011;11(2):93.

106. Kanellopoulou C, Muljo SA, Kung AL, Ganesan S, Drapkin R, Jenuwein T, et al. Dicer-deficient mouse embryonic stem cells are defective in differentiation and centromeric silencing. Genes & development. 2005;19(4):489-501.
107. Shenoy A, Blelloch RH. Regulation of microRNA function in somatic stem cell proliferation and differentiation. Nature Reviews Molecular Cell Biology. 2014.
108. Wong RK, Sagar SM, Chen BJ, Yi GY, Cook R. Phase II Randomized Trial of Acupuncture-Like Transcutaneous Electrical Nerve Stimulation to Prevent Radiation-Induced Xerostomia in Head and Neck Cancer Patients. J Soc Integr Oncol. 2010;8(2):35-42. Epub 2010/04/15. PubMed PMID: 20388444.
109. Cardinali B, Castellani L, Fasanaro P, Basso A, Alema S, Martelli F, et al. Microrna-221 and microrna-222 modulate differentiation and maturation of skeletal muscle cells. PloS one. 2009;4(10):e7607.
110. Dey BK, Gagan J, Dutta A. miR-206 and-486 induce myoblast differentiation by downregulating Pax7. Mol Cell Biol. 2011;31(1):203-14.
111. Rebustini IT, Hayashi T, Reynolds AD, Dillard ML, Carpenter EM, Hoffman MP. miR-200c regulates FGFR-dependent epithelial proliferation via Vldlr during submandibular gland branching morphogenesis. Development. 2012;139(1):191-202.
112. Jevnaker A-M, Osmundsen H. MicroRNA expression profiling of the developing murine molar tooth germ and the developing murine submandibular salivary gland. Archives of oral biology. 2008;53(7):629-45.
113. Metzler M, Venkatesh SG, Lakshmanan J, Carenbauer AL, Perez SM, Andres SA, et al. A Systems Biology Approach Identifies a Regulatory Network in Parotid Acinar Cell Terminal Differentiation. PloS one. 2015. doi: *In production.* 10.1371/journal.pone.0125153.
114. Metzler MA, Appana S, Brock GN, Darling DS. Use of multiple time points to model parotid differentiation. Genomics Data. 2015.
115. Wittliff JL. Laser capture microdissection and its applications in genomics and proteomics. Techniques in Confocal Microscopy, ed by PM Conn (Elsevier, Oxford, 2010). 2010:463-78.
116. Andres SA, Wittliff JL. Relationships of ESR1 and XBP1 expression in human breast carcinoma and stromal cells isolated by laser capture microdissection compared to intact breast cancer tissue. Endocrine. 2011;40(2):212-21.
117. Gautier L, Cope L, Bolstad BM, Irizarry RA. affy--analysis of Affymetrix GeneChip data at the probe level. Bioinformatics. 2004;20(3):307-15. doi: 10.1093/bioinformatics/btg405. PubMed PMID: 14960456.
118. Gentleman R, Carey V, Huber W, Hahne F. Genefilter: Methods for filtering genes from microarray experiments. R package version. 2011;1(0).
119. Brock GN, Mukhopadhyay P, Pihur V, Webb C, Greene RM, Pisano MM. MmPalateMiRNA, an R package compendium illustrating analysis of miRNA microarray data. Source code for biology and medicine. 2013;8(1):1-20.
120. Oh S, Kang DD, Brock GN, Tseng GC. Biological impact of missing-value imputation on downstream analyses of gene expression profiles. Bioinformatics. 2011;27(1):78-86.
121. Benjamini Y, Hochberg Y. Controlling the false discovery rate: a practical and powerful approach to multiple testing. Journal of the Royal Statistical Society Series B (Methodological). 1995:289-300.
122. Smyth GK. Limma: linear models for microarray data. Bioinformatics and computational biology solutions using R and Bioconductor: Springer; 2005. p. 397-420.

123. Jacobs JL, Dinman JD. Systematic analysis of bicistronic reporter assay data. Nucleic acids research. 2004;32(20):e160. doi: 10.1093/nar/gnh157. PubMed PMID: 15561995; PubMed Central PMCID: PMC534638.
124. Livak KJ, Schmittgen TD. Analysis of relative gene expression data using real-time quantitative PCR and the 2(T)(-Delta Delta C) method. Methods. 2001;25(4):402-8. doi: 10.1006/meth.2001.1262. PubMed PMID: WOS:000173949500003.
125. Johnson CL, Kowalik AS, Rajakumar N, Pin CL. Mist1 is necessary for the establishment of granule organization in serous exocrine cells of the gastrointestinal tract. Mechanisms of development. 2004;121(3):261-72. doi: 10.1016/j.mod.2004.01.003. PubMed PMID: 15003629.
126. Zhang X, Cairns M, Rose B, O'Brien C, Shannon K, Clark J, et al. Alterations in miRNA processing and expression in pleomorphic adenomas of the salivary gland. Int J Cancer. 2009;124(12):2855-63. Epub 2009/04/07. doi: 10.1002/ijc.24298. PubMed PMID: 19347935.
127. Akhtar M, Holmgren C, Göndör A, Vesterlund M, Kanduri C, Larsson C, et al. Cell type and context-specific function of PLAG1 for IGF2 P3 promoter activity. Int J Oncol. 2012;41(6):1959-66.
128. Declercq J, Van Dyck F, Van Damme B, Van de Ven WJ. Upregulation of Igf and Wnt signalling associated genes in pleomorphic adenomas of the salivary glands in PLAG1 transgenic mice. Int J Oncol. 2008;32(5):1041-7.
129. Roush S, Slack FJ. The let-7 family of microRNAs. Trends in cell biology. 2008;18(10):505-16.
130. Li VC, Kirschner MW. Molecular ties between the cell cycle and differentiation in embryonic stem cells. Proceedings of the National Academy of Sciences. 2014;111(26):9503-8.
131. Li Z, Gilbert JA, Zhang Y, Zhang M, Qiu Q, Ramanujan K, et al. An HMGA2-IGF2BP2 axis regulates myoblast proliferation and myogenesis. Dev Cell. 2012;23(6):1176-88.
132. Acosta-Alvear D, Zhou Y, Blais A, Tsikitis M, Lents NH, Arias C, et al. XBP1 controls diverse cell type- and condition-specific transcriptional regulatory networks. Molecular cell. 2007;27(1):53-66. doi: 10.1016/j.molcel.2007.06.011. PubMed PMID: 17612490.
133. Hess DA, Humphrey SE, Ishibashi J, Damsz B, Lee AH, Glimcher LH, et al. Extensive pancreas regeneration following acinar-specific disruption of Xbp1 in mice. Gastroenterology. 2011;141(4):1463-72.
134. Ding C, Li L, Su Y-C, Xiang R-L, Cong X, Yu H-K, et al. Adiponectin increases secretion of rat submandibular gland via adiponectin receptors-mediated AMPK signaling. 2013.
135. Zatkova A, Rouillard JM, Hartmann W, Lamb BJ, Kuick R, Eckart M, et al. Amplification and overexpression of the IGF2 regulator PLAG1 in hepatoblastoma. Genes, Chromosomes and Cancer. 2004;39(2):126-37.
136. Hensen K, Braem C, Declercq J, Van Dyck F, Dewerchin M, Fiette L, et al. Targeted disruption of the murine Plag1 proto-oncogene causes growth retardation and reduced fertility. Development, growth & differentiation. 2004;46(5):459-70.
137. Poy MN, Hausser J, Trajkovski M, Braun M, Collins S, Rorsman P, et al. miR-375 maintains normal pancreatic α-and β-cell mass. Proceedings of the National Academy of Sciences. 2009;106(14):5813-8.
138. Dai N, Rapley J, Angel M, Yanik MF, Blower MD, Avruch J. mTOR phosphorylates IMP2 to promote IGF2 mRNA translation by internal ribosomal entry. Genes & development. 2011;25(11):1159-72.
139. Sivakumar S, Mirels L, Miranda AJ, Hand AR. Secretory protein expression patterns during rat parotid gland development. Anat Rec. 1998;252(3):485-97. Epub 1998/11/12. PubMed PMID: 9811227.

140. Geetha C, Venkatesh S, Dunn BF, Gorr S. Expression and anti-bacterial activity of human parotid secretory protein (PSP). Biochemical Society Transactions. 2003;31(4):815-8.
141. Poulsen K, Jakobsen B, Mikkelsen B, Harmark K, Nielsen J, Hjorth J. Coordination of murine parotid secretory protein and salivary amylase expression. Embo J. 1986;5(8):1891.
142. Garcia DM, Baek D, Shin C, Bell GW, Grimson A, Bartel DP. Weak seed-pairing stability and high target-site abundance decrease the proficiency of lsy-6 and other microRNAs. Nature structural & molecular biology. 2011;18(10):1139-46.
143. Lai J-K, Wu H-C, Shen Y-C, Hsieh H-Y, Yang S-Y, Chang C-C. Krüppel-like factor 4 is involved in cell scattering induced by hepatocyte growth factor. Journal of cell science. 2012;125(20):4853-64.
144. Min IM, Pietramaggiori G, Kim FS, Passegue E, Stevenson KE, Wagers AJ. The transcription factor EGR1 controls both the proliferation and localization of hematopoietic stem cells. Cell stem cell. 2008;2(4):380-91. doi: 10.1016/j.stem.2008.01.015. PubMed PMID: 18397757.
145. Liu X, Huang J, Chen T, Wang Y, Xin S, Li J, et al. Yamanaka factors critically regulate the developmental signaling network in mouse embryonic stem cells. Cell Res. 2008;18(12):1177-89. Epub 2008/11/26. doi: 10.1038/cr.2008.309. PubMed PMID: 19030024.
146. Vegliante MC, Palomero J, Pérez-Galán P, Roué G, Castellano G, Navarro A, et al. SOX11 regulates PAX5 expression and blocks terminal B-cell differentiation in aggressive mantle cell lymphoma. Blood. 2013;121(12):2175-85.
147. Shaffer AL, Shapiro-Shelef M, Iwakoshi NN, Lee AH, Qian SB, Zhao H, et al. XBP1, downstream of Blimp-1, expands the secretory apparatus and other organelles, and increases protein synthesis in plasma cell differentiation. Immunity. 2004;21(1):81-93. Epub 2004/09/04. doi: 10.1016/j.immuni.2004.06.010. PubMed PMID: 15345222.
148. Nera KP, Kohonen P, Narvi E, Peippo A, Mustonen L, Terho P, et al. Loss of Pax5 promotes plasma cell differentiation. Immunity. 2006;24(3):283-93. doi: 10.1016/j.immuni.2006.02.003. PubMed PMID: 16546097.
149. Yamamoto K, Yoshida H, Kokame K, Kaufman RJ, Mori K. Differential contributions of ATF6 and XBP1 to the activation of endoplasmic reticulum stress-responsive cis-acting elements ERSE, UPRE and ERSE-II. Journal of biochemistry. 2004;136(3):343-50. doi: 10.1093/jb/mvh122. PubMed PMID: 15598891.
150. Lee AH, Iwakoshi NN, Glimcher LH. XBP-1 regulates a subset of endoplasmic reticulum resident chaperone genes in the unfolded protein response. Mol Cell Biol. 2003;23(21):7448-59. Epub 2003/10/16. PubMed PMID: 14559994; PubMed Central PMCID: PMC207643.
151. Pin CL, Rukstalis JM, Johnson C, Konieczny SF. The bHLH transcription factor Mist1 is required to maintain exocrine pancreas cell organization and acinar cell identity. J Cell Biol. 2001;155(4):519-30. Epub 2001/11/07. doi: 10.1083/jcb.200105060. PubMed PMID: 11696558; PubMed Central PMCID: PMC2198859.
152. Direnzo D, Hess DA, Damsz B, Hallett JE, Marshall B, Goswami C, et al. Induced Mist1 expression promotes remodeling of mouse pancreatic acinar cells. Gastroenterology. 2012;143(2):469-80.
153. Huh WJ, Esen E, Geahlen JH, Bredemeyer AJ, Lee AH, Shi G, et al. XBP1 controls maturation of gastric zymogenic cells by induction of MIST1 and expansion of the rough endoplasmic reticulum. Gastroenterology. 2010;139(6):2038-49. Epub 2010/09/08. doi: 10.1053/j.gastro.2010.08.050. PubMed PMID: 20816838; PubMed Central PMCID: PMC2997137.
154. Lemercier C, Brown A, Mamani M, Ripoche J, Reiffers J. The rat Mist1 gene: structure and promoter characterization. Gene. 2000;242(1-2):209-18. PubMed PMID: 10721714.

155. Cittelly DM, Finlay-Schultz J, Howe EN, Spoelstra NS, Axlund SD, Hendricks P, et al. Progestin suppression of miR-29 potentiates dedifferentiation of breast cancer cells via KLF4. Oncogene. 2013;32(20):2555-64. Epub 2012/07/04. doi: 10.1038/onc.2012.275. PubMed PMID: 22751119.
156. Wellner U, Schubert J, Burk UC, Schmalhofer O, Zhu F, Sonntag A, et al. The EMT-activator ZEB1 promotes tumorigenicity by repressing stemness-inhibiting microRNAs. Nature cell biology. 2009;11(12):1487-95. doi: 10.1038/ncb1998. PubMed PMID: 19935649.
157. Duan Q, Wang X, Gong W, Ni L, Chen C, He X, et al. ER stress negatively modulates the expression of the miR-199a/214 cluster to regulates tumor survival and progression in human hepatocellular cancer. PloS one. 2012;7(2):e31518. doi: 10.1371/journal.pone.0031518. PubMed PMID: 22359598; PubMed Central PMCID: PMC3281082.
158. Oettgen P, Kas K, Dube A, Gu X, Grall F, Thamrongsak U, et al. Characterization of ESE-2, a novel ESE-1-related Ets transcription factor that is restricted to glandular epithelium and differentiated keratinocytes. Journal of Biological Chemistry. 1999;274(41):29439-52.
159. Tamm C, Böwer N, Annerén C. Regulation of mouse embryonic stem cell self-renewal by a Yes–YAP–TEAD2 signaling pathway downstream of LIF. Journal of cell science. 2011;124(7):1136-44.
160. Mills JC, Taghert PH. Scaling factors: transcription factors regulating subcellular domains. Bioessays. 2012;34(1):10-6.
161. Piechocki MP, Burk RD, Ruch RJ. Regulation of connexin32 and connexin43 gene expression by DNA methylation in rat liver cells. Carcinogenesis. 1999;20(3):401-6. Epub 1999/04/06. PubMed PMID: 10190553.
162. Zhu L, Tran T, Rukstalis JM, Sun P, Damsz B, Konieczny SF. Inhibition of Mist1 homodimer formation induces pancreatic acinar-to-ductal metaplasia. Mol Cell Biol. 2004;24(7):2673-81.
163. Vij N, Zeitlin PL. Regulation of the ClC-2 lung epithelial chloride channel by glycosylation of SP1. American journal of respiratory cell and molecular biology. 2006;34(6):754-9.
164. Fergusson D, Campo MS. PEF-1, an epithelial cell transcription factor which activates the long control region of human papillomavirus type 16, is glycosylated with N-acetylglucosamine. Journal of general virology. 1998;79(11):2753-60.
165. Lee AH, Chu GC, Iwakoshi NN, Glimcher LH. XBP-1 is required for biogenesis of cellular secretory machinery of exocrine glands. Embo J. 2005;24(24):4368-80. doi: 10.1038/sj.emboj.7600903. PubMed PMID: 16362047; PubMed Central PMCID: PMC1356340.

CURRICULUM VITA

Melissa Metzler

University of Louisville

Graduate Student

Department of Biochemistry and Molecular Genetics

mametz01@louisville.edu

Education

2009 - present	University of Louisville: doctoral candidate, department of Biochemistry and Molecular Biology
2003 – 2007	Bellarmine University: B.A. in Biology, minor in Chemistry, summa cum laude

Funding

Sept. 2012 – Sept. 2016	NIH/NIDCR	F31OGMB120151: microRNAs and Parotid Acinar Differentiation

Research Positions

January 2010-present: University of Louisville, PhD student under Dr. Douglas S. Darling, Department of Biochemistry and Molecular Biology

January 2007 – July 2007: Bellarmine University, undergraduate research assistant under Dr. David Robbinson, Department of Biology

July 2006 –November 2006: Bellarmine University, undergraduate research assistant under Dr. Steven Wilt, Department of Biology

May 2005 – August 2005: University of Louisville Kentucky Lions Eye Center, undergraduate research assistant under Dr. Nicholas Delamere, Department of Pharmacology and Toxicology

June 2004 – August 2004: University of Kentucky, undergraduate research assistant under Dr. Pete Mirabito, Biology Department

Awards

2012 F31 Fellowship NIH/NIDCR

2011 CGeMM Travel Award. University of Louisville.

2011, Feb. Poster award. Gordon Conference. Salivary Glands and Exocrine Biology. Hotel Galvez. Galveston TX.

2009 – 2011 Graduate Student Fellowship, Integrated Programs in Biomedical Sciences, University of Louisville

2007 Dr. Korn award for excellence in research, Bellarmine University

2004 KBRIN Fellowship, University of Kentucky

Publications

Metzler, Melissa A., Srirangapatnam G. Venkatesh, Jaganathan Lakshmanan, Anne L. Carenbauer, Sara M. Perez, Sarah A. Andres, Savitri Appana, Guy N. Brock, James L. Wittliff, and Douglas S. Darling. "A Systems Biology Approach Identifies a Regulatory Network in Parotid Acinar Cell Terminal Differentiation." *PloS one* 10, no. 4 (2015).

Metzler MA, Appana S, Brock GN, Darling DS. (2015) Use of Multiple Time Points to Model Parotid Differentiation. Genomics Data. Accepted: DOI: 10.1016/j.gdata.2015.05.005

Khundmiri SJ, Metzler MA, Ameen M, Amin V, Rane MJ, Delamere NA.Am J Physiol Cell Physiol 291: C1247-C1257, 2006. Ouabain induces Cell Proliferation through Calcium Dependent Phosphorylation of Akt (Protein Kinase B) in Opossum Kidney Proximal Tubule Cells.

Posters

Melissa Metzler, Srirangapatnam G. Venkatesh, Anne Carenbauer, Sarah Andres, Savitri Appana, Guy Brock, James L. Wittliff, and Douglas S. Darling. A Systems Biology Approach Identifies a Regulatory Network in Parotid Acinar Cell Terminal Differentiation. Research Louisville. University of Louisville. October 29, 2015.

Melissa Metzler, Srirangapatnam G. Venkatesh, Sarah Andres, Savitri Appana, Guy Brock, James L. Wittliff, and Douglas S. Darling. University of Louisville departments of Biochemistry & Molecular Biology, Oral Health and Rehabilitation, and Bioinformatics

and Biostatistics. Parotid Acinar Differentiation: Defining Important Players and Regulatory Steps. Research Louisville. September 24-27, 2013.

Melissa Metzler, Venkatesh G. Srirangapatnam, Sarah Andres, James L. Wittliff, Douglas S. Darling. MicroRNA Changes During *in vivo* Parotid Gland Acinar Differentiation. Cell Symposia. Regulatory RNAs. Wyndam Hotel Chicago IL. Oct. 10 – 12, 2011.

Melissa Metzler, Srirangapatnam Venkatesh, Douglas Darling. MicroRNA Changes in Parotid Gland Acinar Differentiation. Gordon Conference. Salivary Glands and Exocrine Biology. Hotel Galvez. Galveston TX. Feb. 6 – 11, 2011.

Melissa Metzler, Srirangapatnam Venkatesh, Douglas Darling. MicroRNA Changes in Parotid Gland Acinar Differentiation. Research Louisville. University of Louisville 2010.

Melissa Metzler, Srirangapatnam G. Venkatesh, Douglas S. Darling. Acinar cell differentiation: Identifying Regulating Factors. Institute for Molecular Diversity and Drug Design. University of Louisville. 2010.

Invited Talks

A Systems Biology Approach Identifies a Regulatory Network in Parotid Acinar Cell Terminal Differentiation. Institute for Molecular Diversity and Drug Design. University of Louisville. Nov. 10, 2015

Parotid Acinar Differentiation: Defining Important Players and Regulatory Steps. Biochemistry & Molecular Biology Retreat. University of Louisville. Aug. 23, 2013.

MicroRNA Changes in Parotid Gland Acinar Differentiation. Gordon Conference. Salivary Glands and Exocrine Biology. Hotel Galvez. Galveston TX. Feb. 6 – 11, 2011.

Teaching Activities

Fall 2010 Teaching Assistant, BIOC 645/545 Biochemistry. University of Louisville.